TECH LIBRARY KAFB, NM
0060738
NASA CR-16
C. 1
LOAN COPY: RETURN TO
AFWL (WLOL)
KIRTLAND AFB, N MEX

NASA CONTRACTOR REPORT

NASA CR-1632

ANALYSIS OF WING SLIPSTREAM FLOW INTERACTION

by Antony Jameson

Prepared by
GRUMMAN AEROSPACE CORPORATION
Bethpage, N. Y.
for Ames Research Center

NATIONAL AERONAUTICS AND SPACE ADMINISTRATION • WASHINGTON, D. C. • AUGUST 1970

TECH LIBRARY KAFB, NM

0060738

NASA CR-1632

ANALYSIS OF WING SLIPSTREAM FLOW INTERACTION

By Antony Jameson

Distribution of this report is provided in the interest of information exchange. Responsibility for the contents resides in the author or organization that prepared it.

Prepared under Contract No. NAS 2-4658 by
GRUMMAN AEROSPACE CORPORATION
Bethpage, N.Y.

for Ames Research Center

NATIONAL AERONAUTICS AND SPACE ADMINISTRATION

For sale by the Clearinghouse for Federal Scientific and Technical Information
Springfield, Virginia 22151 – CFSTI price $3.00

ACKNOWLEDGEMENT

The starting point of this investigation was a study carried out by John DeYoung with the assistance of Crystal Singleton, the results of which are presented in the Grumman Report, ADR 01-04-66.1, Symmetric Loading of a Wing in a Wide Slipstream. This study introduced the idea of using a rectangular jet as a model for the merged slipstreams of a row of propellers.

SUMMARY

Part 1

Theoretical methods are developed for calculating the interaction of a wing both with a circular slipstream and with a wide slipstream from a row of propellers. Rectangular and elliptic jets are used as models for wide slipstreams. Standard imaging techniques are used to develop a lifting surface theory for a static wing in a rectangular jet. The effect of forward speed is approximated by multiplying the interference potential by a scalar strength factor, derived with the aid of studies of the interaction of a lifting line with an elliptic jet. A closed form solution is found for an elliptic wing exactly spanning the foci of an elliptic jet. A continuous wide jet is found to provide a substantially greater augmentation of lift than multiple separate jets, because of the elimination of edge effects at the gaps. Also it is easier to deflect a wide shallow jet than a deep jet.

Part 2

With aid of the concept of the apparent mass influenced by the wing, simple formulas are developed for the lift and drag of wings in both wide and circular jets. These formulas closely approximate the results of detailed calculations developed in Part 1, and provide the basis of a method suitable for engineering calculations. Predictions using this method show good correlation with existing experimental data for wings without flaps. The method can also be used to estimate the characteristics of propeller-wing-flap combinations if suitable values are assumed for the flap effectiveness α / δ in a jet. It appears from the available evidence that the flap effectiveness is substantially increased in a jet.

TABLE OF CONTENTS

PART 1 - THEORETICAL STUDIES OF THE LIFT OF A WING IN WIDE AND CIRCULAR SLIPSTREAMS

TABLE OF CONTENTS (cont)

PART 2 - ENGINEERING METHOD FOR PREDICTION OF CHARACTERISTICS OF PRACTICAL V/STOL CONFIGURATIONS

PART 1

THEORETICAL STUDIES OF THE LIFT OF A WING IN WIDE AND CIRCULAR SLIPSTREAMS

1. Introduction

The need for V/STOL aircraft to relieve air traffic congestion is becoming increasingly apparent. One of the most promising methods of reducing take off and landing distances is to use propellers or ducted fans to augment the airflow over the wing at low speeds. Interest has therefore been renewed in predicting the effect of slipstream-wing flow interaction on the aerodynamic characteristics of deflected slipstream and tilt wing aircraft.

The lift of a wing spanning a circular slipstream has been quite extensively studied. Early investigators used lifting line theory (refs. 1-5). Later slender body theory was introduced to treat the case when the aspect ratio of the immersed part of the wing is small (refs. 6-9). Neither of these theories agreed well with experimental results. Lifting surface theories were developed by Rethorst (ref. 10), using an analytical approach, and Ribner and Ellis (refs. 16-17), using a numerical approach. These have been shown to give quite good agreement with a limited amount of experimental data, but require lengthy computations. Rethorst's method has been extended to cover the effects of several circular slipstreams, inclined slipstreams, high angle of attack and separated flow (refs. 11-15), but the results of numerical calculations have not been included. Only Sowydra (ref. 18) has attempted to allow for the deflection of the slipstream boundary.

The possibility of the slipstreams from several propellers merging to form a single wide jet has not been considered in any of these investigations. It can be expected, however, that the elimination of the gaps would lead to an increase in efficiency by allowing the circulation to be maintained continuously across the span. In Part 1 of this report a theory is formulated for both wide and circular slipstreams. In Part 2 it is shown how the theory may be used to predict the characteristics of practical V/STOL configurations, and its correlation with existing experimental data is established.

To restrict the complexity of the calculations it is desirable to use the simplest possible analytical models. Two models of a wide slipstream have been found to be amenable to analysis, a rectangular jet and an elliptic jet.

The rectangular jet is particularly suitable for an analysis of the static case, when the aircraft is in a hovering condition. The situation of the blown part of the wing is then similar to that of a wing in an open wind tunnel, and it is possible to draw upon existing theories of wind tunnel interference. The distinguishing features of the present case are that the wing may span the entire jet, and that the aspect ratio of the part of it in the jet may be small, so that it is desirable to allow for both the span-

wise and the chordwise variation of the interference downwash. With a rectangular jet it is possible to satisfy the boundary condition for the static case at every point of the jet surface throughout its length by introducing images, so that a lifting surface theory can quite readily be developed.

Unfortunately this theory is exact only for the static case, since it is no longer possible to satisfy the boundary conditions at the surface of a rectangular jet by introducing images when the aircraft has forward speed. Using an elliptic jet as a model of the slipstream, it is, however, possible to develop a simple lifting line theory which is valid throughout the speed range. From the results of this analysis it is then possible to determine a correction factor for the effect of forward speed on the rectangular jet. In this way an approximate lifting surface theory is obtained for the whole speed range. By using the results of calculations for a square jet to estimate the chordwise variation of the interference downwash, it is also possible to develop a simplified lifting surface theory for a circular jet.

Notation for Part 1

ρ	Air density
V_o	Free stream velocity
V_j	Jet velocity
μ	Velocity ratio $\frac{V_o}{V_j}$
p_o	Pressure in the free stream
p_j	Pressure in the jet
α	Angle of attack
T	Thrust
L	Lift
D	Drag due to lift
L_α	Lift slope $\frac{dL}{d\alpha}$
CL	Lift coefficient referred to jet velocity V_j
CD	Coefficent of induced drag referred to jet velocity V_j
CL_α	Lift slope $\frac{dCL}{d\alpha}$
θ	Jet deflection angle
b	Wing span
c	Wing chord
S	Wing area
AR	Wing aspect ratio
Λ	Wing sweep at 1/4 chord
B	Jet width
H	Jet height
S_j	Jet area
AR_j	Aspect ratio of rectangular jet
λ	Ratio of width to height of elliptic jet

φ_o	Potential in the free stream
φ_j	Potential in the jet
φ_v	Potential of a given vortex distribution in a free stream
Γ	Circulation
w	Downwash velocity
w_j	Downwash velocity due to jet interference
w_{jo}	Downwash velocity at the loadline due to jet interference
x, y, z	Space coordinates
$\bar{x}_c, \bar{y}_c, \bar{z}_c$	Coordinates of horseshoe vortex
$\bar{x}, \bar{y}, \bar{z}$	Coordinates of image vortex
ξ, η, ζ	Nondimensional coordinates $\frac{x}{b/2}, \frac{y}{b/2}, \frac{z}{b/2}$ (in Section 5 ξ, η are elliptic coordinates)
$\bar{\xi}_c, \bar{\eta}_c, \bar{\zeta}_c$	$\frac{\bar{x}_c}{b/2}, \frac{\bar{y}_c}{b/2}, \frac{\bar{z}_c}{b/2}$
$\bar{\xi}, \bar{\eta}, \bar{\zeta}$	$\frac{\bar{x}}{b/2}, \frac{\bar{y}}{b/2}, \frac{\bar{z}}{b/2}$
m, n	Lateral and vertical displacement of image vortex
σ	Ratio of wing span to jet width b/B
a^+	Coordinate of jet downwash function $\frac{\sigma}{2}(\bar{\eta}_c + \eta)$
a^-	Coordinate of jet downwash function $\frac{\sigma}{2}(\bar{\eta}_c - \eta)$
f	Jet downwash function (equation (3.8))
f_x	Longitudinal derivative of jet downwash function (equation (3.11))
A_{nm}	Downwash influence coefficient in a free stream
R_{nm}	Interference downwash influence coefficient
G_m	Nondimensional circulation Γ/bV_j
P	Strength factor of interference influence coefficients
Subscripts n, m	Span stations of load points and control points for calculation of the lift distribution.

2. Mathematical formulation

The general case to be considered is the flow over a wing in the slipstreams generated by one or more propellers, with an external flow due to forward motion of the wing. The slipstreams from a row of closely spaced propellers are assumed to merge to form a single wide jet (sketch 1).

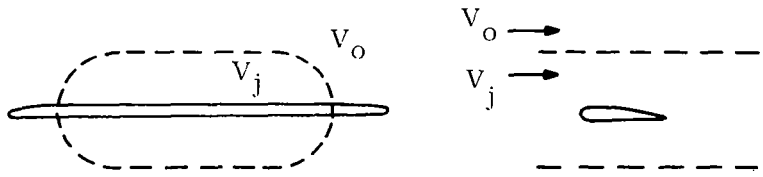

Sketch 1. Wing in a Slipstream and an External Flow

To facilitate the analysis the following simplifying assumptions are also made:

(1) The fluid is inviscid and incompressible
(2) Before it is influenced by the wing the slipstream is a uniform jet such as might be produced by an actuator with a uniform pressure change: transverse velocities and variations of the axial velocity induced by the propellers are ignored.
(3) The jet boundary extends back in a parallel direction: deflection of the jet by the wing is ignored.

In the case of large flap angles the third assumption is not realistic. The deflected jet behind a moving flapped wing would impinge on the external stream like a jet flap, possibly producing an increase in the lift.

Under the first two assumptions the perturbation velocity due to the wing can be represented both inside and outside the slipstream as the gradient of a velocity potential which satisfies Laplace's equation, and according to the third assumption the location of the boundary between the two regions is known. Let V_j and V_o be the unperturbed velocity of the flow inside and outside the slipstream. Also let p_j and φ_j be the pressure and potential inside the slipstream, and p_o and φ_o the pressure

and potential in the external flow. At the boundary both the pressure and potential must be continuous, that is

$$p_j = p_o$$

$$\frac{1}{V_j} \frac{\partial \varphi_j}{\partial n} = \frac{1}{V_o} \frac{\partial \varphi_o}{\partial n}$$

where $\frac{\partial}{\partial n}$ denotes differentiation in the normal direction. Now if the perturbation velocities are small compared with V_j and V_o, then, neglecting the squares of the perturbation velocities in Bernoulli's equation, the pressure changes inside and outside the slipstream are proportional to $V_j \frac{\partial \varphi_j}{\partial x}$ and $V_o \frac{\partial \varphi_o}{\partial x}$. Since these must be equal along the whole length of the boundary, the boundary conditions can be expressed as

$$\varphi_j = \mu \varphi_o \tag{2.1}$$

$$\mu \frac{\partial \varphi_j}{\partial n} = \frac{\partial \varphi_o}{\partial n} \tag{2.2}$$

where

$$\mu = \frac{V_o}{V_j} \tag{2.3}$$

The wing itself will generally be treated as a lifting surface. This leads to the third boundary condition that on the wing surface the downwash is such that the perturbed flow is tangential to the wing. To simplify the calculations the Weissinger approximation will be used (ref. 20). According to this the vorticity of the wing is assumed to be concentrated at the 1/4 chord line, and the tangency condition is required to be satisfied only at the 3/4 chord line. The justification of this approximation is that it yields the same value, 2π, for the lift slope of a two dimensional airfoil as is obtained by more exact theories.

3. Interference for a Horseshoe Vortex in a Jet with No External Flow

The wing will be represented by a distribution of horseshoe vortices (sketch 2), and it is thus necessary to determine the interference for a horseshoe vortex in the slipstream. Initially only the static case will be treated. There is then no external flow and the situation is like that in an open jet wind tunnel. Only the first slipstream boundary condition (2.1) is relevant, and setting the velocity ratio μ equal to zero it becomes

$$\varphi_j = 0 \tag{3.1}$$

In order to simplify the mathematical treatment of the equations it is convenient to use a rectangular jet as a model for a wide slipstream from several propellers. This permits the method of images to be used. Two cases will therefore be considered, a rectangular jet when the slipstream is generated by several propellers, and a circular jet when it is generated by a single propeller or fan.

A. Rectangular jet

For each horseshoe vortex in the distribution the boundary condition (3.1) can be satisfied (ref. 19) by placing a doubly infinite array of image horseshoe vortices in all the external rectangles formed by continuing the jet boundaries to make a lattice (sketch 3). All the vortices in one column have the same sign, and the sign alternates in successive columns. If either the bound or the trailing parts of the vortices are considered, it can be seen that the elements are antisymmetrically disposed about any side of the rectangle containing the jet, so that their contributions cancel each other. The boundary condition is thus satisfied over the whole jet surface in three dimensions. The same proposition is true for a complete wing if image wings lifting upwards and downwards are placed in the external rectangles, and it is evident that this method permits a lifting surface theory to be developed.

It is convenient to separate the downwash due to each vortex from the interference downwash due to its images. Let the original horseshoe vortex be symmetrically placed about the z axis in the jet and suppose that the coordinates of its midspan point are $(\bar{x}_c, o, \bar{z}_c)$. If its semi-span is $\bar{y}_c$ the trailing parts of the vortex are located at $y = \pm\bar{y}_c$. Then the midspan points of the images are at

$$\bar{x} = \bar{x}_c, \ \bar{y} = m\ B, \ \bar{z} = n\ H + (-1)^n\ \bar{z}_c \tag{3.2}$$

where B and H are the breadth and height of the jet. By the Biot Savart law the downwash due to one image of semispan $\bar{y}_c$ is

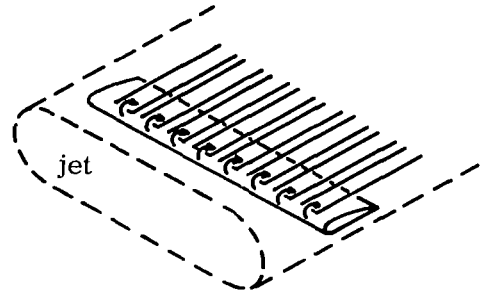

Sketch 2. Representation of the Wing as a Distribution of Horseshoe Vortices

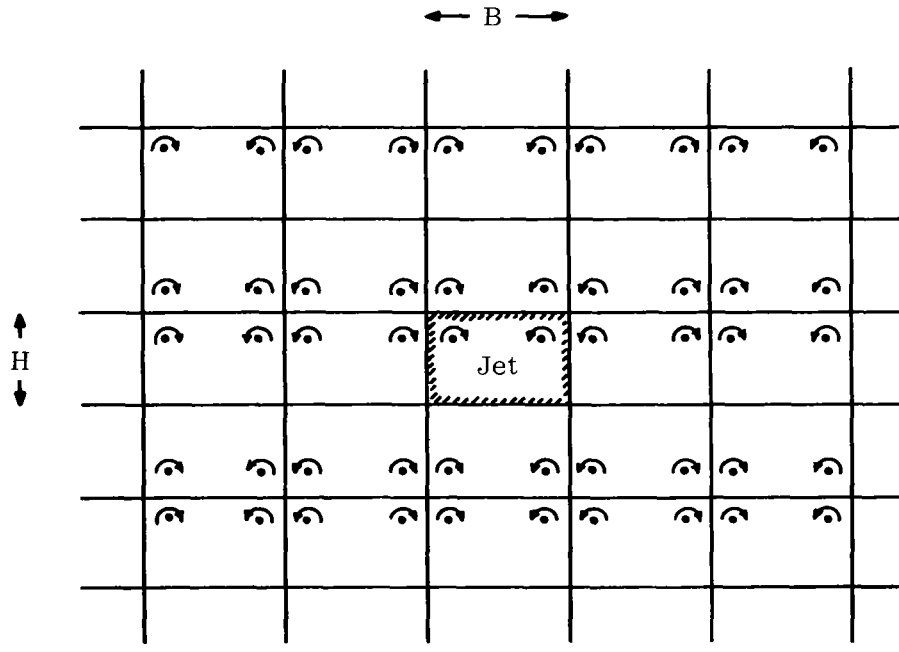

Sketch 3. Images for a Single Horseshoe Vortex in a Rectangular Jet

$$
\begin{aligned}
w_{\substack{\text{one}\\\text{image}}} = \frac{\Gamma}{4\pi} \Bigg\{ & \frac{x-\bar{x}}{(x-\bar{x})^2 + (z-\bar{z})^2} \left[\frac{\bar{y}+\bar{y}_c-y}{\sqrt{(x-\bar{x})^2 + (\bar{y}+\bar{y}_c-y)^2 + (z-\bar{z})^2}} - \frac{\bar{y}-\bar{y}_c-y}{\sqrt{(x-\bar{x})^2 + (\bar{y}-\bar{y}_c-y)^2 + (z-\bar{z})^2}} \right] \\
& + \frac{\bar{y}+\bar{y}_c-y}{(\bar{y}+\bar{y}_c-y)^2 + (z-\bar{z})^2} \left[1 + \frac{x-\bar{x}}{\sqrt{(x-\bar{x})^2 + (\bar{y}+\bar{y}_c-y)^2 + (z-\bar{z})^2}} \right] \\
& - \frac{\bar{y}-\bar{y}_c-y}{(\bar{y}-\bar{y}_c-y)^2 + (z-\bar{z})^2} \left[1 + \frac{x-\bar{x}}{\sqrt{(x-\bar{x})^2 + (\bar{y}-\bar{y}_c-y)^2 + (z-\bar{z})^2}} \right] \Bigg\}
\end{aligned}
\tag{3.3}
$$

The sense of the images can be taken account of by introducing the factor $(-1)^n$.

Summations of a double series of terms of the type given by (3.3) would be laborious. The form of (3.3), however, and the results of calculations for open wind tunnels, indicate that the interference downwash can be satisfactorily approximated in terms of the interference downwash w_{jo} in the plane of the load line and the longitudinal slope of the interference downwash in this plane as

$$
w_j = w_{jo} \left[1 + \frac{x}{\sqrt{\left(w_{jo} \Big/ \frac{dw_j}{dx} \right)^2 + x^2}} \right] \tag{3.4}
$$

In this approximation the form of the longitudinal variation of the downwash is assumed to be independent of the position in the crossplane.

Introduce non dimensional coordinates ξ , η , ζ by dividing by the wing semi span $\frac{b}{B}$. Also let the ratio of the wing span to the jet width be

$$\sigma = \frac{b}{B} \tag{3.5}$$

and define the jet aspect ratio as

$$AR_j = \frac{B}{H} \tag{3.6}$$

Then the equation for the interference downwash in the plane of the loadline due to a horseshoe vortex of strength Γ becomes

$$\frac{w_{jo}}{V_j} = \left(\frac{\Gamma}{bV_j}\right) \sigma \left[f(a^-) + f(a^+) \right] \tag{3.7}$$

where

$$f(a) = \frac{-1}{4\pi} \sum_{m=-\infty}^{\infty}{}' -(-1)^m \sum_{n=-\infty}^{\infty}{}' \frac{m + a}{(m+a)^2 + \left[\frac{n}{AR_j} + (-1)^n \bar{\zeta} - \zeta\right]^2} \tag{3.8}$$

$$f(-a) = -f(a)$$

and

$$a^- = \frac{\sigma}{2} (\bar{\eta}_c - \eta); \; a^+ = \frac{\sigma}{2} (\bar{\eta}_c + \eta) \tag{3.9}$$

The primes on the summations indicate that the term is not summed when m and n are both zero. The slope of the downwash with respect to the longitudinal coordinate is

$$\frac{d}{d\zeta} \frac{w_j}{V_j} = \frac{\Gamma}{bV_j} \sigma^2 \left[f_x(a^-) + f_x(a^+) \right] \tag{3.10}$$

where

$$f_x(a) = \frac{-1}{8\pi} \sum_{m=-\infty}^{\infty}{}' - (-1)^m \sum_{n=-\infty}^{\infty}{}'$$

$$\left(\frac{m+a}{\left[\frac{n}{AR_j} + (-1)^n \bar{\zeta} - \zeta\right]^2 \left\{(m+a)^2 + \left[\frac{n}{AR_j} + (-1)^n \bar{\zeta} - \zeta\right]^2\right\}^{1/2}} + \frac{m+a}{\left\{(m+a)^2 + \left[\frac{n}{AR_j} + (-1)^n \bar{\zeta} - \zeta\right]^2\right\}^{3/2}} \right)$$

$$f_x(-a) = -f_x(a) \tag{3.11}$$

The summation of these series is treated in Appendix A.

B. Circular Jet

When there is only one propeller and the jet is circular, it is convenient to regard the horseshoe vortex of strength Γ as composed of a two dimensional part consisting of two trailing line vortices of strength $\frac{\Gamma}{2}$, and a part antisymmetric in the longitudinal direction consisting of horseshoe vortices of strength $\frac{\Gamma}{2}$ extending backwards and forwards (sketch 4). The two parts cancel each other ahead of the load line and reinforce each other behind it.

The downwash in the plane of the load line is contributed entirely by the two dimensional part. For this the boundary condition can be satisfied (ref. 1) by introducing images at the inverse points (sketch 5)

$$y = \pm \frac{\left(\frac{B}{2}\right)^2}{\bar{y}_c} \tag{3.12}$$

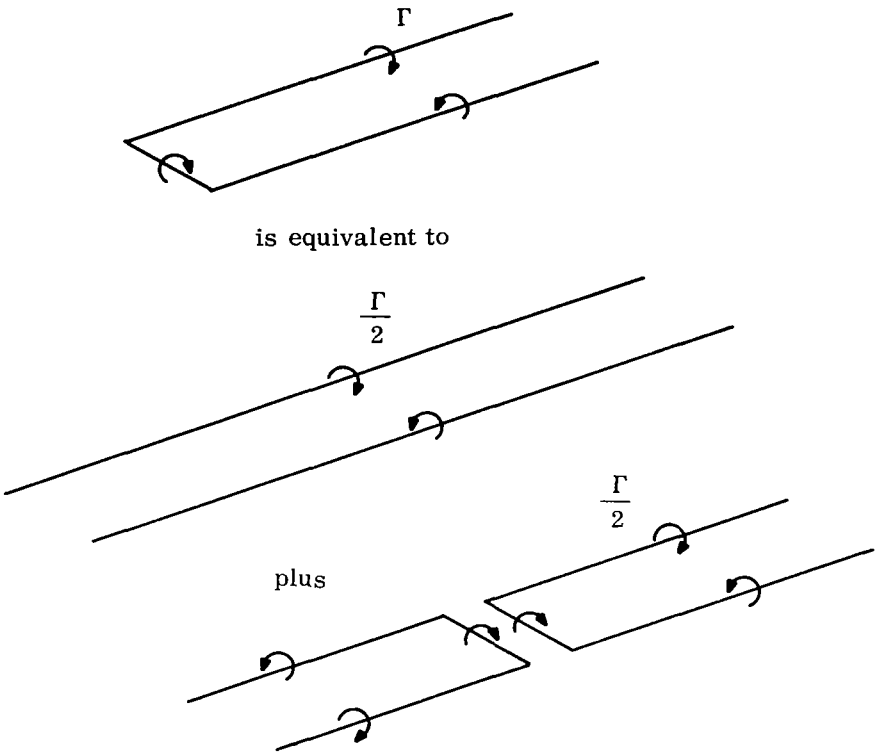

Sketch 4. Decomposition of a Horseshoe Vortex into two Dimensional and Anti-symmetric Parts

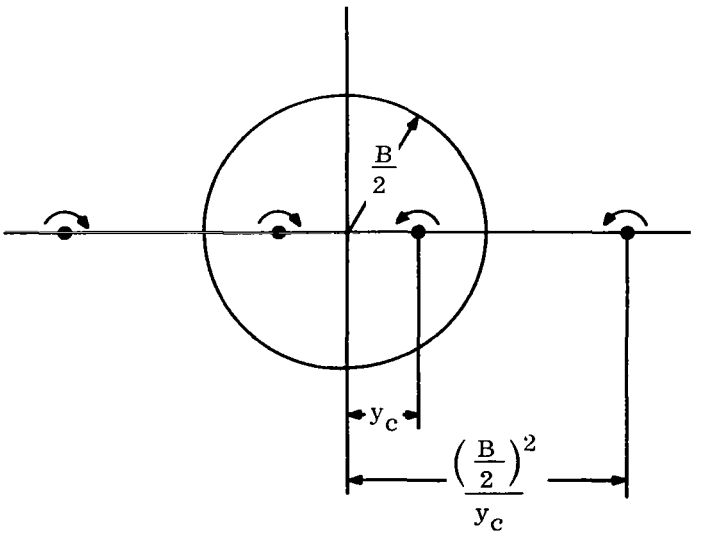

Sketch 5. Images for a Vortex Pair in a Circular Jet

where B is the jet diameter. Then in terms of the nondimensional coordinates

$$\frac{w_{jo}}{V_j} = \left(\frac{\Gamma}{bV_j}\right) \frac{\sigma}{2\pi} \left(\frac{1}{\frac{1}{\sigma\bar{\eta}c} - \sigma\eta} + \frac{1}{\frac{1}{\sigma\bar{\eta}c} + \sigma\eta} \right) \tag{3.13}$$

Using the notation of (3.4) this becomes

$$\frac{w_{jo}}{V_j} = \left(\frac{\Gamma}{bV_j}\right) \left[f(a^-) + f(a^+) \right] \tag{3.14}$$

where

$$f(a) = \frac{1}{2\pi a} ; \; a^- = \frac{1}{\sigma\bar{\eta}c} - \sigma\eta \; ; \; a^+ = \frac{1}{\sigma\bar{\eta}c} + \sigma\eta$$

$$f(-a) = -f(a) \tag{3.15}$$

The longitudinal variation of the downwash is due to the antisymmetric part. The interference potential due to this cannot be represented by images. It has been evaluated in terms of Bessel functions by Rethorst (ref. 10). The results of wind tunnel theory, however, indicate that the ratio of the slope of the downwash to the downwash at the load line is nearly the same for circular and square jets. Thus to estimate the slope of the downwash at the load line for a circular jet, this ratio can be calculated for a square jet by the methods described earlier in this section, and used to multiply the downwash at the load line for the circular jet. Then formula (3.4) may be used. In this way the need to evaluate the antisymmetric potential is obviated.

4. Determination of the circulation for a static wing by Weissinger lifting surface theory

With the aid of the results for the interference experienced by a horseshoe vortex in a jet with no external flow, the properties of a static wing can be calculated by the methods of standard wing theory. Only the case of a wing which is symmetric in the jet will be treated.

The vorticity of the wing is assumed to be concentrated at the 1/4 chord line and the spanwise distribution of the lift is represented by the circulation at a finite number of span stations. The induced downwash angle due to the combined effects of the wing vorticity and the interference vortices is then required to be equal to the wing surface angle at a corresponding number of spanwise control points along the 3/4 chord line. This leads to a set of algebraic equations for the circulation. Because of the symmetry it is only necessary to calculate the circulation at the span stations across one semi-span. Let η_m denote the ^{m}th span station at which the circulation is to be calculated and let

$$G_m = \frac{\Gamma(\eta_m)}{bV} \tag{4.1}$$

where Γ is the circulation. Let A_{nm} be the contribution to the downwash angle at the nth control point due to unit circulation, $G_m = 1$, at the mth station on each semispan. Also let R_{nm} be the contribution due to the corresponding images representing the jet interference. Then if α_n is the wing surface angle at the ^{n}th control point

$$\alpha_n = \sum (A_{nm} + R_{nm})\ G_m \tag{4.2}$$

where the summation is over the circulation stations. Since α_n is known from the distribution of twist and camber, the determination of the circulation and corresponding lift and drag is reduced to the solution of these equations, and the determination of the influence coefficients A_{nm} and R_{nm}.

The influence coefficients A_{nm} for the free wing can be calculated accurately by the method of de Young and Harper (ref. 20), who used Fourier series to represent the continuous distribution of circulation in terms of the circulation at a finite number of span stations. Since the contribution of the image vortex distributions is a secondary effect, a direct summation of horseshoe vortices is sufficient for the calculation of the interference influence coefficients R_{nm}. To conform the interference coefficients to the free wing coefficients the horseshoe vortices are distributed with varying spans (sketch 6). One vortex is placed on the wing center line, so that when the circulation is to be calculated at N span stations from the tip to the center across one semispan,

the total number of vortices across the full span is 2N-1. The lateral limits of the horseshoes are then defined by the points

$$\bar{\eta}_m = \cos \frac{(2m-1)\pi}{4N} \tag{4.3}$$

The vortices are given the strength of the circulation at the span stations

$$\bar{\eta}_m = \cos \frac{m\pi}{2N} \tag{4.4}$$

and are located on the 1/4 chord line at these stations so that their longitudinal coordinates are

$$\bar{\xi}_m = \bar{\eta}_m \tan \Lambda \tag{4.5}$$

where Λ is the sweepback angle of the 1/4 chord line. The lateral and longitudinal coordinates of the control points on the 3/4 chord line are

$$\eta_n = \cos \frac{n\pi}{2N} \tag{4.6}$$

$$\xi_n = \eta_n \tan \Lambda + \frac{c(\eta_n)}{b} \tag{4.7}$$

where $c(\eta_n)$ is the local chord. Each influence coefficient is calculated for a symmetric pair of vortices at corresponding stations on either semi-span. Such a pair can be replaced by the difference between two wide vortices, the first spanning the outer limits and the second the inner limits of the vortices in the original pair (sketch 7). The symmetry assumed in section 3 is preserved, and following (3.4) the interference influence coefficients can be expressed as

$$R_{nm} = R_{o_{nm}} \left[1 + \frac{(\xi_n - \bar{\xi}_m)}{\sqrt{\left(\frac{R_{o_{nm}}}{R_{x_{nm}}}\right)^2 + (\xi_n - \bar{\xi}_n)^2}} \right] \tag{4.8}$$

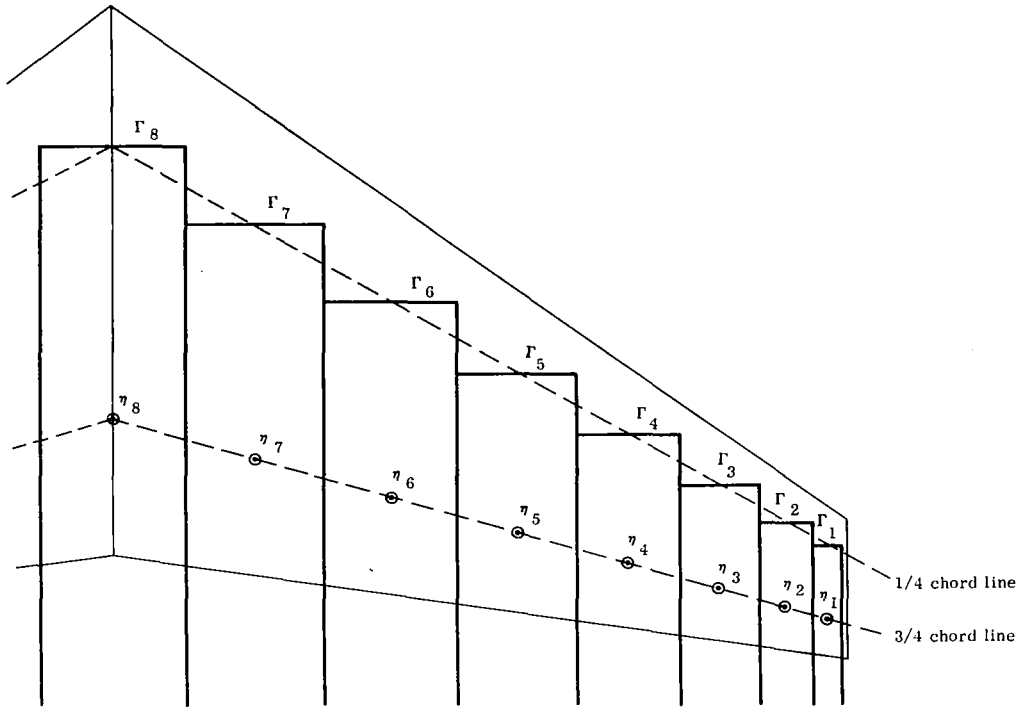

Sketch 6. Distribution of Horseshoe Vortices Γ and Control Points η

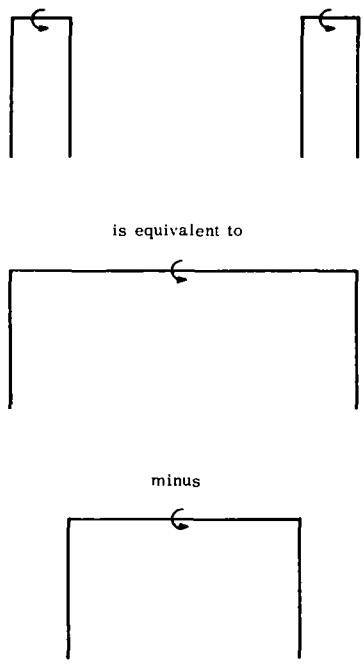

Sketch 7. Decomposition of a Pair of Horseshoe Vortices into the Difference Between Two Wide Vortices

where

$$R_{onm} = \sigma \left[f(a^{-}_{nm}) + f(a^{+}_{nm}) - f(a^{-}_{n,m+1}) - f(a^{+}_{n,m+1}) \right] \tag{4.9}$$

$$R_{x_{nm}} = \sigma^{2} \left[f_x(a^{-}_{nm}) + f_x(a^{-}_{nm}) - f_x(a^{+}_{n,m+1}) - f_x(a^{+}_{n,m+1}) \right] \tag{4.10}$$

and

$$a^{-}_{nm} = \frac{\sigma}{2} (\bar{\eta} c_m - \eta_n), \quad a^{+}_{nm} = \frac{\sigma}{2} (\bar{\eta} c_m + \eta_n) \tag{4.11}$$

5. Analysis of the effect of forward speed using lifting line theory for circular and elliptic jets

When the wing has forward speed so that there is an external flow, both the boundary conditions (2.1) and (2.2) should be satisfied at the slipstream surface. Unfortunately it turns out that these conditions cannot be jointly satisfied for a rectangular jet by the introduction of images to represent the interference effects. This is proved in Appendix B. For the purpose of analyzing the effect of forward speed on a wing in a wide slipstream, the rectangular jet is not a convenient model, because the external region, with corners introduced by the rectangular cut-out, is very difficult to treat mathematically. The use of an elliptic jet as a model results in a much more convenient shape for the external region. A lifting surface theory in an elliptic jet would require lengthy calculations. An analysis of a lifting line in circular and elliptic jets will therefore be used to gain insight into the effect of forward speed. The results of this analysis will be used to determine a correction factor which will allow the lifting surface theory of the previous sections to be extended through the speed range.

For a lifting line analysis it is only necessary to determine the downwash at the load line. Thus if a horseshoe vortex is decomposed into a two dimensional and an anti-asymmetric part as in sketch 4 of section 3, only the two dimensional part need be considered. For a circular jet it was already shown by Koning (ref. 1) that the boundary conditions for a vortex pair are satisfied throughout the speed range if the strength of the image vortices is multiplied by the factor.

$$P = \frac{1 - \mu^2}{1 + \mu^2} \tag{5.1}$$

where μ is the velocity ratio.

In order to analyze the interference potential due to trailing vortices in an elliptic jet (sketch 8), it is convenient to introduce elliptic cylinder coordinates by the

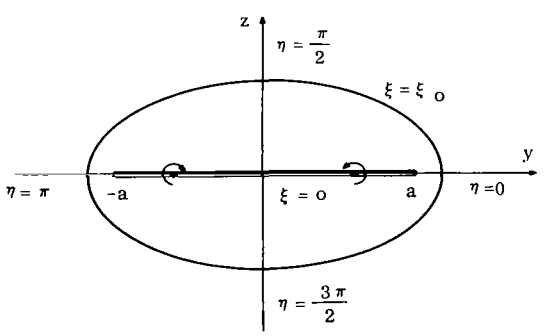

Sketch 8. Vortex Pair in Slipstream

transformation

$$y + iz = a \cosh(\xi + i\eta),$$

$$y = a \cosh\xi \cos\eta, \quad z = a \sinh\xi \sin\eta \tag{5.2}$$

The lines of constant ξ are confocal ellipses with foci at $y = \pm a$, and the lines of constant η are branches of hyperbolas. The line $\xi = 0$ is a slit between the foci, and the slipstream boundary is at $\xi = \xi_o$.

Let φ_v be the potential due to a symmetric distribution of trailing vortices in the absence of a slipstream boundary, and let the potential inside and outside the slipstream be

$$\varphi_j = \varphi_v + \Delta\varphi_j \tag{5.3}$$

$$\varphi_o = \varphi_v + \Delta\varphi_o \tag{5.4}$$

The boundary conditions (2.1) and (2.2) then require that at $\xi = \xi_o$

$$\Delta\varphi_j = \mu\Delta\varphi_o - (1-\mu)\varphi_v \tag{5.5}$$

$$\mu\frac{\partial}{\partial\xi}\Delta\varphi_j = \frac{\partial}{\partial\xi}\Delta\varphi_o + (1-\mu)\frac{\partial}{\partial\xi}\varphi_v \tag{5.6}$$

Laplace's equation remains unchanged in the elliptic coordinates as

$$\frac{\partial^2\varphi}{\partial\xi^2} + \frac{\partial^2\varphi}{\partial\eta^2} = 0$$

Let

$$\varphi = Y(\xi)\ Z(\eta)$$

Then

$$\frac{Y''}{Y} = \frac{-Z''}{Z} = n^2 \text{ say}$$

so that the basic separated solutions are

$$e^{n\xi} \cos n\eta \ , \quad e^{n\xi} \sin n\eta \ , \quad e^{-n\xi} \cos n\eta \ , \quad e^{-n\xi} \sin n\eta$$

where n must be an integer to preserve continuity between $\eta = 0$ and $\eta = 2\pi$. The only combinations of these solutions which are continuous and have continuous first deriviatives across the line $\xi = 0$ between the foci are (ref. 21, p. 536)

$$\cosh n\xi \cos n\eta \ , \quad \sinh n\xi \sin n\eta$$

Assuming that the wing is located in the center of the jet, φ_v must be symmetric about the vertical axis $\left(\eta = \frac{\pi}{2} \text{ and } \frac{3\pi}{2}\right)$, and antisymmetric about the horizontal axis ($\eta = 0$ and π). $\Delta\varphi_o$ and $\Delta\varphi_o$ must have the same symmetry. Also φ_v and $\Delta\varphi_o$ must vanish at infinity, and $\Delta\varphi_j$ must be continuous across the line $\xi = 0$. Thus they can be represented as

$$\varphi_v = \sum_{n=1,3,5\ldots}^{\infty} A_n \, e^{-n\xi} \sin n\eta \tag{5.7}$$

$$\Delta\varphi_j = \sum_{n=1,3,5\ldots}^{\infty} B_n \sinh n\xi \sin n\eta \tag{5.8}$$

$$\Delta\varphi_o = \sum_{n=1,3,5\ldots}^{\infty} C_n \, e^{-n\xi} \sin n\eta \tag{5.9}$$

The corresponding stream functions are represented by the same series with $\sin \eta$ replaced by $\cos n\eta$. The stream function for a vortex pair was determined by Tani and Sanuki. For vortices at (ξ_1, η_1) and (ξ_1, $\pi - \eta_1$), where on the centerline either $\xi_1 = 0$ or $\eta_1 = 0$, they found that

$$A_n = \frac{2}{\pi n} \cosh n\xi_1 \cos n\eta_1 \tag{5.10}$$

On substituting the series for φ_v, $\Delta\varphi$ and $\Delta\varphi_o$ in the boundary conditions (5.5) and (5.6) it follows that

$$\sum B_n \sinh n\xi_o \sin n\eta = \sum \left[\mu C_n - (1-\mu) A_n\right] e^{-n\xi_o} \sin n\eta$$

$$\sum \mu n B_n \cosh n\xi_o \sin n\eta = -\sum \left[C_n + (1-\mu) A_n\right] n e^{-n\xi_o} \sin n\eta$$

These are satisfied if

$$B_n \frac{e^{2n\xi_o}-1}{2} = \mu C_n - (1-\mu) A_n$$

$$\mu B_n \frac{e^{2n\xi_o}+1}{2} = -C_n - (1-\mu) A_n$$

whence

$$B_n = -\frac{1-\mu^2}{1+\mu^2 \coth n\xi_o} \frac{2A_n}{e^{2n\xi_o}-1}$$

$$C_n = -\frac{(1-\mu)(1-\mu \coth n\xi_o)}{1+\mu^2 \coth n\xi_o} A_n$$

The ratio of the width to the height of the slipstream is

$$\lambda = \coth \xi_o \tag{5.11}$$

and

$$e^{2\xi_o} = \frac{\lambda+1}{\lambda-1}$$

Also let $F_n(\lambda)$ be defined as

$$F_n(\lambda) = \coth n\xi_o = \frac{\left(\frac{\lambda+1}{\lambda-1}\right)^n + 1}{\left(\frac{\lambda+1}{\lambda-1}\right)^n - 1} \tag{5.12}$$

The complete solution for $\Delta\varphi_j$ and $\Delta\varphi_o$ is then given by (5.8) and (5.9) where

$$B_n = -\frac{1-\mu^2}{1+\mu^2 F_n(\lambda)} \frac{2A_n}{\left(\frac{\lambda+1}{\lambda-1}\right)^n - 1} \tag{5.13}$$

$$C_n = -\frac{(1-\mu)(1-\mu F_n(\lambda))}{1+\mu^2 F_n(\lambda)} A_n \tag{5.14}$$

The variation of the interference potential inside the slipstream with forward speed is determined by the factor $\frac{1-\mu^2}{1+\mu^2 F_n(\lambda)}$ in B_n. Since this factor varies from term to term, the dependence of the interference potential on forward speed is different at different points in space.

When the wing extends exactly between the foci of the ellipse (sketch 9), a simple closed form solution can be obtained. On the line $\xi = 0$ between the foci the downwash is

$$\frac{\partial\varphi}{\partial z} = \frac{1}{a \sin\eta} \frac{\partial\varphi}{\partial\xi}$$

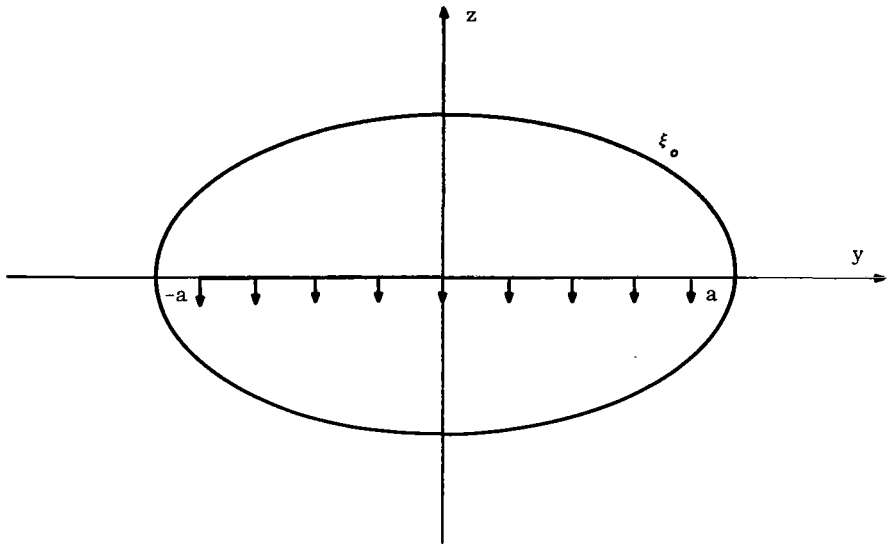

Sketch 9. Wing Spanning Foci of Slipstream

It can be seen that the first term of the series for φ_V or φ_j represents a uniform downwash between the foci. Thus for a wing with an elliptic lift distribution only this term remains, and

$$\varphi_V = A\,(\cosh\xi - \sinh\xi)\,\sin\eta \tag{5.15}$$

$$\varphi_j = A\left(\cosh\xi - \frac{\lambda + \mu^2}{1 + \lambda\mu^2}\,\sinh\xi\right)\,\sin\eta \tag{5.16}$$

The vorticity is contributed entirely by the first term, which is discontinuous across the line $\xi = 0$, and the downwash is contributed entirely by the second term. For a given lift the effect of the slipstream is simply to increase the downwash by the factor

$$\frac{\lambda + \mu^2}{1 + \lambda\mu^2}$$

The wing thus behaves as if its aspect ratio were divided by this factor. This is a generalization of a result obtained by Glauert (ref. 23) for open wind tunnels. Also the interference potential is

$$\Delta\varphi_j = A\,(\lambda - 1)\,\frac{1 - \mu^2}{1 + \lambda\mu^2}\,\sinh\xi\,\sin\eta \tag{5.17}$$

The dependence of the interference potential on forward speed is thus expressed by the factor

$$P = \frac{1 - \mu^2}{1 + \lambda\mu^2} \tag{5.18}$$

This formula differs from the formula (5.1) for a circular jet by the appearance of $\lambda\mu^2$ instead of μ^2 in the denominator.

The foregoing analysis shows that the dependence of the interference potential on forward speed is different at different points in space except in the case of a wing with an elliptic lift distribution spanning the foci of the ellipse. However, when the ratio of width to height of the ellipse is 2, the span between the foci is already a fraction $\frac{\sqrt{3}}{2} = .866$ of the slipstream width. Thus if $\lambda > 2$ and the wing extends beyond the foci it may be expected that the first term of the series for the potential is the principal term, so that a reasonable approximation would be obtained by assuming the whole interference potential to have the same dependence on forward speed at all points.

The slender body analysis of Graham et al. (ref. 6) can also quite easily be applied to a wing in an elliptic jet (ref. 24), since it only requires two dimensional potentials. The general case of a wing of intermediate aspect ratio would require evaluation of the antisymmetric part of the potential in terms of Mathieu functions, but this hardly seems worth the effort required, since the actual jet cross-section would not be elliptic.

6. Extension of lifting surface theory to allow for forward speed

The analysis of the last section indicates that the two dimensional part of the interference potential for a wing in a circular jet or a wing spanning the foci of an elliptic jet depends in the same way on forward speed everywhere in space. If this were true for the whole interference potential, it would mean that all the interference influence coefficients R_{nm} in equation (4.2) would vary with forward speed in exactly the same way. This suggests a simple procedure for extending the lifting surface theory of sections 3 and 4 to allow for the effect of forward speed. The interference influence coefficients R_{nm} will all be multiplied by a single scalar factor P, representing the strength of the interference. Thus equation (4.2) is replaced by

$$\alpha_n = (A_{nm} + P\, R_{nm})\, G_m \tag{6.1}$$

The approximation is here made of neglecting the variation at different points in space of the way in which the interference potential depends on forward speed. The exact equations for the static case are obtained by setting $P = 1$ when $\mu = 0$. Also when $\mu = 1$ the wing is in a free stream, and the exact equations are then obtained by setting $P = 0$. It remains to determine a rule for estimating P at intermediate speeds.

For a wing in a circular jet the variation with forward speed of the two dimensional part of the potential is given by (5.1). It will be assumed that any difference in the way in which the antisymmetric part of the potential varies with forward speed is not important, so that the same factor can be applied to the whole potential. Thus (5.1) will be used to determine the strength factor P in (6.1).

The case of a wing in a rectangular jet is more difficult. It can be expected that the interference potential due to a wide rectangular jet will vary with forward speed in much the same way as the interference potential due to a wide elliptic jet. For a wing spanning the foci of the elliptic the effect of forward speed is given by (5.18). If the wing does not exactly span the foci there would be additional terms in the series (5.8) for the interference potential, each of which would vary in a different way with forward speed. It will be assumed, however, that the first term is the most important term, and that it is also representative of the behaviour of a rectangular jet. Therefore, introducing the jet aspect ratio AR_j instead of λ as a measure of the jet width, the strength factor for a rectangular jet will be taken to be

$$P = \frac{1 - \mu^2}{1 + AR_j\, \mu^2} \tag{6.2}$$

For a square jet this gives the same effect of forward speed as for a circular jet.

Once the strength factor P has been determined the remainder of the calculations are performed exactly as in section 4.

7. Aerodynamic coefficients

If the slipstream velocity V_j is used as the reference velocity, the aerodynamic coefficients can be determined from the circulation exactly as in the theory for a free wing (ref. 20). The local lift coefficient is

$$2\frac{b}{c}\,G_n \tag{7.1}$$

where c is the chord. Using a trigonometric quadrature formula, the lift coefficient for the complete wing is found to be

$$CL = \frac{\pi AR}{2N}\left[G_N + 2\sum_{n=1}^{N-1} G_n \sin \eta_n\right] \tag{7.2}$$

where AR is the aspect ratio. The contribution of each span station to the induced drag is found by rotating the local lift vector back through the local induced downwash angle at the load line. This angle can be determined from the influence coefficients $A_{o_{nm}}$ and $R_{o_{nm}}$ for the downwash at the load line as

$$\alpha_{o_n} = \sum_{n=1}^{N} (A_{o_{nm}} + R_{o_{nm}})\, G_m \tag{7.3}$$

Then assuming that the downwash angle is small the coefficient of induced drag can be evaluated as

$$CD = \frac{\pi AR}{2N}\left[G_N \alpha_{o_N} + 2\sum_{n=1}^{N-1} G_n\, \alpha_{o_n} \sin \eta_n\right] \tag{7.4}$$

The effectiveness of the wing in converting the propeller thrust into lift can be measured by the ratio of lift to thrust. Suppose that the jet is generated by an actuator which causes the flow velocity in the jet to increase from the free stream velocity V_o to a final velocity V_j, once the pressure is equalized inside and outside. Then the thrust can be determined from the increase in the momentum multiplied by the mass flow, that is

$$T = \rho S_j V_j (V_j - V_o) \tag{7.5}$$

where ρ is the density and S_j the jet area. The lift slope is

$$L_\alpha = \frac{1}{2} \rho \quad S V_j^2 CL_\alpha \tag{7.6}$$

where S is the wing area and CL_α is the slope of the lift coefficient. Also

$$S = \frac{b^2}{AR}$$

and for a rectangular jet

$$S_j = HB = \frac{B^2}{AR_j} = \frac{b^2}{\sigma^2 AR_j}$$

where AR_j is the jet aspect ratio defined by (3.6) and σ is the span ratio defined by (3.5). Thus

$$\frac{L_\alpha}{T} = \frac{\sigma^2}{2(1-\mu)} \frac{AR_j}{AR} CL_\alpha \tag{7.7}$$

For a circular jet the same formula holds if the jet aspect ratio is defined as the jet width divided by its mean height, or

$$AR_j = \frac{B^2}{S_j} = \frac{4}{\pi} \tag{7.8}$$

8. Properties of a wing vertically off center in the jet

The determination of the effect of shifting the wing vertically in the jet can be carried out in detail using formulas (3.7) - (3.11). At certain heights, however, it is possible to use symmetry to obtain the interference influence coefficients in terms of the coefficients for a wing centered in the jet without any extra calculations.

When the wing is at a height $z = \pm \frac{H}{2}$, so that it coincides with the edge of the jet, the images in adjacent zones move vertically to coincide at alternate boundaries (sketch 10). It follows that

$$R_{nm}\left(AR_j,\ z = \frac{H}{2}\right) = 2R_{nm}\left(\frac{AR_j}{2},\ z = 0\right) + A_{nm}$$

where the term A_{nm} represents the image coinciding with the wing. In the static case when the strength factor $P = 1$ the total influence coefficient is then

$$A_{nm} + R_{nm}\left(AR_j,\ z = \frac{H}{2}\right) = 2\left\{A_{nm} + R_{nm}\left(\frac{AR_j}{2},\ z = 0\right)\right\}$$

whence the solution of (5.2) yields

$$CL_\alpha\left(AR_j,\ z = \frac{H}{2}\right) = \frac{1}{2}CL_\alpha\left(\frac{AR_j}{2},\ z = 0\right)$$

$$\frac{CD}{CL^2}\left(AR_j,\ z = \frac{H}{2}\right) = 2\frac{CD}{CL^2}\left(\frac{AR_j}{2},\ z = 0\right)$$

Symmetry is also obtained when the wing is at a height $z = \pm \frac{H}{4}$. Then the image system can be resolved as in sketch 11 into the sum of three patterns which are symmetric about the wing and one which is antisymmetric. The antisymmetric pattern produces no downwash at the plane of the wing. Thus

$$R_{nm}\left(AR_j,\ z = \frac{H}{4}\right) = \frac{1}{2}R_{nm}(2AR_j,\ z = 0) - \frac{1}{2}R_{nm}(AR_j,\ z = 0) + R_{nm}\left(\frac{AR_j}{2},\ z = 0\right)$$

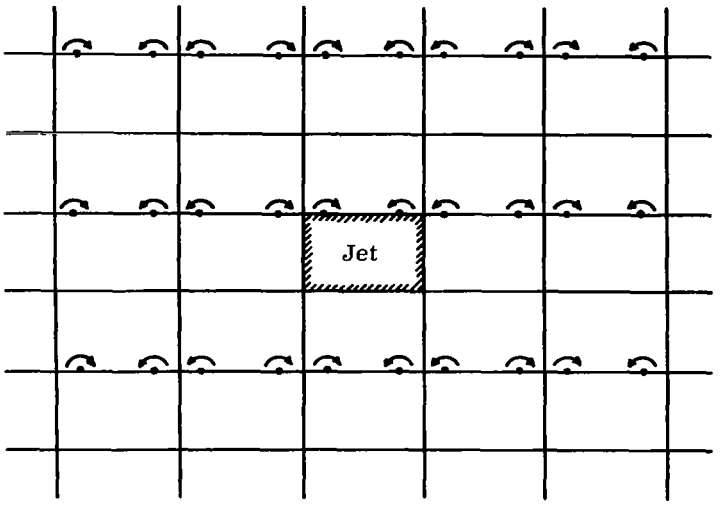

Sketch 10. Images for a Horseshoe Vortex at the Edge of a Rectangular Jet

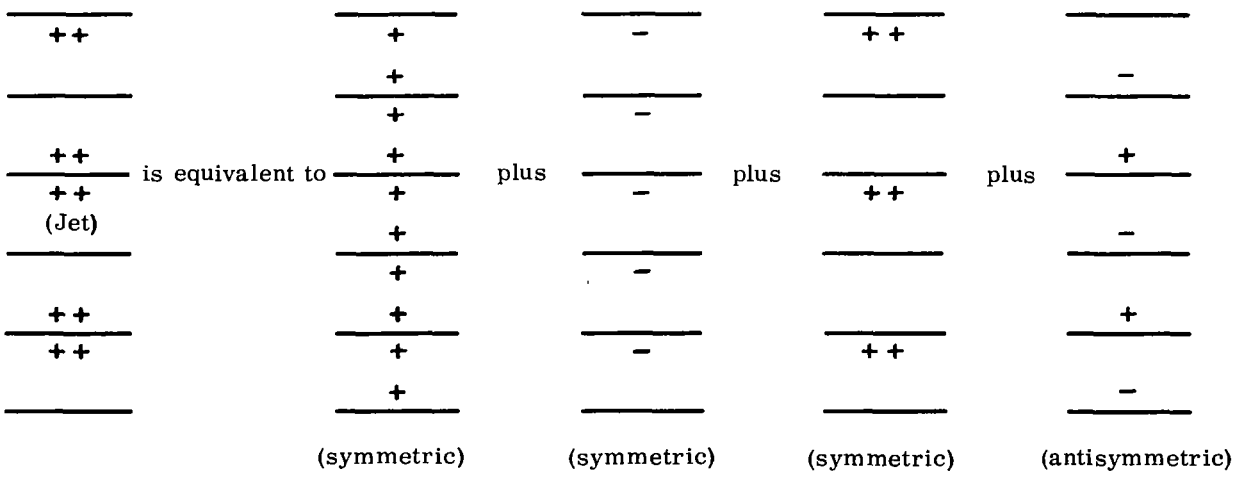

Sketch 11. Decomposition of the Image Pattern for a Horseshoe Vortex Midway Between the Edge and the Center of a Rectangular Jet

and the loading and aerodynamic coefficients can be determined by substituting these values in (6.1).

With the wing characteristics known at $z = 0$, $\frac{H}{4}$ and $\frac{H}{2}$, the characteristics at other vertical positions can be estimated by using a power series. Let N represent G, CL_α or $\frac{CD}{CL^2}$. Since the characteristics are the same for equal displacements up or down use an even series

$$N(z) = N(0) + t_1 z^2 + t_2 z^4$$

Then solving for t_1 and t_2 yields

$$N(z) = N(0) + \left\{5\,N(0) - \frac{16}{3} N\left(\frac{H}{4}\right) + \frac{1}{3} N\left(\frac{H}{2}\right)\right\} z^2$$

$$+ \left\{4\,N(0) - \frac{16}{3} N\left(\frac{H}{4}\right) + \frac{4}{3} N\left(\frac{H}{2}\right)\right\} z^4$$

9. Typical results

The methods of the previous sections have been incorporated in a computer program for the calculation of the lift of a wing in a rectangular slipstream. This program incorporates the method of deYoung and Harper (ref. 20) for the calculation of the influence coefficients A_{nm} for a wing in a free stream defined in section 4. The program permits the user to specify the number of vortices to be used to represent the wing. Calculations to determine typical trends have been made using 8 vortices per semi-span. The results of some of these calculations and of some additional hand calculations are presented in fig. 1-4.

Figure 1 shows the effect of jet width on the characteristics of rectangular wings at velocity ratios of 0, .6 and 1.0. Figure 2 shows operational curves of the behaviour of some typical wings through out the speed range. All coefficients are referred to the slipstream velocity. With this convention the lift coefficient decreases as the external velocity is decreased because of the reduced mass flow influenced by the wing. When the aircraft is static the jet deflection angle θ equals the ratio of lift to thrust. Figure 3 shows the static turning effectiveness $\theta/\alpha = L_\alpha/T$. For a given jet aspect ratio the turning effectiveness increases towards a limiting value as the wing chord is increased or its aspect ratio reduced. The turning effectiveness is also increased by an increase in the aspect ratio of the jet or reduction of its height: it is easier to deflect an airflow which is close to the wing.

Sketch 12 illustrates the influence which these trends could have on a design. When the aircraft is static the absence of an external flow prevents parts of the wing outside a jet from influencing conditions in the jet, and if there are several jets they do not interact, so that the total lift is simply the sum of the independent contributions from each jet. The performance of a wing in a large square jet is compared with its performance in four small jets and in a single wide jet of aspect ratio 4. The wing has a constant chord equal to the height of the small jets or the wide shallow jet. In the large square jet $L_\alpha/T = .365$. In the four small jets it is .480 because of the increase in the ratio of wing chord to jet height, and in the wide jet it is further increased to .835 by the elimination of the gaps. The return to atmospheric pressure in each gap causes a loss of circulation which extends into the jets. It is evident that if several propellers are used it is beneficial to place them close enough to each other to ensure that their slipstreams merge. Also a larger fraction of the thrust is converted into lift when a single large propeller is replaced by a row of small propellers arranged to give a shallow jet of the same width. This would compensate for the reduction in thrust from a given input of power, attendant upon the increase in disc loading. The power absorbed by an ideal actuator of area S_p is proportional to V_j^3 and its thrust to $S_p V_j^2$, so that if the power were fixed in the case illustrated, the thrust of the wide actuator would be

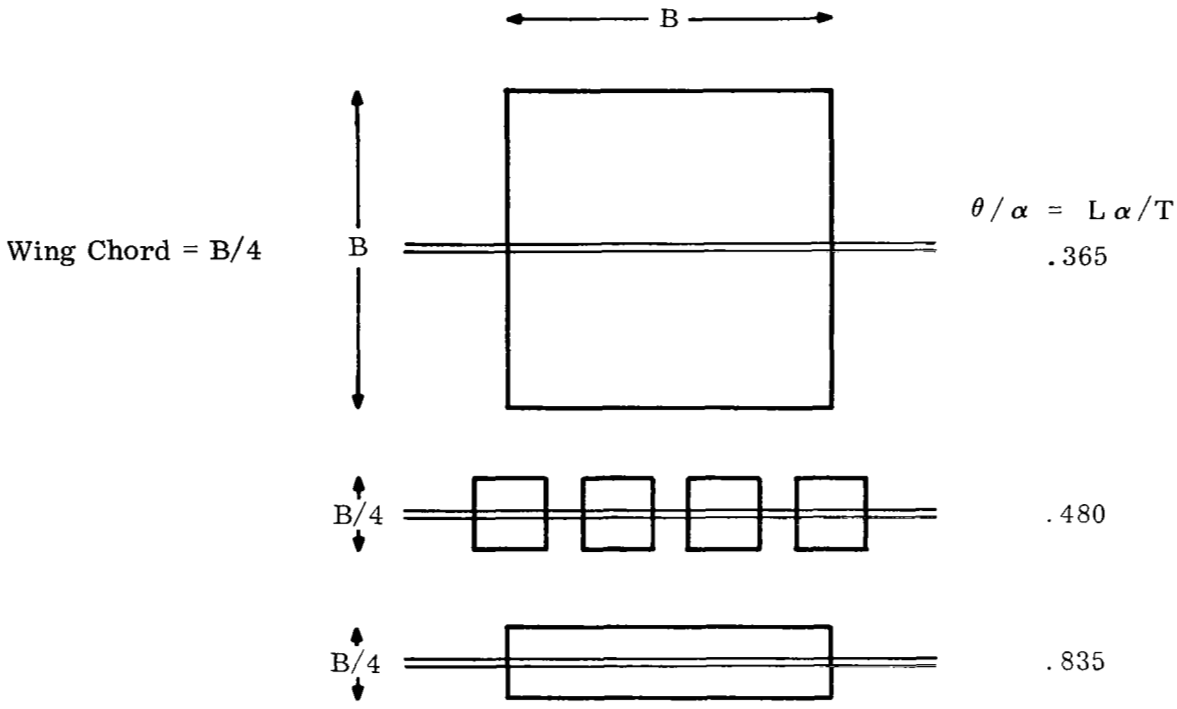

Sketch 12. Effect of the Disposition of Jets on the Static Turning Effectiveness of a Rectangular Wing

$(1/4)^{1/3}$ = .630 of the thrust of the square actuator. At a given angle of attack the lift of the wing in the wide jet would then be .630 x .835/.365 = 1.44 times its lift in the square jet. It thus appears that the propellers of a deflected slipstream STOL aircraft might well be optimized for the cruise without penalizing its low speed performance.

Finally figure 4 illustrates the effect of the vertical position of the wing in the jet for the case of a static low aspect ratio wing. The lift is maximized and the drag minimized when the wing is centered in the jet. It should be remembered that the effects of momuniform axial velocity and rotation in the slipstream have been ignored in these calculations. In practice there may be advantages in locating the wing off the vertical center of the jet.

REFERENCES

1. Koning, C.: Influence of the Propeller on Other Parts of the Airplane Structure. Vol. IV of Aerodynamic Theory, W. F. Durand, ed., Julius Springer (Berlin), 1935, pp. 361-430.

2. Franke, A. and Weinig F.: The Effect of the Slipstream on an Airplane Wing. NACA TM920, 1939.

3. Smelt, R. and Davies, H.: Estimation of Increase in Lift Due to Slipstreams. R. and M. No. 1788, British A.R.C., 1937.

4. Squire, H.B. and Chester, W.: Calculation of the Effect of Slipstream on Lift and Induced Drag. R. and M. No. 2368, British A.R.C., 1950.

5. Ferrari, C.: Propeller and Wing Interaction at Subsonic Speeds. Aerodynamic Components of Aircraft at High Speeds, A. F. Donovan and H. R. Lawrence, ed., High Speed Aerodynamics and Jet Propulsion, Vol. 7, Princeton University Press, pp. 364-416.

6. Graham, E.W., Lagerstrom, P.A., Licher, R.M., and Beane, B.J.: A Preliminary Theoretical Investigation of the Effects of Propeller Slipstream on Wing Lift. Douglas Rep. SM 14991, 1953.

7. Goland, L., Miller, N., and Butler, L.: Effect of Propeller Slipstream on V/STOL Aircraft Performance and Stability, Dynasciences Rep. DCR 137, 1964.

8. Butler, L., Goland, L, and Huang, Kuo P.: An Investigation of Propeller Slipstream Effects on V/STOL Aircraft Performance and Stability. Dynasciences Rep. DCR 174, 1966.

9. George, M., and Kisielowski, E.: Investigation of Propeller Slipstream Effects on Wing Performance. Dynasciences Rep. DCR 234, 1967.

10. Rethorst, S.: Aerodynamics of Nonuniform Flows as Related to an Airfoil Extending Through a Circular Jet. J. Aero. Sc., vol. 25, no. 1, Jan. 1958, pp. 11-28.

11. Rethorst, S., Royce, W.W., and Wu, T. Yao-tsu: Lift Characteristics of Wings Extending through Propeller Slipstreams. Vehicle Research Corp. Rep. 1, 1958.

12. Wu, T. Yao-tsu, and Talmadge, Richard B.: A Lifting Surface Theory for Wings Extending Through Multiple Jets. Vehicle Research Corp. Rep. 8, 1961.

13. Cumberbatch, E.: A Lifting Surface Theory for Wings at High Angles of Attack Extending Through Multiple Jets. Vehicle Research Corp. Rep. 9, 1963.

14. Wu, T. Yao-tsu: A Lifting Surface Theory for Wings at High Angles of Attack Extending Through Inclined Jets. Vehicle Research Corp. Rep. 9a, 1963.

15. Cumberbatch, E., and Wu, T. Yao-tsu: A Lifting Surface Theory for Wings Extending Through Multiple Jets in Separated Flow Conditions. Vehicle Research Corp. Rep. 10, 1963.

16. Ribner, H. S.: Theory of Wings in Slipstreams. U.T.I.A. Rep. 60, 1959.

17. Ribner, H. S. and Ellis, N. D.: Theory and Computer Study of Wing in a Slipstream. Preprint 66-466, AIAA, 1966.

18. Sowydra, A.: Aerodynamics of Deflected Slipstreams, Part I, Formulation of the Integral Equations. Cornell Aero. Lab. Rep. AI-1190-A-6, 1961.

19. Theodorsen, Theodore: Interference on an Airfoil of Finite Span in an Open Rectangular Wind Tunnel. NACA TR 461, 1933.

20. DeYoung, John, and Harper, Charles W.: Theoretical Symmetric Span Loading at Subsonic Speeds for Wings Having Arbitrary Planform. NACA TR 921, 1948.

21. Jeffreys, H. and Jeffreys, B. S.: Methods of Mathematical Physics, Cambridge University Press, 1956.

22. Tani, Itiro and Sanuki, Matao: The Wall Interference of a Wind Tunnel of Elliptic Cross Section, NACA TM 1075, 1944.

23. Glauert, H.: Some General Theorems Concerning Wind Tunnel Interference on Aerofoils. R. and M. no. 1470, British A.R.C., 1932.

24. Jameson, Antony: Preliminary Investigation of the Lift of a Wing in an Elliptic Slipstream. Grumman Aero. Rep. 393-68-2, 1968.

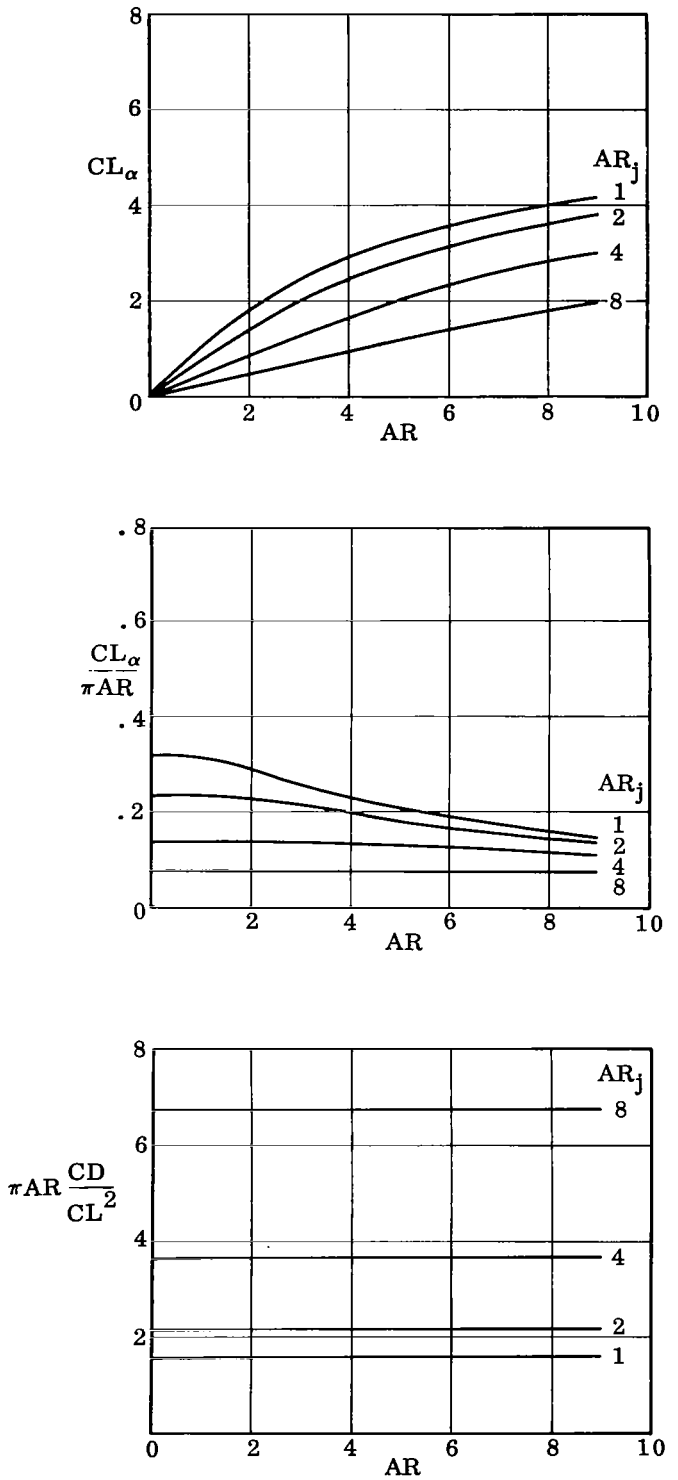

Figure 1(a). Rectangular Wings Spanning Rectangular Jets
Static Case: $\mu = 0$

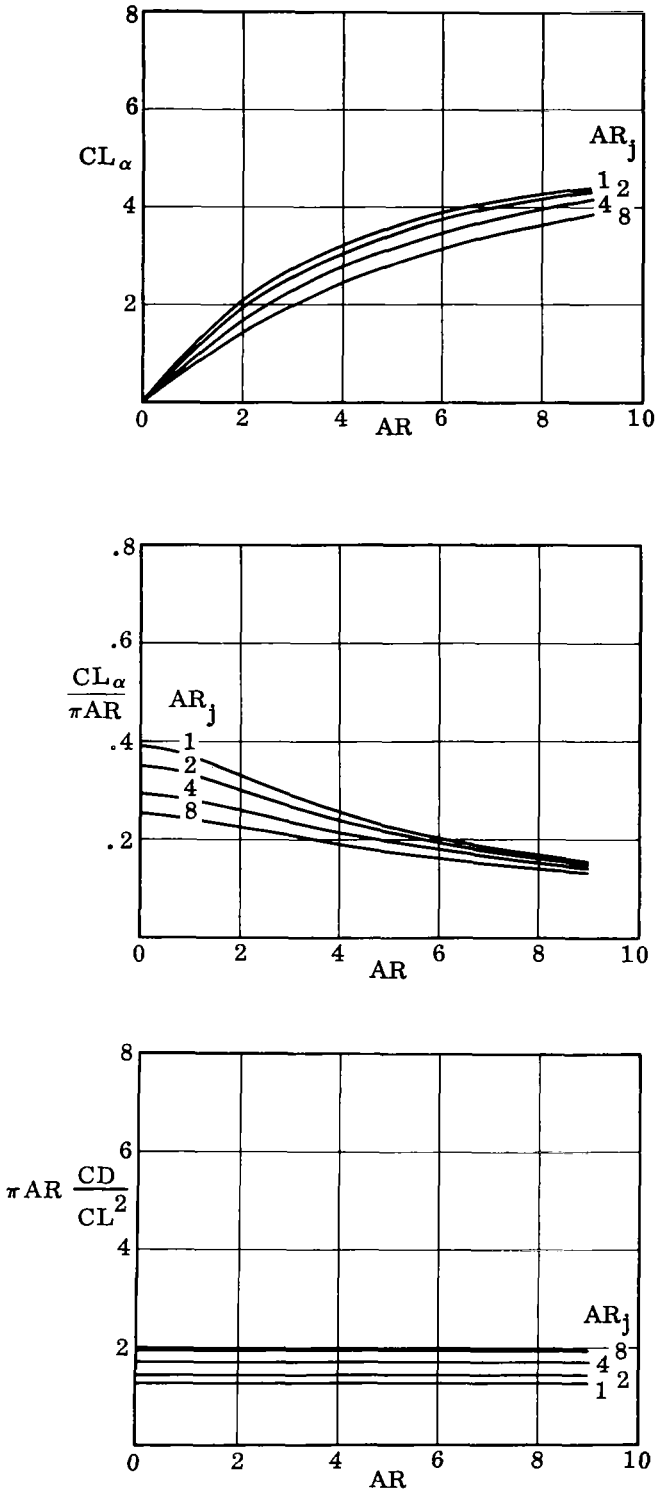

Figure 1(b). Rectangular Wings Spanning Rectangular Jets
$\mu = .6$

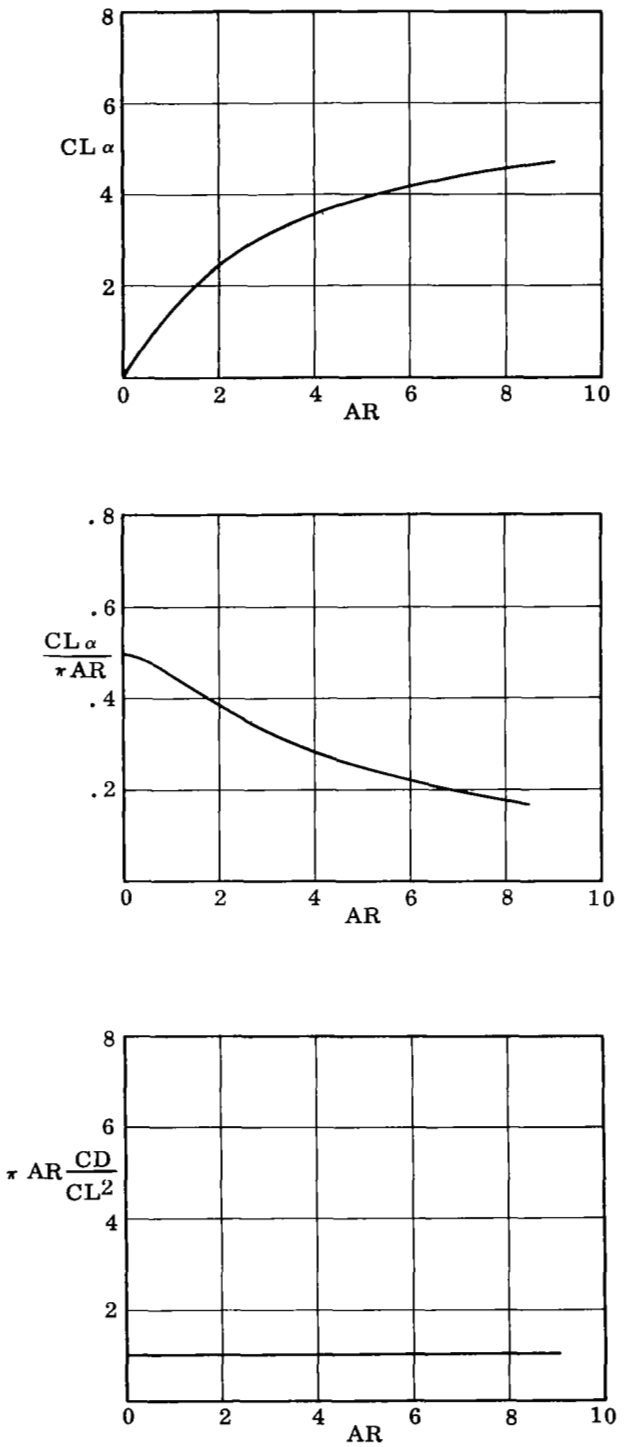

Figure 1(c). Rectangular Wings In a Free Stream
$\mu = 1$

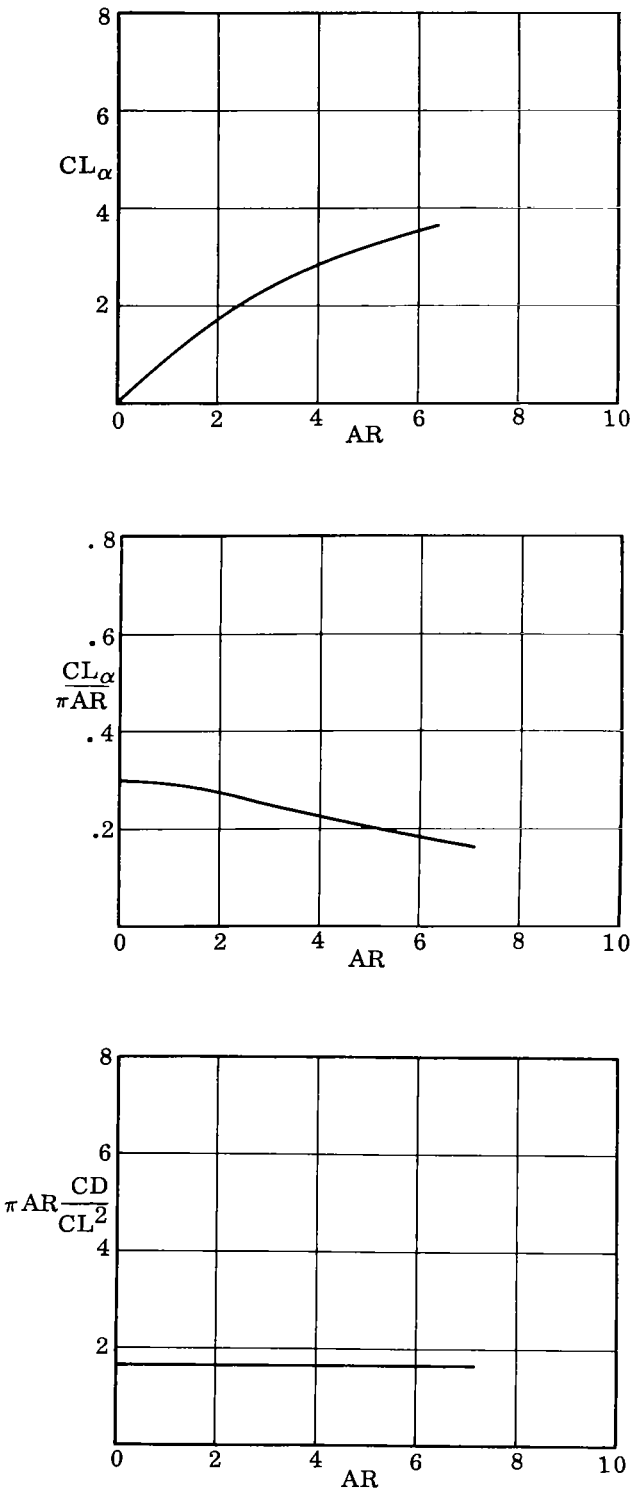

Figure 1(d). Rectangular Wings Spanning Circular Jets
Static Case: $\mu = 0$

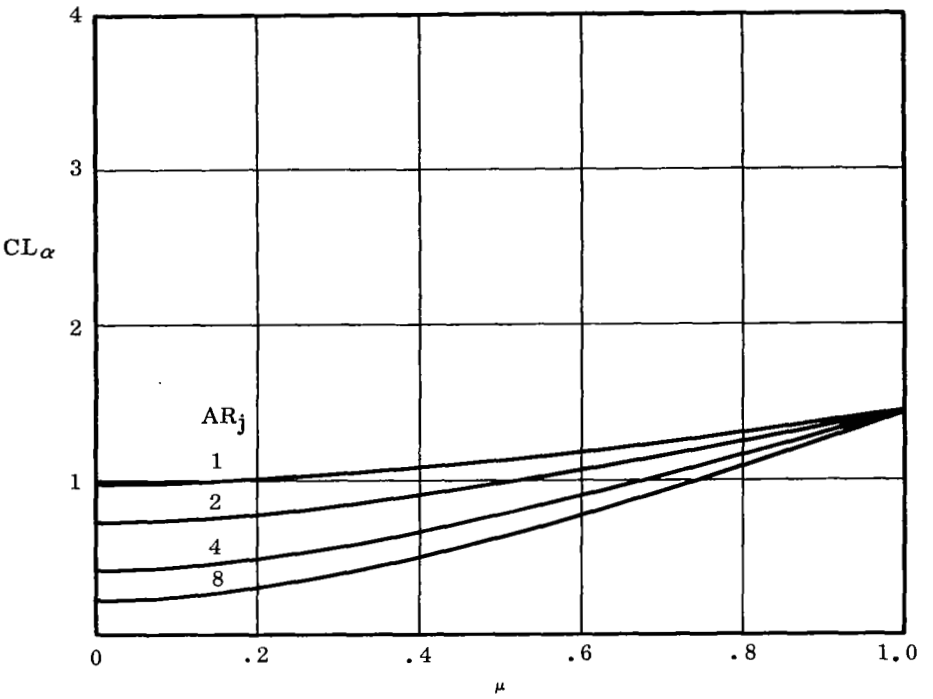

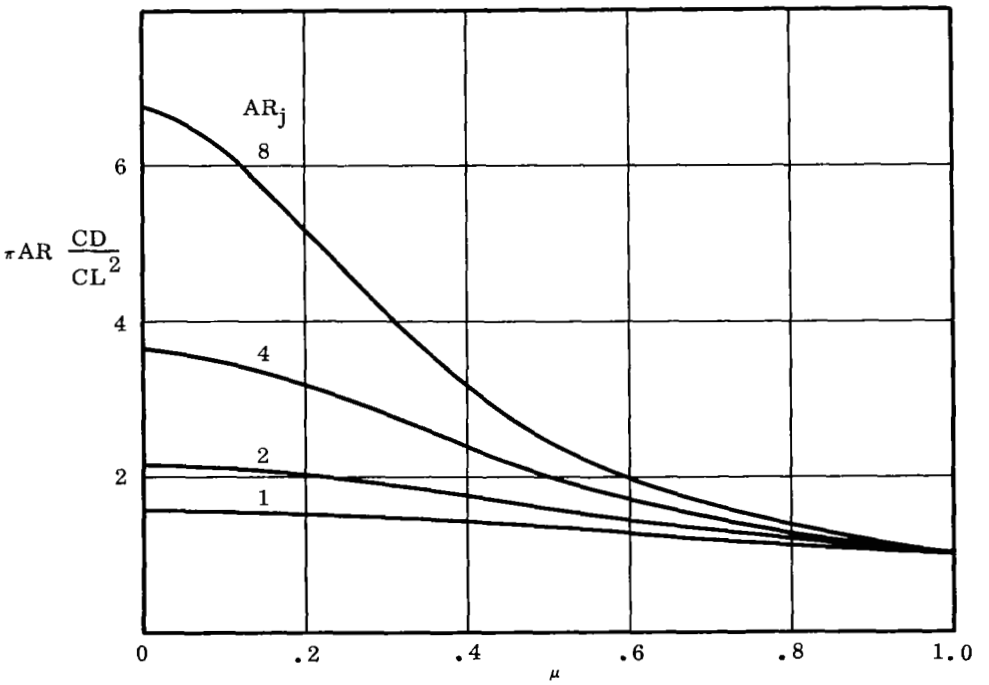

Figure 2(a). Operational Curves for a Rectangular Wing
AR = 1

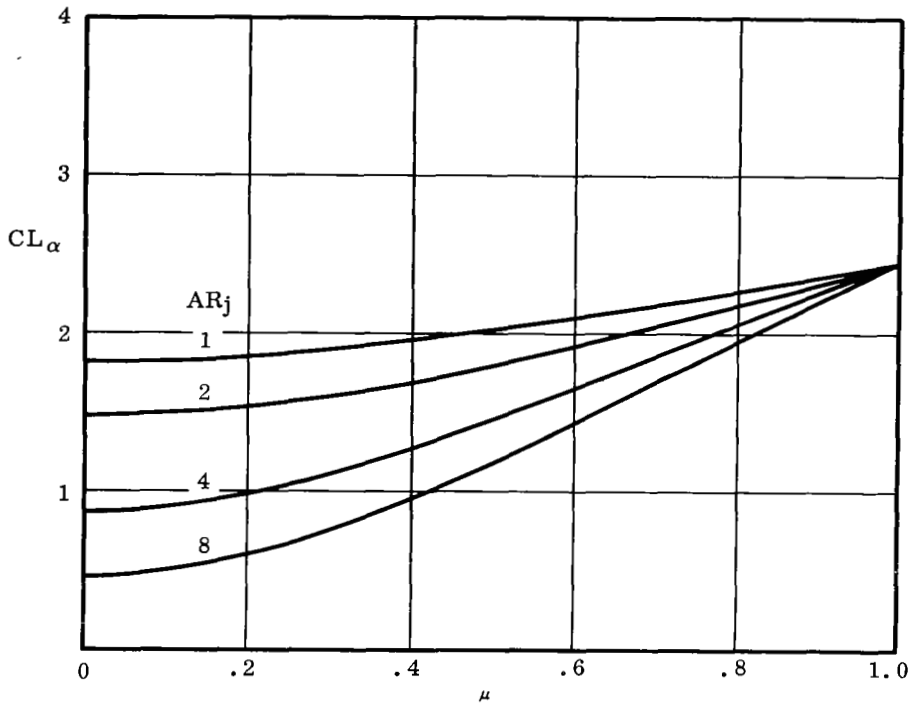

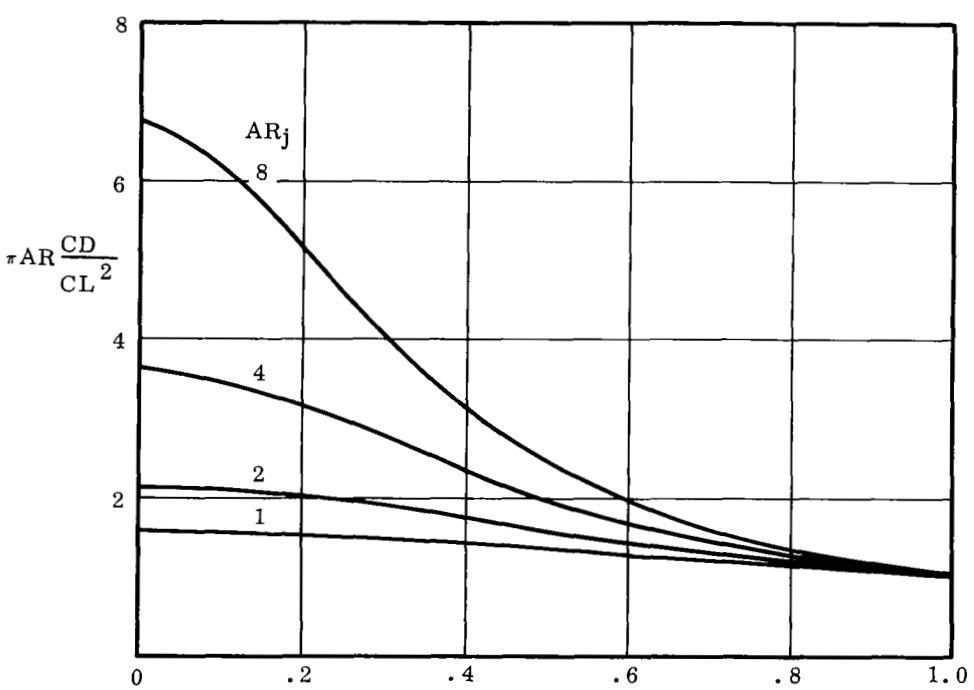

Figure 2(b). Operational Curves for a Rectangular Wing
AR = 2

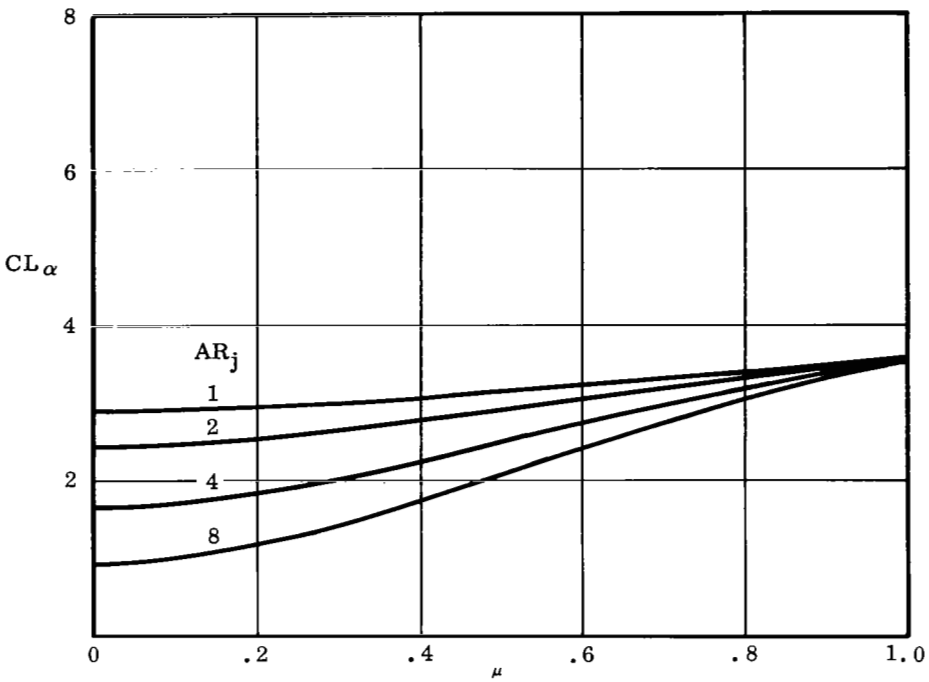

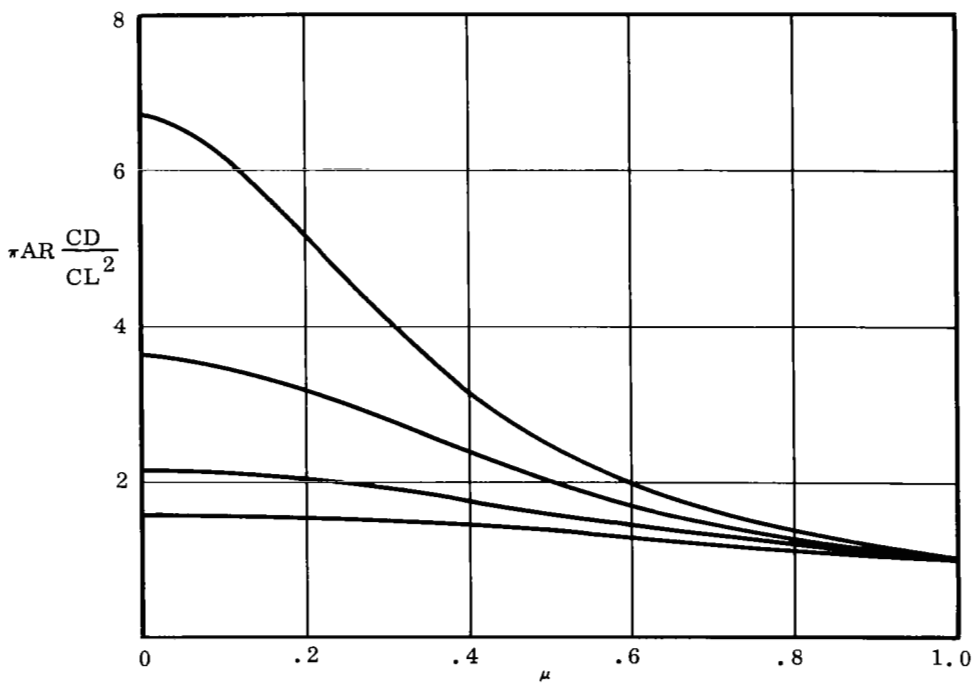

Figure 2(c). Operational Curves for a Rectangular Wing
AR = 4

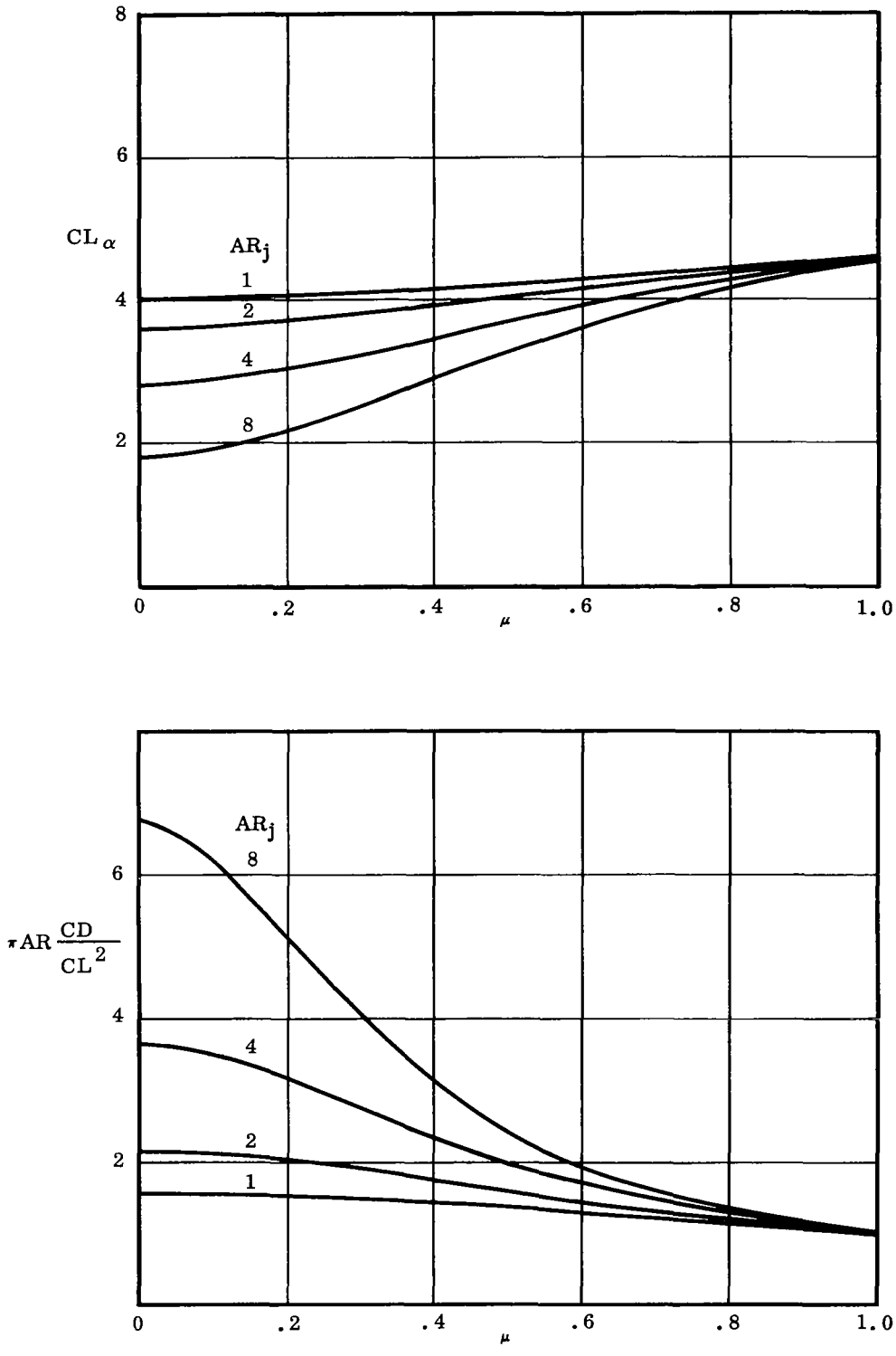

Figure 2(d). Operational Curves for a Rectangular Wing
AR = 8

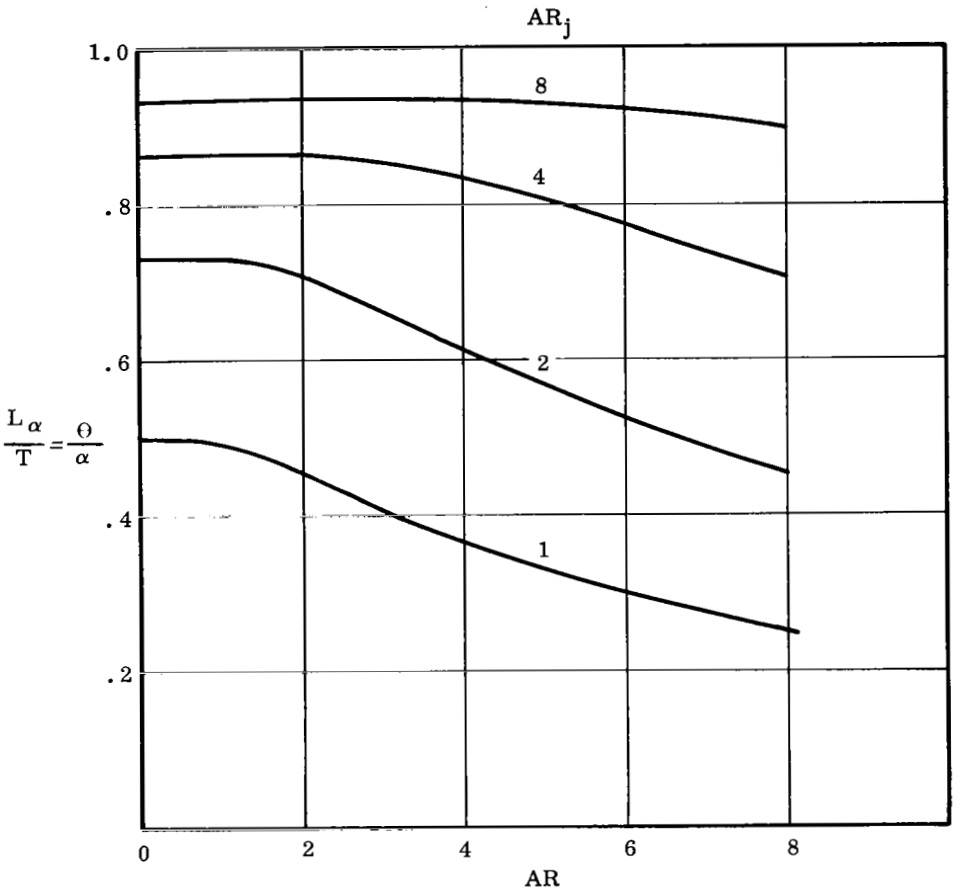

Figure 3. Turning Effectiveness of Rectangular Wings in a Static Jet
$\mu = 0$

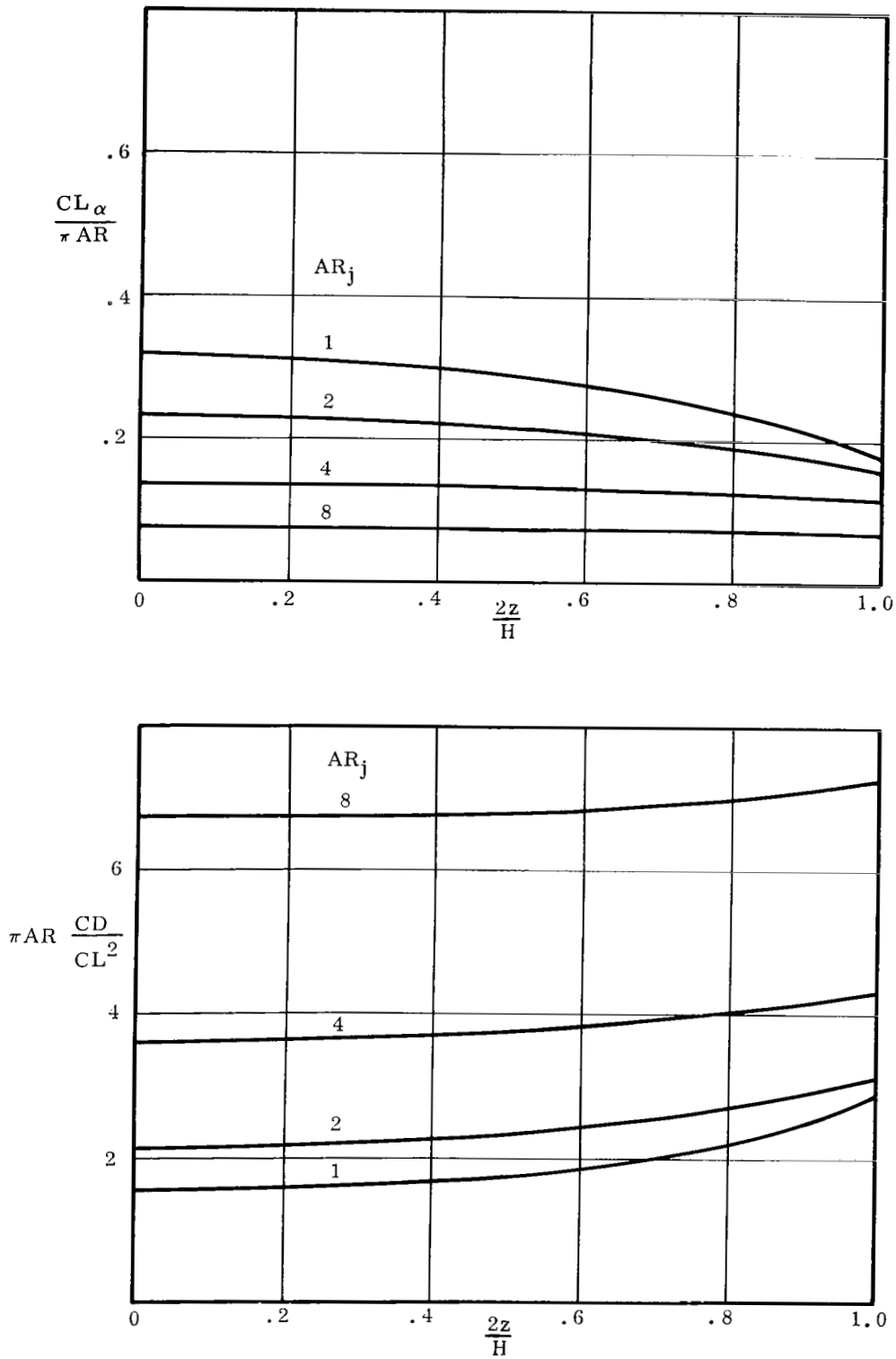

Figure 4. Effect of Vertical Position of the Wing in the Jet
Slender Wing: AR ≡ 0

Appendix A Summation of Contributions of Image Vortices

The evaluation of the interference downwash for a single horseshoe vortex requires the summation of the double series in equations (3.8) and (3.11) for f(a) and $f_x(a)$. Unfortunately these do not converge very rapidly. However, they may be simplified when the wing is vertically centered in the jet. Since it is only necessary to evaluate the downwash in the plane of the wing, then both $\bar{\zeta}$ and ζ can be set equal to zero. Also known analytic results can be used for much of the summation.

When $\bar{\zeta} = \zeta = 0$ (3.8) becomes

$$4\pi f(a) = 2a \sum_{n=1}^{\infty} \frac{1}{n^2 + \frac{n^2}{AR_j^2}} + 2a \sum_{m=1}^{\infty} \frac{-(-1)^m}{m^2 - a^2} - 2 \sum_{m=1}^{\infty} \sum_{n=1}^{\infty}$$

$$-(-1)^m \left[\frac{m+a}{(m+a)^2 + \frac{n^2}{AR_j^2}} - \frac{m-a}{(m-a)^2 + \frac{n^2}{AR_j^2}} \right] \tag{A1}$$

Now the following summations are known results (ref. A1, p. 264)

$$\sum_{n=1}^{\infty} \frac{1}{n^2 + a^2} = \frac{1}{2a^2} (\pi a \coth \pi a - 1) \tag{A2}$$

$$\sum_{n=1}^{\infty} \frac{-(-1)^n}{n^2 - a^2} = \frac{1}{2a^2} (\pi a \csc \pi a - 1) \tag{A3}$$

Using these (A1) becomes

$$f(a) = \frac{-1}{4\pi a} + \frac{AR_j}{4} \coth \pi AR_j a + \frac{AR_j}{4} \sum_{m=1}^{\infty}$$

$$-(-1)^m \left[\coth \pi AR_j (m-a) - \coth \pi AR_j (m+a) \right] \tag{A4}$$

This single series converges rapidly when a is small. When a approaches 1 a relation between f (1-a) and f (a) can be used. (A4) can be expanded as

$$f(a) = \frac{-1}{4\pi a} + \frac{AR_j}{4} \coth \pi AR_j a + \frac{AR_j}{4} \coth \pi AR_j(1-a)$$

$$- \frac{AR_j}{4} \coth \pi AR_j(1+a) - \frac{AR_j}{4} \coth \pi AR_j(2-a)$$

$$+ \frac{AR_j}{4} \coth \pi AR_j(2+a) + \ldots\ldots \tag{A5}$$

Then substituting (1-a) for a in (A5)

$$f(1-a) = \frac{-1}{4\pi(1-a)} + \frac{AR_j}{4} \coth \pi AR_j(1-a) + \frac{AR_j}{4} \coth \pi AR_j a$$

$$- \frac{AR_j}{4} \coth \pi AR_j(2-a) - \frac{AR_j}{4} \coth \pi AR_j(1+a)$$

$$+ \frac{AR_j}{4} \coth \pi AR_j(3-a) + \ldots\ldots \tag{A6}$$

Subtracting (A6) from (A5) gives the relation

$$f(a) = f(1-a) + \frac{1}{4\pi} \left(\frac{1}{1-a} - \frac{1}{a}\right) \tag{A7}$$

Since the series (A4) converges very rapidly in the desirable range of $1/2 \leq AR_j < \infty$, it can be truncated after a few terms. Expanding the coth terms the following formulas are finally obtained for computing f(a):

for $\infty > AR_j \geq 1/2$: and $a \leq 1/2$

$$f(a) = -\frac{1}{4\pi a} + \frac{AR_j}{4}\coth \pi AR_j a + \frac{AR_j}{4}\coth \pi AR_j(1-a) - \frac{AR_j}{4}\coth \pi AR_j(1+a)$$

$$- AR_j \left(\frac{1}{e^{4\pi AR_j} + e^{2\pi AR_j}} + \frac{2}{e^{8\pi AR_j}} + \frac{1}{e^{12\pi AR_j}} \right) \sinh 2\pi AR_j a$$

$$- 4AR_j \left(\frac{1}{e^{8\pi AR_j}} + \frac{3}{e^{12\pi AR_j}} + \frac{11}{e^{16\pi AR_j}} \right) \sinh 2\pi AR_j a \sinh^2 \pi AR_j a \qquad \text{(A8a)}$$

when $a \to 0$

$$f(a) = \pi AR_j^2 \left(\frac{1}{12} + \frac{1}{2}\operatorname{csch}^2 \pi AR_j - \frac{2}{e^{4\pi AR_j} + e^{2\pi AR_j}} - \frac{4}{e^{8\pi AR_j}} - \frac{2}{e^{12\pi AR_j}} \right) a \qquad \text{(A8b)}$$

when $AR_j = 0$:

$$f(a) = \frac{1}{4}\left(\csc \pi a - \frac{1}{\pi a}\right) \qquad \text{(A8c)}$$

when $AR_j = 0$ and $a \rightarrow 0$

$$f(a) = \frac{\pi}{24} a \tag{A8d}$$

also

$$f(-a) = -f(a)$$

and when $> 1/2$ use (A7)

Similar methods can be employed in the evaluation of $f_x(a)$. When $\bar{\zeta} = \zeta = 0$ (3.11) becomes

$$f_x(a) = \frac{1}{8\pi} \sum_{m=-\infty}^{\infty} - (-1)^m \sum_{m=-\infty}^{\infty} \left(\frac{m+a}{\left(\frac{n}{AR_j}\right)^2 \left\{ (m+a)^2 + \left(\frac{n}{AR_j}\right)^2 \right\}^{1/2}} + \frac{m+a}{\left\{ (m+a)^2 + \left(\frac{n}{AR_j}\right)^2 \right\}^{3/2}} \right) \tag{A9}$$

The following known results may be used (ref. A1, p. 267 and p. 811)

$$\sum_{m=1}^{\infty} \frac{-(-1)^m}{(m \pm a)^2} = \frac{1}{4} \psi'\left(\frac{1}{2} \pm \frac{a}{2}\right) - \frac{1}{4} \psi'\left(1 \pm \frac{a}{2}\right) \tag{A10}$$

$$\sum_{m=1}^{\infty} \frac{-(-1)^m}{m^k} = (1-2^{1-k})\, \zeta(k) \tag{A11}$$

where ψ' is a trigamma function and ζ is a Riemann Zeta function. Then (A9) may be written as

$$f_x(a) = \frac{1}{16\pi}\left[\frac{1}{a^2} - \pi^2 \csc \pi a \cot \pi a + \psi'\left(1+\frac{a}{2}\right) - 2\,\psi'(1+a)\right]$$

$$+ \frac{AR_j^{\,2}}{4\pi} \sum_{n=1}^{\infty}\left[\frac{AR_j a}{n^2\left[n^2 + (AR_j a)^2\right]^{1/2}} + \frac{AR_j a}{\left[n^2 + (AR_j a)^2\right]^{3/2}}\right]$$

$$- \frac{AR_j^{\,2}}{4\pi} \sum_{m=1}^{\infty} -(-1)^m \left\{ \sum_{n=1}^{\infty}\left[\frac{AR_j\,(m+a)}{n^2\left[n^2 + AR_j^{\,2}(m+a)^2\right]^{1/2}} + \frac{AR_j\,(m+a)}{\left[n^2 + AR_j^{\,2}(m+a)^2\right]^{3/2}}\right]\right.$$

$$\left. -\left[\frac{AR_j\,(m-a)}{n^2\left[n^2+AR_j^{\,2}(m-a)^2\right]^{1/2}} + \frac{AR_j\,(m-a)}{\left[n^2 + AR_j^{\,2}(m-a)^2\right]^{3/2}}\right]\right\} \tag{A12}$$

A relation similar to (A7) can be found between $f_x(a)$ and $f_x(1-a)$

$$f_x(a) = f_x(1-a) + \frac{1}{16\pi}\left[\frac{1}{(1-a)^2} - \frac{1}{a^2}\right] \tag{A13}$$

and this may be used as before to limit the range to $a < 1/2$. The same series in n appears in three places in (A12). It has been found that the summation

$$\sum_{n=1}^{\infty}\left[\frac{1}{n^2(n^2+e^2)^{1/2}} + \frac{1}{(n^2+e^2)^{3/2}}\right]$$

$$= \frac{\pi^2}{6}\left[\frac{1}{(1.7058+e^2)^{1/2}} + \frac{.6995}{(1.0034+e^2)^{3/2}}\right] \tag{A14}$$

is accurate to four figures. Incorporating this in (A12) the formulas for computing $f_x(a)$ are finally reduced to:

$$
\begin{aligned}
f_x(a) = \frac{1}{16\pi}\Bigg[\frac{1}{a^2} - \pi^2 \csc \pi a \quad \cot \pi a + \psi'\left(1+\frac{a}{2}\right) - 2\psi'(1+a)\Bigg] \\
+ \frac{\pi a}{24}\left[\frac{AR_j^{\,2}}{\left(\frac{1.7058}{AR_j^{\,2}} + a^2\right)^{1/2}} + \frac{.6995}{\left(\frac{1.0034}{AR_j^{\,2}} + a^2\right)^{3/2}}\right] \\
- \frac{\pi}{24}\sum_{m=1}^{\infty} - (-1)^m \Bigg\{\frac{(m+a)\, AR_j^{\,2}}{\left[\frac{1.7058}{AR_j^{\,2}} + (m+a)^2\right]^{1/2}} \\
- \frac{(m-a)\, AR_j^{\,2}}{\left[\frac{1.7058}{AR_j^{\,2}} + (m-a)^2\right]^{1/2}} + \frac{.6995\,(m+a)}{\left[\frac{1.0034}{AR_j^{\,2}} + (m+a)^2\right]^{3/2}} \\
- \frac{.6995\,(m-a)}{\left[\frac{1.0034}{AR_j^{\,2}} + (m-a)^2\right]^{3/2}}\Bigg\}
\end{aligned}
\tag{A15a}
$$

when $a \rightarrow 0$, using term by term differentiation

$$f_x(a) \rightarrow \left\{ \frac{3\,\zeta(3)}{16\,\pi} + \frac{\zeta(3)\,AR_j^{\,3}}{2\,\pi} - \frac{\pi}{12} \sum_{m=1}^{\infty} -(-1)^m \left[\frac{1.7058}{\left(\frac{1.7058}{AR_j^2} + m^2\right)^{3/2}} + \frac{.6995\left(\frac{1.0034}{AR_j^2} - 2m^2\right)}{\left(\frac{1.0034}{AR_j^2} + m^2\right)^{5/2}} \right] \right\} a \tag{A15b}$$

when $AR_j = 0$

$$f_x(a) = \frac{1}{16\,\pi} \left[\frac{1}{a^2} - \pi \csc \pi a \cot \pi a + \psi'\left(1 + \frac{a}{2}\right) - 2\,\psi'(1+a) \right] \tag{A15c}$$

when $AR_j = 0$ and $a \rightarrow 0$

$$f_x(a) \rightarrow \frac{3\,\zeta(3)}{16\,\pi}\, a \tag{A15d}$$

also

$$f_x(-a) = -f_x(a)$$

and when $a > 1/2$ use (A13).

Reference

A1 Abramowitz, M., and Stegun, I. A., ed.: Handbook of Mathematical Functions with Formulas, Graphs, and Mathematical Tables. National Bureau of Standards, 1955.

Appendix B Limitations of the Representation of the Interference Potential by Images

The treatment of the lift of a wing in a static rectangular jet rests on the representation of the interference potential by images. It is the purpose of this appendix to determine whether this method can be extended to allow for forward speed. Two cases are examined:

1. When the jet passes through a strip of infinite width but limited height.
2. When the jet extends through an infinite quadrant in the crossplane so that it has a single corner.

In each case the interference potential for a single trailing vortex is considered, and the boundary conditions to be satisfied are those given in section 2 of the text:

$$\varphi_j = \mu \varphi_o \tag{B1}$$

$$\mu \frac{\partial \varphi_j}{\partial n} = \frac{\partial \varphi_o}{\partial n} \tag{B2}$$

where

$$\mu = \frac{V_o}{V_j} \tag{B3}$$

Note that the boundary condition for a closed wind tunnel

$$\frac{\partial \varphi_j}{\partial n} = 0$$

is obtained by setting $\mu = \infty$ in (B2).

The first case has been treated by von Karman (ref. B1). The analysis is repeated here for convenience. It is found that the interference potential can be represented by images, but that the strength of each image has a different dependence on μ, so that they cannot all be multiplied by a single strength factor. In the second case it is found that the interference potential can only be represented by images in the cases of the open and closed windtunnels ($\mu = 0$ and $\mu = \infty$). Thus the image method is not strictly applicable to the case of a wing in a rectangular slipstream at forward speed.

Case 1: Interference for a Vortex in a Slipstream Filling an Infinite Strip

Consider first a unit vortex lying parallel to the x axis in a slipstream occupying the whole space to the left of a vertical boundary at $y = a$ (fig. B1). If the vortex is at $y = y_1$, its potential in the absence of a slipstream boundary would be

$$F\ (y_1) = \frac{1}{2\pi}\ \tan^{-1}\frac{z}{y-y_1} \tag{B4}$$

Consider also a unit vortex at the image point $y = 2a - y_1$ obtained by reflecting the original vortex in the boundary. With the addition of a constant its potential would be

$$G = F\,(2a - y_1) + \text{constant} \tag{B5}$$

The constant, which does not represent any flow, can be chosen so that on the boundary

$$F = -G \tag{B6}$$

$$\frac{\partial F}{\partial y} = \frac{\partial G}{\partial y} \tag{B7}$$

Suppose that the potential in the slipstream is

$$\varphi_j = F + P\,G \tag{B8}$$

and that the potential outside it is

$$\varphi_o = Q\ F \tag{B9}$$

In view of (B6) and (B7) the boundary conditions (B1) and (B2) are then satisfied if

$$1 - P = \mu Q$$

$$\mu(1+P) = Q$$

or

$$P = \frac{1 - \mu^2}{1 + \mu^2} \quad , \quad Q = \frac{2\mu}{1 + \mu^2} \tag{B10}$$

Consider now a slipstream occupying an infinite strip parallel to the z axis with boundaries at $y = \pm a$ (fig. B2). Considering each boundary separately, the original vortex at $y = -y_1$ gives rise to two primary images of strength P at $y = 2a - y_1$ and $y = -2a - y_1$. But now at the right hand boundary the potential due to the primary image on the left is just like the potential of the original vortex, and must be compensated by the introduction of a secondary image on the right with strength P^2. Similarly the primary image to the right gives rise to a secondary image to the left. The secondary images in turn must be compensated by tertiary images, and by repeated reflection a series of images of successively higher order is obtained. Thus the potential in the slipstream is

$$\varphi_j = F(y_1) + P\left[F(2a-y_1) + F(-2a-y_1)\right] + P^2\left[F(4a-y_1) + F(-4a-y_1)\right] \ldots + \text{constant} \tag{B11}$$

where $F(y_1)$ is the potential of a vortex at $y = y_1$ given by (B4). Also the potential to the right of the slipstream boundary is

$$\varphi_o = Q\left[F(y_1) + P\,F(-2a-y_1) + P^2\,F(-4a-y_1) \ldots\right] + \text{constant} \tag{B12}$$

and the potential to the left is given by a similar expression. The downwash in the slipstream is

$$w = \frac{1}{2\pi}\left[\frac{1}{y-y_1} + P\left(\frac{1}{y-2a+y_1} + \frac{1}{y+2a+y_1}\right) + P^2\left(\frac{1}{y-4a+y_1} + \frac{1}{y+4a+y_1}\right)\ldots\right] \tag{B13}$$

Exactly the same arguments may be used when the infinite line vortex is replaced by a horseshoe vortex. Thus the three dimensional interference potential due to a slipstream occupying either a vertical or a horizontal strip of infinite extent can be represented by images. When the aircraft has forward speed, however, these

images are not multiplied by a constant strength factor P, but images of successively higher order are multiplied by successively higher powers of P.

Case 2: Interference for a Vortex in a Slipstream Filling a Quadrant

As the simplest case of a slipstream with a cross-section including a corner consider a slipstream filling an infinite quadrant between the negative y and z axes (fig. B3). The only possible images are then the reflections of the original vortex in the y and z axes and an image in the quadrant opposite the slipstream which is obtained by reflection of either of the primary images in the z or y axes respectively. Let the potential of the original vortex be F_1, and let the potentials of vortices at the image points in the other quadrants be F_2, F_3, and F_4 respectively where the constant terms in the potentials are chosen so that on the y axis

$$F_1 = -F_4, \quad F_2 = -F_3 \tag{B14}$$

$$\frac{\partial F_1}{\partial z} = \frac{\partial F_2}{\partial z}, \quad \frac{\partial F_3}{\partial y} = \frac{\partial F_4}{\partial y} \tag{B15}$$

and on the z axis

$$F_1 = -F_2, \quad F_3 = -F_4 \tag{B16}$$

$$\frac{\partial F_1}{\partial y} = \frac{\partial F_2}{\partial y}, \quad \frac{\partial F_3}{\partial y} = \frac{\partial F_4}{\partial y} \tag{B17}$$

Denote the potentials in the four quadrants by φ_1, φ_2, φ_3, and φ_4. In the second, third and fourth quadrants there can be no singularity. Therefore let

$$\varphi_2 = Q_1 F_1 + Q_2 F_2 + Q_4 F_4$$

$$\varphi_3 = R_1 F_1 + R_2 F_2 + R_3 F_3$$

Now there is no slipstream boundary between the second and third quadrants.

Thus on the positive y axis

$$\varphi_2 = \varphi_3$$

$$\frac{\partial \varphi_2}{\partial z} = \frac{\partial \varphi_3}{\partial z}$$

whence in view of (B14) and (B15)

$$(Q_1 - Q_4)\ F_1 - Q_3\ F_2 = (R_1 - R_4)\ F_1 + R_2\ F_2$$

$$(Q_1 + Q_4)\ \frac{\partial F_1}{\partial z} + Q_3\ \frac{\partial F_2}{\partial z} = (R_1 + R_4)\ \frac{\partial F_1}{\partial z} + R_2\ \frac{\partial F_2}{\partial z}$$

But since, F_1, F_2, $\frac{\partial F_2}{\partial z}$ and $\frac{\partial F_2}{\partial z}$ are distinct functions these can only be satisfied if

$$Q_1 - Q_4 = R_1 - R_4$$

$$Q_1 + Q_4 = R_1 + R_4$$

$$Q_3 = -R_2$$

$$Q_3 = R_2$$

or

$$Q_1 = R_1\ ,\quad Q_4 = R_4\ ,\quad Q_3 = R_2 = 0$$

But by a similar argument applied to the third and fourth quadrants it also follows that

$$R_4 = 0$$

Thus the only possible representation for the potential in the second, third and fourth quadrants is

$$\varphi_2 = \varphi_3 = \varphi_4 = Q\, F_1$$

where Q is a constant to be determined.

Suppose that the potential in the slipstream is

$$\varphi_1 = F_1 + P_2\, F_2 + P_3\, F_3 + P_4\, F_4$$

Then the boundary conditions (B1) and (B2) are satisfied on the negative y axis if

$$(1-P_4)\ F_1 + (P_2 - P_3)\ F_2 = \mu Q\ F_1$$

$$\mu\,(1 + P_4)\ \frac{\partial F_1}{\partial z} + \mu\,(P_2 + P_3)\ \frac{\partial F_2}{\partial z} = Q\ \frac{\partial F_1}{\partial z}$$

It is thus necessary that

$$1 - P_4 = \mu Q$$

$$\mu\,(1 + P_4) = Q$$

$$P_2 - P_3 = 0$$

$$\mu\,(P_2 + P_3) = 0$$

Similarly the boundary conditions on the negative z axis require that

$$1 - P_2 = \mu Q$$

$$\mu\,(1 + P_2) = Q$$

$$P_4 - P_3 = 0$$

$$\mu\,(P_4 + P_3) = 0$$

If μ is finite and not zero then

$$P_2 = P_3 = P_4 = 0$$

whence

$$\mu Q = 1, \quad Q = \mu$$

which is only possible if

$$\mu = 1 \ , \quad Q = 1$$

This is the trivial case when the slipstream boundary vanishes. The open wind-tunnel is obtained when $\mu = 0$. Then the well known solution

$$P_2 = P_3 = P_4 = 1, \quad Q = 0$$

is obtained. The closed wind tunnel is represented by $\mu = \infty$. Only the terms containing μ need be retained, and the solution is

$$P_2 = P_3 = -1, \quad P_4 = 1, \quad Q = 0$$

It may be concluded that the boundary conditions cannot be satisfied by the introduction of images except in the cases of the open and closed wind tunnels.

Reference

B1 VonKarman, Theodore: General Aerodynamic Theory - Perfect Fluids. Vol. II of Aerodynamic Theory, W. F. Durand, ed., Julius Springer (Berlin), 1935.

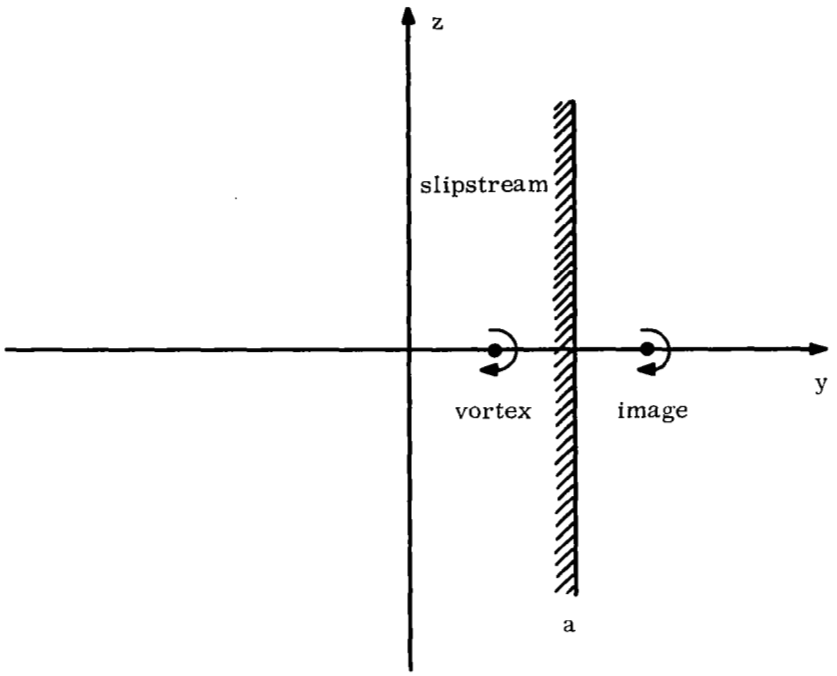

Figure B1. Vortex in a Semi-Infinite Slipstream

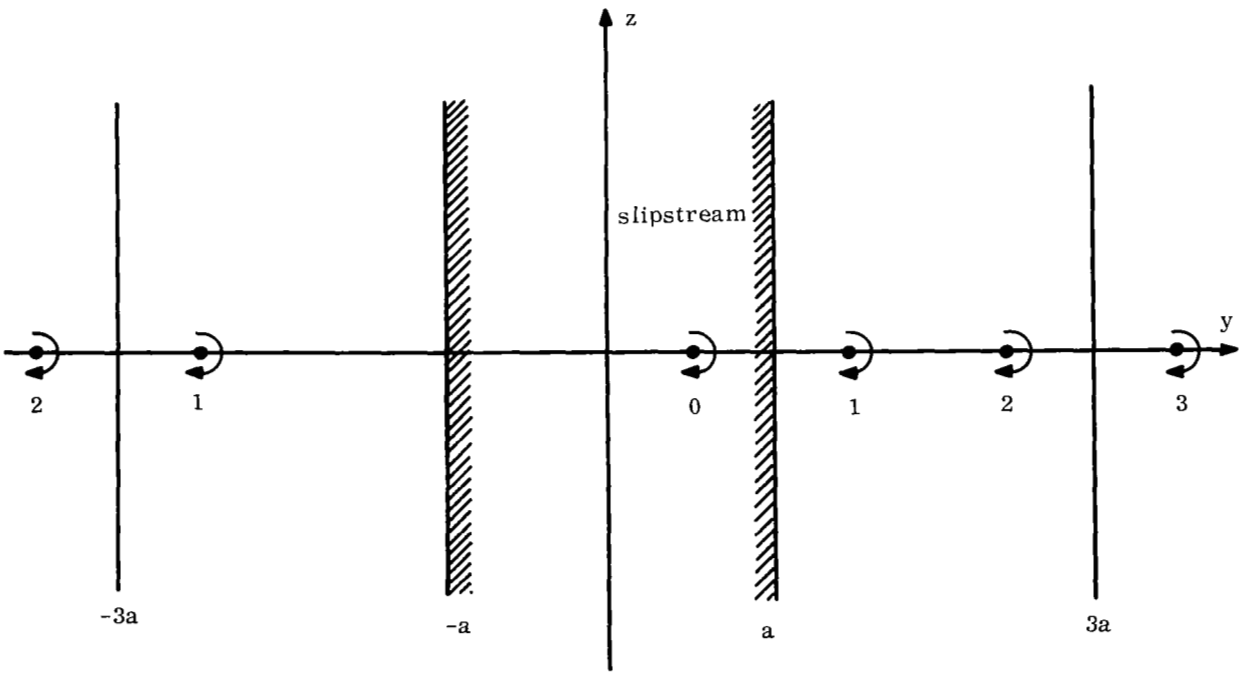

Figure B2. Vortex in a Slipstream Filling an Infinite Strip

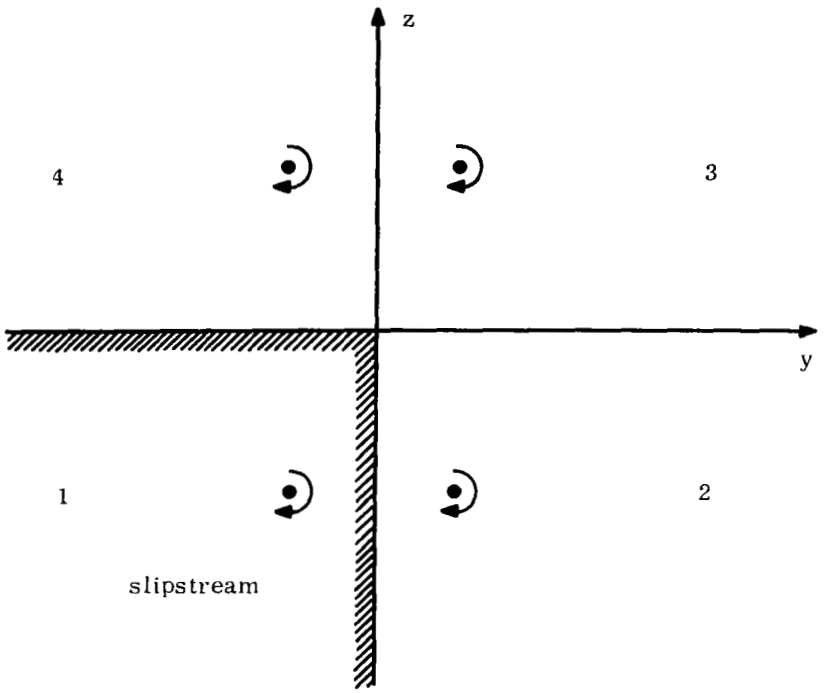

Figure B3. Vortex in a Slipstream Filling a Quadrant

PART 2

ENGINEERING METHOD FOR PREDICTION OF CHARACTERISTICS OF PRACTICAL V/STOL CONFIGURATIONS

1. Introduction

In this second part of the report, a method is given for estimating the aerodynamic characteristics of practical configurations for propeller-driven V/STOL aircraft. The results of a number of sample calculations are presented to establish the correlation of the theory with existing experimental data.

The additional lift required to permit a V/STOL aircraft to fly at low speeds may be generated by tilting the propeller-wing combination or by lowering flaps to deflect the slipstream, or by a combination of these methods. In order to estimate the lift and drag of an inclined propeller-wing combination (sketch 1), it is necessary to allow for the vertical and horizontal components of

(1) the thrust of the propellers,
(2) the normal force in the plane of the propellers due to the inclination of the inflow velocity,
(3) the lift and drag of the wing under the influence of the propeller slipstream.

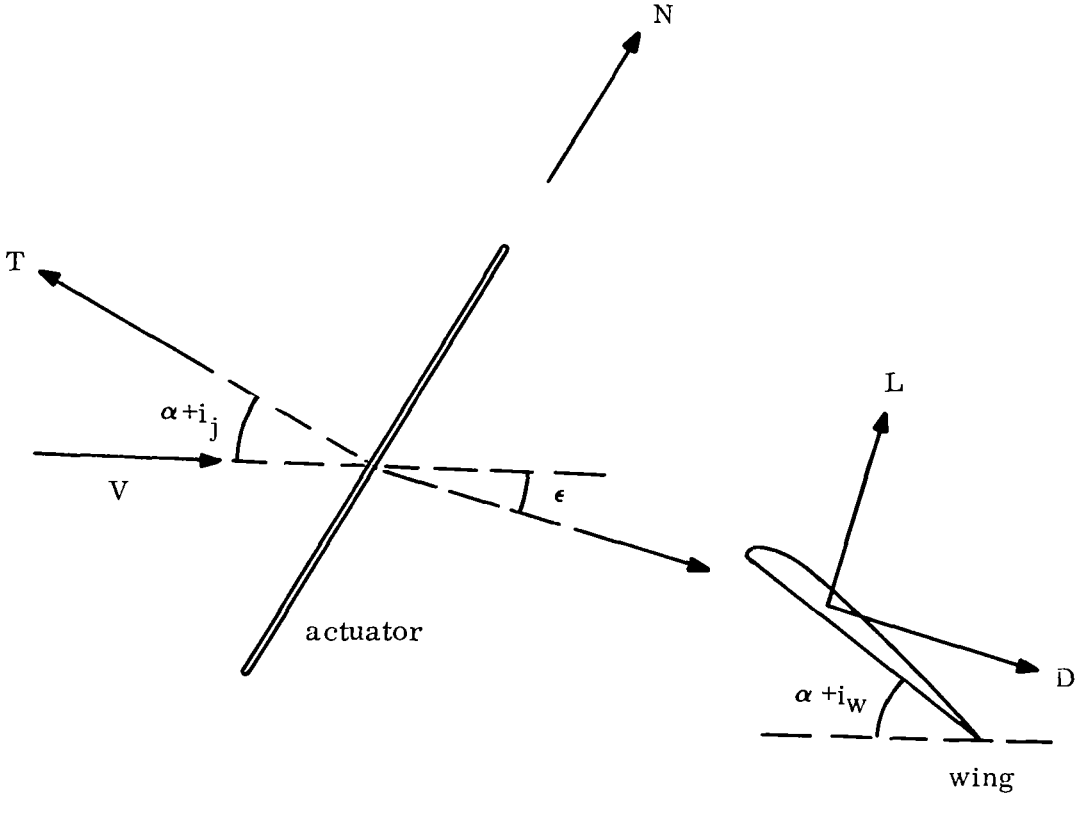

Sketch 1. Inclined Actuator-Wing Combination: Actuator Incidence i_j, Wing Incidence i_w, Slipstream Downwash Angle ϵ

The propeller slipstream has three principal effects on the wing: it increases the dynamic pressure, it alters the wing angle of attack, and its interference with the flow over the wing causes changes in the lift slope and the induced drag factor. The theory of Part 1 may be used to estimate the effect due to interference. In section 2, some simple formulas are developed which approximate the theoretical results to within about 3% in the range of practical calculations; these will be used to eliminate the need for detailed calculations. The theory strictly applies only to a wing that is completely contained in a single jet. If the wing extends beyond the slipstream, or spans several slipstreams, there will be additional interference effects which have not been included. It is assumed, however, that the effect of a jet on the part of the wing outside the jet is relatively small. A simple method of superposition will therefore be used to calculate the lift and drag of a wing with sections in the free stream. The increase in the lift of each blown part of the wing, treated as if it were an independent planform, is added to the lift of the whole wing in the free stream. The upwash outside an inclined jet is approximated by treating the jet as an infinite falling cylinder. Slipstream rotation will be ignored; it is assumed that the decrease in lift due to downwash on one side of the slipstream would be about equal to the increase in lift due to upwash on the other side, so that the estimate of total lift in the slipstream should be reasonably accurate as long as the wing spans the entire slipstream. (When propellers are placed at the wing tips, they are usually of large diameter so that most of the lift is produced directly by the thrust of the inclined propellers, and the contribution of the wing is small.) The effect of flap deflection is considered in section 4 and large angles of attack are treated in section 5.

The complete procedure for estimating the forces of a wing propeller combination is described in section 6. DeYoung's method (ref. 2) is used to estimate the forces on an inclined propeller. The drag due to lift is assumed to be the principal contribution to drag, and so profile drag is not estimated, though it would not be difficult to add an allowance for it. Section 7 contains the comparison of theoretical and experimental results.

Notation for Part 2

Symbols unique to Part 2 are defined as they are introduced in the text. In addition, all the formulas for prediction of the aerodynamic characteristics of a propeller driven V/STOL aircraft are collected in section 6; and for convenience, the definition of the symbols is included there together with the formulas in which they are used. Those symbols used in both Parts 1 and 2 are defined in the notation list, page 4.

2. Formulas for quick estimation of the lift and drag of a wing spanning a slipstream.

Estimation of the lift by the full theory of Part 1 requires lengthy calculations. In this section, simple formulas are derived for a wing of constant chord fully immersed in a slipstream. These approximate the results of the full calculations to an accuracy which is quite acceptable for evaluation of a proposed design.

When a wing immersed in a slipstream is compared with a wing in a stream of the same velocity extending through the whole space, the essential difference is a reduction by the ratio μ of the mass flow outside the slipstream, and consequently a reduction in the mass flow influenced by the wing. In the case of a free wing, the mass flow that is influenced is that passing through a tube of area $\pi b^2/4$ just containing the wing tips. The smaller mass flow influenced by the wing in a slipstream is thus equivalent to a reduction in the effective span or aspect ratio of the wing.

The lift of the wing in the static case will first be considered. Compared with a free wing, a given lift is developed by deflection of a smaller mass flow through a greater downwash angle. As a first approximation, assume that the additional downwash due to the presence of the jet boundary is a constant fraction p of the downwash of the wing in a free stream. (It was shown in section 5 of Part 1 that this is exactly true for a wing with an elliptic lift distribution spanning the foci of an elliptic jet.) In this case, the jet effect is equivalent to a decrease in the effective aspect ratio from AR to

$$AR_o = \frac{AR}{1 + p}$$

According to lifting line theory, the lift slope would then be

$$CL_{\alpha_o} = \frac{a_o}{1 + \frac{a_o\,(1+p)}{\pi AR}}$$

where a_o is the lift slope of the two dimensional airfoil. Also, the lift slope CL_{α_1} of the wing in a free stream would be

$$CL_{\alpha_1} = \frac{a_o}{1 + \frac{a_o}{\pi AR}}$$

Thus the ratio of the lift slopes would be

$$\frac{CL_{\alpha_o}}{CL_{\alpha_1}} = \frac{1 + \dfrac{a_o}{\pi AR}}{1 + \dfrac{a_o\,(1+p)}{\pi AR}} = \frac{AR + \dfrac{a_o}{\pi}}{AR + \dfrac{a_o}{\pi}\,(1+p)}$$

Accepting the thin airfoil value 2π for a_o, this suggests the functional form

$$\frac{CL_{\alpha_o}}{CL_{\alpha_1}} = \frac{AR + 2}{AR + a}$$

where a depends on the jet aspect ratio.

The results of full calculations for rectangular wings spanning rectangular jets are shown in fig. 1. It can be seen that for a fixed jet aspect ratio, each curve of $\frac{CL_{\alpha_o}}{CL_{\alpha_1}}$ has a point of inflexion for a value of AR that is less than AR_j; but to the right of this, the curves have a shape consistent with the proposed form. In fact, good agreement is obtained for values of AR_j from 1 to 4 and $\frac{AR}{AR_j} > \frac{1}{2}$ by taking the following values of a:

AR_j	a
1	3.35
2	4.8
3	6.7
4	8.8

This dependence of a on AR_j can be rather well represented by

$$a = 2AR_j + \frac{2.5}{1 + AR_j}$$

Thus, in the specified range of AR and AR_j, the static lift of a rectangular wing spanning a rectangular jet can be determined from its lift in a free stream by the formula

$$\frac{CL_{\alpha_0}}{CL_{\alpha_1}} = \frac{AR + 2}{AR + 2AR_j + \frac{2.5}{1 + AR_j}} \tag{2.1}$$

It is in fact unlikely that a practical design would fall outside the range in which this formula is valid; since, for a wing of constant chord c spanning a jet of height H

$$\frac{AR}{AR_j} = \frac{H}{c}$$

so the limitation is that the wing chord should not be more than twice the jet height or propeller diameter.

The dependence of the lift on the ratio μ of the external velocity to the slipstream velocity can be treated in a similar way. For the case of a wing spanning the foci of an elliptic jet, it was found in section 5 of Part 1 that the downwash is increased by the factor

$$\frac{\lambda + \mu^2}{1 + \lambda\mu^2}$$

This is equivalent to a decrease in the effective aspect ratio to the value

$$AR_\mu = AR \frac{1 + \lambda\mu^2}{\lambda + \mu^2}$$

where λ is the ratio of width to height of the slipstream. According to lifting line theory, the corresponding lift slope would be

$$CL_{\alpha_\mu} = \frac{a_0}{1 + \frac{a_0}{AR_\mu}}$$

When $\mu = 0$, the effective aspect ratio and lift slope become

$$AR_o = \frac{AR}{\lambda}$$

$$CL_{\alpha_o} = \frac{a_o}{1 + \frac{a_o}{\pi AR_o}}$$

Also, the lift slope for a free stream is

$$CL_{\alpha_1} = \frac{a_o}{1 + \frac{a_o}{\pi AR}}$$

Then

$$\frac{\frac{CL_{\alpha_1}}{CL_{\alpha_\mu}} - 1}{\frac{CL_{\alpha_1}}{CL_{\alpha_o}} - 1} = \frac{\frac{1}{AR_\mu} - \frac{1}{AR}}{\frac{1}{AR_o} - \frac{1}{AR}}$$

where

$$\begin{aligned}\frac{1}{AR_\mu} - \frac{1}{AR} &= \frac{1}{AR}\left(\frac{\lambda + \mu^2}{1 + \lambda\mu^2} - 1\right) \\ &= \left(\frac{\lambda}{AR} - \frac{1}{AR}\right)\frac{1 - \mu^2}{1 + \lambda\mu^2} \\ &= \left(\frac{1}{AR_o} - \frac{1}{AR}\right)\frac{1 - \mu^2}{1 + \lambda\mu^2}\end{aligned}$$

Thus

$$\frac{CL_{\alpha_1}}{CL_{\alpha_\mu}} - 1 = \left(\frac{CL_{\alpha_1}}{CL_{\alpha_o}} - 1\right)\frac{1 - \mu^2}{1 + \lambda\mu^2}$$

The dependence of the wing characteristics on forward speed is here expressed in terms only of the lift in a free stream and the lift in a static jet, with no explicit reference to the two dimensional lift slope or the aspect ratio. It will be assumed that the lift of a wing in a rectangular jet varies with forward speed in a similar way, where, for the rectangular jet, the jet aspect ratio AR_j should be used instead of λ as a measure of jet width. This leads to

$$\frac{CL_{\alpha_\mu}}{CL_{\alpha_1}} = \frac{1}{1 + \left(\frac{CL_{\alpha_1}}{CL_{\alpha_o}} - 1\right) \frac{1 - \mu^2}{1 + AR_j \mu^2}} \tag{2.2}$$

Simple formulas can also be found for the induced drag. Let r denote $\frac{CD}{CL^2}$ and let r_o, r_1, and r_μ be the values of this ratio for a wing in a static jet, in a free stream, and in a slipstream with velocity ratio μ. On inspecting the results of the full calculations for rectangular wings spanning rectangular jets, it is found that for a fixed jet aspect ratio AR_j, the ratio $\frac{r_o}{r_1}$ is almost independent of wing aspect ratio. Some typical values of $\frac{r_o}{r_1}$ are tabulated below:

AR_j	AR = 0	AR = 4	AR = 8
.5	1.45	1.45	1.46
1	1.57	1.57	1.57
2	2.15	2.14	2.12
4	3.63	3.61	3.54
8	6.73	6.69	6.56

The variation of $\frac{r_o}{r_1}$ with AR_j when AR = 4 is plotted in fig. 2, and it can be seen that it is almost linear when $AR_j > 2$. It has been found that it is well approximated by the formula

$$\frac{r_o}{r_1} = .76\,(AR_j + e^{-AR_j}) + .53 \tag{2.3}$$

In the case of forward speed, $\frac{r_\mu}{r_1}$ should approach $\frac{r_o}{r_1}$ when μ approaches 0, and it should approach 1 when μ approaches 1. Also, the assumed variation of CL with μ implies a factor $1 + AR_j\mu^2$ in the denominator of the effective aspect ratio. This leads to the formula

$$\frac{r_\mu}{r_1} = \frac{\frac{r_o}{r_1} + \left(1 + AR_j - \frac{r_o}{r_1}\right)\mu^2}{1 + AR_j\mu^2} \tag{2.4}$$

These formulas permit the lift and drag of a wing spanning a slipstream to be determined from the lift and drag of the same wing in a free stream. Equations (2.1) and (2.3) give the static lift and induced drag, and equations (2.2) and (2.4) may then be used to calculate the effect of forward speed. The formulas have been compared with the results of the full calculations for rectangular wings spanning rectangular jets over the full range of forward speed from $\mu = 0$ to $\mu = 1$. For jet aspect ratios from 1 to 8 and wing aspect ratios greater than half the jet aspect ratio, the maximum error has been found to be about 3%.

For a rectangular wing spanning a circular jet, it has been found similarly that a good approximation to the lift is given by

$$\frac{CL_{\alpha_o}}{CL_{\alpha_1}} = \frac{AR + 2}{AR + 3.54} \tag{2.5}$$

$$\frac{CL_{\alpha_\mu}}{CL_{\alpha_1}} = \frac{1}{1 + \left(\frac{CL_{\alpha_1}}{CL_{\alpha_o}} - 1\right)\frac{1 - \mu^2}{1 + \mu^2}} \tag{2.6}$$

and to the drag by

$$\frac{r_o}{r_1} = 1.68 \tag{2.7}$$

$$\frac{r_\mu}{r_1} = \frac{1.68 + .32\,\mu^2}{1 + \mu^2} \tag{2.8}$$

3. Lift and drag of a wing partially immersed in one or more slipstreams

In many designs, the wing tips extend beyond the region of the slipstreams. Also, even if the propellers on each semispan are close enough for their slipstreams to merge, the presence of the fuselage will ensure separation of the slipstreams on the two sides. It is thus necessary to consider the case of a wing that extends through more than one slipstream. When the aircraft is static, the lift is simply the sum of the independent contributions of each part of the wing that is in a slipstream. When the aircraft has forward speed, however, not only will there be a contribution to the lift from the part of the wing in the free stream, but also the presence of a part of the wing beyond each slipstream and of other slipstreams will cause a modification of the flow over the wing inside each slipstream. These additional interactions have not been cosidered in the theory, and, strictly, would require recalculation of the circulation in each slipstream. Instead, an approximate estimate of the lift will be derived by a simple method of superposition. This procedure is consistent with the aim of avoiding massive calculations, and it leads to an estimate that reduces to the usual result for a wing in a free stream when the velocity ratio is unity, and to the sum of the independent contributions from each slipstream when the aircraft is static.

The lift will be calculated as the sum of the lift of the whole wing at free stream velocity plus the increase due to the part of the wing in each slipstream, calculated as if that part were an isolated planform, not extending beyond the jet. Thus, the increase will be estimated simply as the difference between the lift of that planform if it were an independent wing in a free stream, and its lift if it just spanned a slipstream. Let V be the external velocity and V_j the jet velocity. Then if S_{wj} is the area of the wing inside a jet of width B_j, the increase due to the jet is

$$\Delta L = \frac{1}{2} \rho S_{wj} \quad (V_j^2 \, CL_{\alpha_{j\mu}} \alpha_{wj\mu} - V^2 \, CL_{\alpha_1} \alpha_{wj1})$$

where $CL_{\alpha_{j\mu}}$ is the lift slope of the part of the wing in the jet at a velocity ratio $\mu = \frac{V}{V_j}$, calculated for a planform of aspect ratio $\frac{B_j^2}{S_{wj}}$; CL_{α_1} is the lift slope of this planform when $\mu = 1$, or the lift slope in a free stream; $\alpha_{w_{j\mu}}$ is the angle of attack of the wing in the jet; and $\alpha_{w_{j1}}$ is the angle of attack of this section in the free stream. The angle of attack of the wing in the jet is reduced from the angle

of attack in the free stream by the jet downwash angle ϵ . It can be seen that ΔL is the lift in an independent slipstream when $V = 0$. Also, $\Delta L = 0$ when $V = V_j$, provided that in this case $\alpha_{wj\mu} = \alpha_{wj1}$. In fact, an inclined propeller can create a downwash at zero thrust, and it is possible to allow for the resulting interference by using separate estimates of α_{wj1} and $\alpha_{wj\mu}$ when $V = V_j$.

When a slipstream is inclined to the free stream, it will also create an external upwash. This can be approximated by regarding the slipstream as a falling cylinder. The upwash at a distance of y from the center of the jet is then

$$\frac{\left(\frac{B_j^2}{2}\right)}{y^2}\epsilon$$

If y_1 is the distance to the wing tip, the average upwash over the span beyond the jet is then

$$\int_{\frac{B_j}{2}}^{y_1} \frac{B_j^2}{4y^2}\epsilon \quad dy = \frac{B_j}{2y_1}\epsilon$$

Thus the average upwash over the external part of the wing is approximately equal to $\frac{S_{wj}}{S}\epsilon$, where S is the total wing area. The increase in lift due to the upwash may then be estimated by multiplying together the area of the unblown part of the wing, the increase in the angle of attack due to the upwash of all the jets, and the lift slope CL_{α_1} calculated for the complete wing in a free stream.

Provided that the angle of attack α in the free stream and the jet downwash angles are small, the total lift can now be calculated from the relation

$$\overline{V}^2\overline{S}CL = V^2SCL_{\alpha_1}\ \alpha + V^2CL_{\alpha_1}\left(S - \sum_{jets} S_{wj}\right)\sum_{jets}\frac{S_{wj}}{S}\ \epsilon$$

$$+ \sum_{jets} S_{wj}\left(V_j^2CL_{\alpha_{j\mu}}\ \alpha_{wj\mu} - V^2CL_{\alpha_{j1}}\ \alpha_{wj1}\right) \tag{3.1}$$

where $\overline{V}$ is the reference velocity, which might be V or V_j, and $\overline{S}$ is the reference area. This equation can be written as

$$\overline{V}^2\overline{S}CL = \left(S - \sum_{jets} S_{wj}\right) V^2CL_f + \sum_{jets} S_{wj}\ V_j^2\ CL_{j\mu} \tag{3.2}$$

where CL_f and α_f are the lift coefficient and angle of attack attributed to the unblown part of the wing

$$CL_f = CL_{\alpha_1}\ \alpha_f \tag{3.3}$$

$$\alpha_f = \alpha + \sum_{jets}\frac{S_{wj}}{S}\ \epsilon \tag{3.4}$$

and $CL_{j\mu}$ is the lift coefficient attributed to each blown section

$$CL_{j\mu} = CL_{\alpha_{j\mu}}\ \alpha_{wj\mu} + \frac{V^2}{V_j^2}\left(CL_{\alpha_1}\alpha - CL_{\alpha_{j1}}\ \alpha_{wj1}\right) \tag{3.5}$$

The angle of attack should be measured relative to the zero lift angle. It should also be remembered that the lift in each jet will be perpendicular to the local flow velocity, so that $CL_{j\mu}$ actually represents a force which is rotated back through an angle ϵ. Since the theory of wing jet interaction has only been developed for a wing that is symmetric in the jet, the planform in the jet must be replaced by a rectangular planform of equal area when the slipstream is on one side of a tapered wing.

The induced drag can be estimated in a similar way. Let the average induced downwash angle be

$$\alpha_i = r\ CL$$

so that the induced drag at small angles of attack is

$$CD = \alpha_i\ CL = r\ CL^2$$

The change in the induced drag of the part of a wing in a jet will be calculated as the free stream lift of this section multiplied by the change in the induced downwash angle, plus the new induced downwash angle multiplied by the change in the lift. If the lift coefficient of this part in the free stream is assumed to be

$$CL_{j1} = CL_{\alpha_1}\ \alpha \tag{3.6}$$

the change in the drag is

$$\Delta D = \frac{1}{2}\ \rho\ S_{wj}\ V^2 CL_{j1} \left(r_{j\mu}\ CL_{j\mu} - r_{j1} CL_{j1} \right)$$

$$+ S_{wj} \left(V_j^{\,2} CL_{j\mu} - V^2 CL_{j1} \right)\ r_{j\mu}\ CL_{j\mu}$$

where $CL_{j\mu}$ is calculated from (3.5), $r_{j\mu}$ is the induced drag factor of the part of the wing in the jet at a velocity ratio μ, calculated as if it were an independent planform not extending beyond the jet, and r_{j1} is the induced drag factor of this planform if it were an independent planform in a free stream.

If it is assumed that this part of the wing is the source of a fraction of the total drag in the free stream proportional to its area, its contribution to the drag in the free stream would have been

$$D = S_{w_j} V^2 r_1 CL_{j_1}{}^2$$

where r_1 is the induced drag factor of the complete wing in the free stream. The drag to be attributed to the part of the wing in each jet is then $D + \Delta D$ plus a contribution due to the rotation of the lift back through the downwash angle ϵ .

The drag of the unblown part of the wing will be calculated as the lift of this section multiplied by the new induced downwash angle, which may be estimated as the lift multiplied by the induced drag factor r_1 of the free wing. The lift is given by (3.3) and (3.4).

Finally, if the angle of attack and the jet downwash angles are small, the total induced drag may be calculated from the relation

$$\overline{V}^2\overline{S}CD = \left(S - \sum_{\text{jets}} S_{w_j}\right) V^2 CD_f + \sum_{\text{jets}} S_{w_j} V_j{}^2 \left(CD_{j\mu} + CL_{j\mu}\,\epsilon\right) \tag{3.7}$$

where

$$CD_f = r_1 CL_f{}^2 \tag{3.8}$$

and

$$CD_{j\mu} = \frac{V^2}{V_j^2} \; CL_{j1}\left(r_{j\mu}CL_{j\mu} + r_1 CL_{j1} - r_{j1}CL_{j1}\right)$$

$$+ \left(CL_{j\mu} - \frac{V^2}{V_j^2} \; CL_{j1}\right) r_{j\mu}CL_{j\mu} \qquad (3.9)$$

4. Effect of flaps

Lowry and Polhamus have described a quick method for estimating the effect of flap deflection on the lift of wings of finite span (ref. 3). With flaps deflected the lift coefficient can be expressed as

$$CL = CL_{\alpha} (\alpha + \alpha/\delta \ \delta) \tag{4.1}$$

where CL_{α} is the lift slope of the planform, δ is the flap deflection and α/δ the three dimensional flap effectiveness. If the three dimensional flap effectiveness is expressed in terms of the effectiveness of the same flap applied to a two dimensional airfoil as

$$\alpha/\delta = K \ \alpha/\delta_{2D}$$

then according to Lowry and Polhamus K depends to a first approximation only on α/δ_{2D} and the aspect ratio AR. They give curves for K based on lifting surface calculations.

To facilitate the incorporation of this method in a computer program it is desirable to replace the curves by a formula. Now in the limit of low aspect ratio, slender wing theory indicates that the lift is completely determined by the trailing edge angle, so that $\alpha/\delta = 1$ (ref. 4). Also $K \rightarrow 1$ as $AR \rightarrow \infty$ by definition. This suggests the form

$$K = \frac{1 + F}{\alpha/\delta_{2D} + F}$$

where F is a function of α/δ_{2D} and AR which $\rightarrow 0$ as $AR \rightarrow \infty$. From Lowry and Polhamus' curves the following table can be constructed.

$\alpha/\delta_{2D} = .2$	AR	K	F	$\frac{F}{\sqrt{\alpha/\delta_{2D}}}$
	1	1.73	.895	2.0
	2	1.49	1.43	3.20
	4	1.30	2.50	5.60
	8	1.16	4.86	10.9

$\alpha/\delta_{2D} = .4$	AR	K	F	$\frac{F}{\sqrt{\alpha/\delta_{2D}}}$
	1	1.39	1.14	1.8
	2	1.25	2.0	3.16
	4	1.14	3.72	5.88
	8	1.08	7.29	11.5

$\alpha/\delta_{2D} = .6$	AR	K	F	$\frac{F}{\sqrt{\alpha/\delta_{2D}}}$
	1	1.20	1.35	1.75
	2	1.13	2.48	3.20
	4	1.08	4.26	5.50
	8	1.04	10.5	13.5

It can be seen that $\frac{F}{\sqrt{\alpha/\delta_{2D}}}$ is more or less independent of α/δ_{2D}, depending on AR only, and it has been found that $\frac{F}{\sqrt{\alpha/\delta_{2D}}}$ can be quite well approximated as

$$\frac{F}{\sqrt{\alpha/\delta_{2D}}} = AR \frac{AR + 4.5}{AR + 2}$$

Substituting for F finally leads to a simple formula for computing α/δ ,

$$\alpha/\delta = \frac{\sqrt{\alpha/\delta_{2D}} + \alpha/\delta_{2D} \dfrac{AR + 4.5}{AR + 2} AR}{\sqrt{\alpha/\delta_{2D}} + \dfrac{AR + 4.5}{AR + 2} AR} \tag{4.2}$$

Assuming that a deflected slipstream or tilt wing aircraft would have full span flaps, the application of this procedure is nevertheless complicated by the fact that the effective aspect ratio of a section of the wing immersed in the slipstream is less than the aspect ratio of the complete wing, and depends on the velocity ratio, so that separate calculations are required for sections of the wing in each slipstream and in the free stream.

In the absence of measurements of α/δ for a wing in a jet or a detailed calculation it is uncertain what value should be attributed to it. Since, however, the effective aspect ratio of a wing in an isolated circular jet is generally small, α/δ should approach 1. A simple rule that gives the correct value when the velocity ratio approaches 1 is then

$$\alpha/\delta_{j\mu} = 1 - \mu^2 + \mu^2 \ \alpha/\delta_1 \tag{4.3}$$

where $\alpha/\delta_{j\mu}$ is the flap effectiveness for the section of the wing in the jet, and α/δ_1 the flap effectiveness for the free wing. From static tests of flaps behind one and two propellers on a half wing (ref. 5) it appears that the turning angle in a wide jet is about the same as in a circular jet. Since the theory indicates that the turning effectiveness of a wing is greater in a wide jet, it may be concluded that under static conditions α/δ decreases in a wide jet. To allow for this effect the following rule may be used for flaps in a rectangular jet:

$$\alpha/\delta_{j\mu} = \frac{1}{2}\left(1 + \frac{1}{AR_j}\right)(1 - \mu^2) + \mu^2 \ \alpha/\delta_1. \tag{4.4}$$

5. Large angles of attack

A tilt wing aircraft will fly at large angles of attack during transition. Since the propellers are aligned with the wing, the added velocity imparted by them will reduce the angle of attack of the blown sections of the wing. The different parts of the wing can then be expected to stall at different angles, and the aircraft may fly at an angle such that the unblown part of the wing is stalled while the blown parts are not yet stalled. In such circumstances, it is extremely difficult to predict the forces accurately, but even a rough estimate may be useful. The method described here should be regarded as giving no more than that.

First, since the jet downwash angles may be large, (3.2) and (3.7) should be replaced by

$$\overline{V}^2\overline{S}CL = \left(S - \sum_{\text{jets}} S_{wj}\right) V^2 CL_f + \sum_{\text{jets}} S_{wj} V_j^2 \left(CL_{j\mu} \cos\epsilon - CD_{j\mu} \sin\epsilon\right) \tag{5.1}$$

$$\overline{V}^2\overline{S}CD = \left(S - \sum_{\text{jets}} S_{wj}\right) V^2 CD_f + \sum_{\text{jets}} S_{wj} V_j^2 \left(CL_{j\mu} \sin\epsilon + CD_{j\mu} \cos\epsilon\right) \tag{5.2}$$

Then the lift and drag coefficients of each part of the wing must be estimated at large angles of attack. Below the stall, the lift can be expected to vary as the sine of the angle of attack. Also, one can allow roughly for the stall by assuming that beyond it the lift varies as the cosine of the angle of attack. Then, for each section of the wing

$$CL = CL_\alpha \sin\alpha, \quad \alpha \leq \alpha_{max}$$

$$CL_\alpha \sin\alpha_{max} \frac{\cos\alpha}{\cos\alpha_{max}}, \quad \alpha > \alpha_{max}$$

where α is the angle of attack, and α_{max} is the angle of maximum lift, both measured from the zero lift angle of that section.

If the propellers are not aligned with the zero lift angle of the wing, the zero lift angles of the blown and unblown parts of the wing will be different and must be calculated separately. Let ϵ', $\alpha'_{wj\mu}$, and α'_{wj1} be the changes in the jet downwash angle, the angle of attack of the wing in a jet, and the angle of attack of this part of the wing in a free stream resulting from a unit change of α. The lift slope CL_{α_f} of the unblown part of the wing and CL_{α} of each blown part of the wing can be determined by setting $\alpha = 1$ and substituting ϵ', $\alpha'_{wj\mu}$, and α'_{wj1} for ϵ, $\alpha_{wj\mu}$, and α_{wj1} in (3.1) - (3.5). Then, if CL_f and $CL_{j\mu}$ are calculated for $\alpha = 0$, the zero lift angles of the blown and unblown sections are

$$\alpha_{of} = -\frac{CL_f}{CL_{\alpha_f}} \tag{5.3}$$

$$\alpha_{oj\mu} = -\frac{CL_{j\mu}}{CL_{\alpha_j}} \tag{5.4}$$

The lift coefficients at large angles may now be calculated as

$$CL_f = CL_{\alpha_1} \sin(\alpha_f - \alpha_{of}), \quad \alpha_f - \alpha_{of} \leq \alpha_{max_f}$$

$$CL_{\alpha_1} \tan \alpha_{max_f} \cos(\alpha_f - \alpha_{of}), \quad \alpha_f - \alpha_{of} > \alpha_{max\ f} \tag{5.5}$$

$$CL_{j\mu} = C_{\alpha_j} \sin(\alpha_{wj\mu} - \alpha_{oj\mu}), \quad \alpha_{wj\mu} - \alpha_{oj\mu} \leq \alpha_{max_{j\mu}}$$

$$CL_{\alpha_j} \tan \alpha_{max_{j\mu}} \cos(\alpha_{wj\mu} - \alpha_{oj\mu}), \quad \alpha_{wj\mu} - \alpha_{oj\mu} > \alpha_{max_{j\mu}} \tag{5.6}$$

where α_{max_f} and $\alpha_{max_{j\mu}}$ are the maximum lift angles of the unblown part of the wing and the part in each jet, which remain to be determined.

It will be assumed that the maximum lift angle of the two dimensional airfoil is known. The three dimensional wing will stall later than the two dimensional airfoil because the local angle of attack is reduced by the downwash. If the aspect ratio is large, the flow can be regarded locally as two dimensional, so that if a_o is the two dimensional lift slope

$$CL = a_o \alpha_e$$

where α_e is the average effective angle of attack. Then

$$\frac{\alpha_e}{\alpha} = \frac{CL_\alpha}{a_o}$$

If the downwash is uniform, the local angle of attack is α_e. If the downwash is not uniform, the maximum local angle of attack is still proportional to α_e. The stall can be expected to begin when any section reaches the two dimensional stall angle. Thus, for a high aspect ratio wing, it may be expected that

$$\alpha_{max} = K \frac{a_o}{CL_\alpha} \alpha_{max_{2D}}$$

where K is a constant ≤ 1 to allow for nonuniformity of the downwash. This formula is not satisfactory for low aspect ratio wings, since then $CL_\alpha \rightarrow \pi/2$ AR, so that the estimate of α_{max} becomes very large. To allow for this, one may introduce an additional factor $\frac{1}{\sqrt{1 + \left(\frac{a_o}{\pi AR}\right)^2}}$ which approaches 1 when AR is large and $\frac{\pi AR}{a_o}$ when AR is small. Then

$$\alpha_{max} = \frac{K}{CL_\alpha} \frac{a_o}{\sqrt{1 + \left(\frac{a_o}{\pi AR}\right)^2}} \alpha_{max_{2D}} \tag{5.7}$$

If CL_α is estimated by Lowry and Polhamus' formula (ref. 2) as

$$CL_\alpha = \frac{a_o}{\frac{a_o}{\pi AR} + \sqrt{1 + \frac{a_o}{\pi AR}^2}}$$

this reduces to

$$\alpha_{max} = K\left(1 + \frac{\frac{a_o}{\pi AR}}{\sqrt{1 + \left(\frac{a_o}{\pi AR}\right)^2}}\right)\alpha_{max_{2D}} \tag{5.8}$$

A good average value of K is .8. Taking $\alpha_o = 2\pi$, the maximum lift angle of the wing in a free stream may be estimated according to (5.7) as

$$\alpha_{max_1} = \frac{1.6\pi}{CL_{\alpha_1}} \frac{AR}{\sqrt{AR^2 + 4}} \alpha_{max_{2D}} \tag{5.9}$$

Then, for the unblown part it will be assumed that

$$\alpha_{max_f} = \alpha_{max_1} \tag{5.10}$$

The effective aspect ratio of the part of the wing in each jet depends on the velocity ratio. In the absence of better information, the following rule can be used. When $\mu = 0$, use (5.8) with K = .8 and $a_o = 2\pi$ so that

$$\alpha_{max_{jo}} = .8\left(1 + \frac{2}{\sqrt{AR^2 + 4}}\right)\alpha_{max_{2D}} \tag{5.11}$$

when $\mu > 0$, take

$$\alpha_{max_{j\mu}} = (1 - \mu^2)\ \alpha_{max_{jo}} + \mu^2\ \alpha_{max_1} \tag{5.12}$$

which yields the correct value for a wing in a free stream when $\mu = 1$.

When flaps are deflected, the same procedure can be used; but in calculating CL_f and $CL_{j\mu}$ at $\alpha = 0$, the increase of the effective angle of attack due to the flaps should be included, and $\alpha_{max_{2D}}$ should be measured from the zero lift angle of the section with the flaps down.

6. Complete procedure for estimating the forces of a propeller wing combination

The formulas of section 2-5 provide the basis for estimating the contribution of the wing to the force experienced by a propeller driven V/STOL aircraft, given the dimensions, induced velocity, and downwash angle of each slipstream. They need to be complemented, therefore, by a procedure for estimating the characteristics of an inclined propeller. The procedure given by De Young (ref. 2) is simple and convenient. It will be used here. In the light of the approximations already introduced in the analysis of the wing, it does not appear that it would be fruitful to incorporate a more elaborate analysis.

In the absence of better information about when the slipstreams of two or more propellers merge, it will arbitrarily be assumed that if any two propellers on the same semispan are separated by not more than 1/10 propeller diameter, their slipstreams merge. The wide slipstream is then approximated by the slipstream of a rectangular actuator with an area equal to the sum of the areas of the propeller disks, so that the induced velocity in the jet is the same when the total thrust is the same. The aspect ratio of the rectangle is taken to be the ratio of the width spanned by the outer edges of the propeller disks to their height. In determining the size of the blown regions of the wing, one should allow for the contraction of the slipstreams behind the propeller. For the sake of simplicity, it will be assumed that the slipstreams are fully contracted in the region of the wing. A wide slipstream does not necessarily contract equally in the vertical and lateral directions. A formula for the contraction of a rectangular slipstream is derived in Appendix A. It is also necessary to determine the downwash in the slipstream, and required formulas are obtained in Appendix B. The analysis in these appendices is due to DeYoung.

The various elements can now be combined into a complete procedure which is listed below:

A. Propeller forces

Symbols:

ρ	density
V	free stream velocity
V_j	final jet velocity
μ	$\frac{V}{V_j}$

S	wing area
S_p	area of propeller disk or rectangular actuator
AR_p	aspect ratio of rectangular actuator
AR_j	aspect ratio of contracted jet
B_p	width of actuator or propeller diameter
H_p	height of actuator or propeller diameter
B_j	diameter or width of contracted slipstream
N_b	number of propeller blades
$\bar{b}$	average blade chord which may be estimated as $.16\left(\frac{5}{4}b_{.25} + 2b_{.5} + 2b_{.75} + b_{.95}\right)$ where b_r is the blade chord at a radius fraction r.
σ	solidity $= \frac{4N_b}{3\pi} \frac{\bar{b}}{B_p}$ for a propeller
β	blade angle at a radius fraction of .75 in degrees
T	thrust
N	normal force
CN	normal force coefficient
CN_α	slope of normal force coefficient
x	distance downstream from actuator
α_j	inflow angle to propeller or actuator
ϵ	downwash in the slipstream
E	constant of proportionality between downwash and inflow angle

Actuator equation:

$$\mu = \frac{1}{\sqrt{1 + \frac{T}{\frac{1}{2}\rho V^2 S_p}}} = \sqrt{1 - \frac{T}{\frac{1}{2}\rho V_j^2 S_p}} \tag{6.1}$$

Slipstream contraction:

For a circular slipstream

$$B = B_p \sqrt{\frac{1+\mu}{2}} \tag{6.2}$$

and AR_j does not need to be defined since it is not contained in the formulas for a circular slipstream; for a rectangular slipstream according to Appendix A

$$B = \frac{B_p}{2\sqrt{AR_p}} \left[\sqrt{1 + AR_p + 2\mu \sqrt{AR_p}} + \sqrt{AR_p} - 1 \right] \tag{6.3}$$

$$AR_j = \frac{1}{2(1+\mu)} \left[\sqrt{1 + AR_p + 2\mu \sqrt{AR_p}} + \sqrt{AR_p} - 1 \right]^2 \tag{6.4}$$

Normal force:

Assume that the normal force is proportional to the sine of the inflow angle,

$$C_N = C_{N_\alpha} \sin \alpha_j \tag{6.5}$$

where (ref. 2, equations (5) and (7))

$$C_{N_\alpha} = \frac{\mu}{2}\left(1 + \frac{\mu}{2} + \frac{\mu}{1+\mu^2}\right)\frac{4.25\sigma}{1+2\sigma}\sin(\beta + 8) \tag{6.6}$$

and for a rectangular actuator, C_{N_α} is the average for the propellers.

Downwash:

$$\epsilon = E\alpha_j \tag{6.7}$$

where according to Appendix B

$$E = \frac{E_\infty}{2}\left[\frac{\frac{2x}{B_p} + e + \sqrt{1 + \left(\frac{2x}{B_p} + e\right)^2}}{\frac{2x}{H_p} + e}\right] \tag{6.8}$$

$$E_\infty = \frac{1-\mu}{1+\mu^2} + \frac{\mu}{4}\,\frac{2+\mu+\mu^2}{1+\mu^2}\,\frac{4.25\sigma}{1+2\sigma}\sin(\beta + 8) \tag{6.9}$$

$$e = \frac{E_\infty}{2\sqrt{1-E_\infty}} \tag{6.10}$$

and for a rectangular actuator E_∞ is the average for the propellers.

B. Induced downwash angles

Symbols:

α	angle of attack of fuselage
i_j	incidence of actuator axis to fuselage
i_w	incidence of wing to fuselage

α_j	inflow angle to actuator
α_{wj}	angle of attack of the wing in the jet
AR	wing aspect ratio
c	wing chord at the jet center
$x_{L.75}$, $x_{R.75}$	distance of actuator to wing leading edge at 3/4 jet semispan to the left and right of the jet center
$y_{L.75}$, $y_{R.75}$	distance of fuselage to points at 3/4 jet semispan to the left and right of the jet center
$\Delta y_{L.75}$, $\Delta y_{R.75}$	distance from one jet center line to points at 3/4 jet semispan to the left and right of the center of another jet
D_{fus}	fuselage diameter

Equation for actuator inflow angles:

For each jet

$$\alpha_j = \alpha + i_j + U_w(\alpha + i_w) + U_f \quad \alpha + \sum_{\text{other jets}} U_{o_j} \epsilon \tag{6.11}$$

where U_w, U_f, and U_{o_f} are upwash factors due to the wing circulation, to the fuselage treated as an infinite falling cylinder, and to the other slipstreams treated as semi-infinite falling cylinders (ref. 2, equations (12), (13), and (14) with a factor μ to allow for the increased velocity in the slipstream).

$$U_w = \frac{2\mu\,AR}{9(AR+10)} \left[\frac{1}{\frac{x_{L.75}}{c} + .1} + \frac{1}{\frac{x_{R.75}}{c} + .1} \right] \tag{6.12}$$

$$U_f = \frac{\mu}{8} \left[\left(\frac{D_{fus}}{y_{L.75}} \right)^2 + \left(\frac{D_{fus}}{y_{R.75}} \right)^2 \right] \tag{6.13}$$

$$U_{oj} = \frac{\mu}{16} \left[\left(\frac{B_j}{\Delta y_{L.75}} \right)^2 + \left(\frac{B_j}{\Delta y_{R.75}} \right)^2 \right] \tag{6.14}$$

Substituting

$$\epsilon = E \ \alpha_j$$

this set of equations can be solved for α_j for each jet, whence ϵ is also determined.

Wing inflow angles:

$$\alpha_{wj1} = \alpha + i_w + U_f \ \alpha \tag{6.15}$$

$$\alpha_{wj\mu} = \alpha_{wj1} - \epsilon + \sum_{\text{other jets}} U_{\infty j} \ \epsilon \tag{6.16}$$

where, since the wing is behind the actuator, the upwash factor $U_{\infty j}$ due to the other slipstreams is calculated as if they were infinite falling cylinders, that is

$$U_{\infty j} = 2U_{oj} \tag{6.17}$$

C. Lift and induced drag of the wing at small angles

Symbols:

$\overline{V}$	reference velocity
$\overline{S}$	reference area
S	actual wing area allowing for chord extension due to flaps
S_{wj}	area of the part of a wing in a slipstream
AR	aspect ratio
AR_{wj}	aspect ratio of the part of a wing in a slipstream
$CL_{\alpha 1}$	lift slope of the wing in a free stream
$CL_{\alpha j\mu}$	lift slope of the part of a wing in a jet calculated as if it were an independent planform not extending beyond the jet
$CL_{\alpha j1}$	lift slope of the same planform if it were an independent wing in a free stream
$CL_{\alpha jo}$	lift slope of the same planform in a static jet
r_1	induced drag factor $\frac{CD}{CL^2}$ for a wing in a free stream
$r_{j\mu}$	induced drag factor of the part of the wing in a jet calculated as if it were an independent planform not extending beyond the jet
r_{j1}	induced drag factor of the same planform if it were an independent wing in a free stream
r_{jo}	induced drag factor of the same planform in a static jet
CL_f	lift coefficient of the unblown part of the wing
α_f	effective angle of attack of the unblown part of the wing
$CL_{j\mu}$	lift coefficient of the part of the wing in a jet
CL_{j1}	lift coefficient attributed to this part of the wing when the whole wing is in a free stream
CD_f	coefficient of induced drag of the unblown part of the wing
$CD_{j\mu}$	coefficient of induced drag of the part of the wing in a jet

Lift and induced drag in a free stream:

These can be calculated by Weissinger lifting surface theory as developed by De Young and Harper (ref. 1). Assuming that the wing is not twisted, the induced drag is proportional to the square of the lift

$$CD = r\,CL^2$$

and the induced downwash angle is

$$\alpha_i = r\,CL$$

where r is the induced drag factor.

For a rectangular untwisted wing, a quick estimate can be made by the following formulas which have been found to be in close agreement with the results of detailed calculations.

$$CL_\alpha = 2\pi \frac{AR}{AR + 3\,\dfrac{AR^2 + 2}{AR^2 + 1.5}} \tag{6.18}$$

$$r = \frac{1 + .006AR}{\pi AR} \tag{6.19}$$

Lift slope and induced drag factors for the section of a wing in a jet:

The blown region is replaced by a rectangular planform of equal area, and the lift slope and induced drag factors for an isolated wing of this planform in a free stream must then be calculated by lifting surface theory, or else estimated by the formulas given above with the aspect ratio of the blown planform as

$$CL_{\alpha_{j1}} = 2\pi \frac{AR_{wj}}{AR_{wj} + 3\,\dfrac{AR_{wj}^2 + 2}{AR_{wj}^2 + 1.5}} \tag{6.20}$$

$$r_{j1} = \frac{1 + .006AR_{wj}}{\pi AR_{wj}} \tag{6.21}$$

Then, for a circular slipstream (equations (2.5) - (2.8) of section 2)

$$\frac{CL_{\alpha_{jo}}}{CL_{\alpha_{j1}}} = \frac{AR_{wj} + 2}{AR_{wj} + 3.54} \tag{6.22}$$

$$\frac{CL_{\alpha_{j\mu}}}{CL_{\alpha_{j1}}} = \frac{1}{1 + \left(\frac{CL_{\alpha_{j1}}}{CL_{\alpha_{jo}}} - 1\right) \frac{1-\mu^2}{1+\mu^2}} \tag{6.23}$$

$$\frac{r_{jo}}{r_{j1}} = 1.68 \tag{6.24}$$

$$\frac{r_{j\mu}}{r_{j1}} = \frac{1.68 + .32\mu^2}{1 + \mu^2} \tag{6.25}$$

and for a rectangular slipstream (equations (2.1) - (2.4) of section 2)

$$\frac{CL_{\alpha_{jo}}}{CL_{\alpha_{j1}}} = \frac{AR_{wj} + 2}{AR_{wj} + 2AR_j + \frac{2.5}{1 + AR_j}} \tag{6.26}$$

$$\frac{CL_{\alpha_{j\mu}}}{CL_{\alpha_{j1}}} = \frac{1}{1 + \left(\frac{CL_{\alpha_{j1}}}{CL_{\alpha_{jo}}} - 1\right) \frac{1 - \mu^2}{1 + AR_{j\mu}^{\ 2}}} \tag{6.27}$$

$$\frac{r_{jo}}{r_{j1}} = .76(AR_j + e^{-AR_j}) + .53 \tag{6.28}$$

$$\frac{r_{j\mu}}{r_{j1}} = \frac{\frac{r_{jo}}{r_{j1}} + \left(1 + AR_j - \frac{r_{jo}}{r_{j1}}\right) \mu^2}{1 + AR_j \mu^2} \tag{6.29}$$

Lift and induced drag of the wing at small angles:

$$\overline{V}^2 \overline{S} CL = \left(S - \sum_{jets} S_{wj}\right) V^2 CL_f + \sum_{jets} S_{wj} V_j^2 CL_{j\mu} \tag{6.30}$$

$$\overline{V}^2 \overline{S} CD = \left(S - \sum_{jets} S_{wj}\right) V^2 CD_f$$

$$+ \sum_{jets} S_{wj} V_j^2 \left(CD_{j\mu} + CL_{j\mu} \epsilon\right) \tag{6.31}$$

where $\overline{V}$ is the reference velocity

$$CL_f = CL_{\alpha_1} \alpha_f \tag{6.32}$$

$$\alpha_f = \alpha + \sum_{jets} \frac{S_{wj}}{S} \epsilon_j \tag{6.33}$$

$$CL_{j\mu} = CL_{\alpha j\mu}\,\alpha_{wj\mu} + \frac{V^2}{V_j^2}\left(CL_{\alpha 1}\,\alpha - CL_{\alpha j1}\,\alpha_{wj1}\right) \tag{6.34}$$

$$CL_{j1} = CL_{\alpha 1}\,\alpha \tag{6.35}$$

$$CD_f = r_1\,CL_f^2 \tag{6.36}$$

$$CD_{j\mu} = \frac{V^2}{V_j^2}\,CL_{j1}\left(r_{j\mu}\,CL_{j\mu} + r_1\,CL_{j1} - r_{j1}\,CL_{j1}\right) + \left(CL_{j\mu} - \frac{V^2}{V_j^2}\,CL_{j1}\right) r_{j\mu}\,CL_{j\mu} \tag{6.37}$$

Lift slope of the wing:

The lift slope can be obtained by solving (6.11), (6.15), and (6.16) for the change in upwash which results from a unit change of α, and substituting these values in (6.32) - (6.37); that is, by calculating CL_f and $CL_{j\mu}$ when $i_w = i_j = 0$ and $\alpha = 1$.

Reference velocity:

Usually it is most convenient to take $\overline{V} = V_j$, so that a meaning can be attached to CL and CD when V = 0. If the jet velocity is different in different slipstreams, the same formulas can be used, and then it is convenient to define $\overline{V}$ as the root mean square jet velocity

$$\frac{\sum_{\text{jets}} S_p V_j^2}{\sum_{\text{jets}} S_p}$$

where for each jet, S_p is the area of the actuator by which it was generated.

D. Effect of flaps

Symbols:

δ	flap deflection
α/δ_{2D}	flap effectiveness in two dimensions
α/δ_1	flap effectiveness for three dimensional wing in a free stream
$\alpha/\delta_{j\mu}$	flap effectiveness for the section of a wing in a jet
i_{w1}	effective incidence of the wing in a free stream
$i_{wj\mu}$	effective incidence of the section of the wing in a jet

Effective wing incidence:

The wing incidence i_w is increased by the equivalent angle of attack due to flap deflection; for the wing outside the jet, the equivalent incidence is

$$i_{w1} = i_w + \alpha/\delta_1 \, \delta \tag{6.38}$$

where

$$\alpha/\delta_1 = \frac{\sqrt{\alpha/\delta_{2D}} + \alpha/\delta_{2D} \dfrac{AR + 4.5}{AR + 2} AR}{\sqrt{\alpha/\delta_{2D}} + \dfrac{AR + 4.5}{AR + 2} AR} \tag{6.39}$$

For a section of the wing in a slipstream, the equivalent incidence is

$$i_{wj\mu} = i_w + \alpha/\delta_{j\mu} \, \delta \tag{6.40}$$

where for a circular jet

$$\alpha/\delta_{j\mu} = 1 - \mu^2 + \mu^2 \quad \alpha/\delta_1 \tag{6.41}$$

and for a rectangular jet

$$\alpha/\delta_{j\mu} = \frac{1}{2}\left(1 + \frac{1}{AR_j}\right)(1 - \mu^2) + \mu^2 \; \alpha/\delta_1 \tag{6.42}$$

i_{w1} and $i_{wj\mu}$ should be substituted for i_w in (6.11) and (6.15).

Chord extension:

If there is a chord extension due to the flaps, the aspect ratio and area of the wing (and of its blown sections) should be corrected to allow for this, although it may be preferred to use the original wing area as the reference area in (6.30) and (6.31).

E. Wing forces at large angles of attack

Symbols:

$CL_{\alpha f}$	lift slope of the unblown part of the wing
$CL_{\alpha j}$	lift slope of the part of the wing in a jet
α_{of}	zero lift angle of the unblown part of the wing
$\alpha_{oj\mu}$	zero lift angle of the part of the wing in a jet
$\alpha_{max_{2D}}$	angle of maximum lift of the two dimensional airfoil, measured from the zero lift angle
α_{max1}	angle of maximum lift of the wing in a free stream
α_{maxf}	angle of maximum lift of the unblown part of the wing
$\alpha_{max_{j\mu}}$	angle of maximum lift of the part of the wing in a jet

Zero lift angles of the blown and unblown parts of the wing:

Find the lift slopes CL_{α_f} and CL_{α_j} of the unblown part of the wing and each part in a jet by setting $i_w = i_j = 0$ and $\alpha = 1$ in (6.11), (6.15), (6.16), and (6.32) - (6.37); calculate the lift coefficients CL_f and $CL_{j\mu}$ when $\alpha = 0$; then

$$\alpha_{of} = -\frac{CL_f \; (\alpha = 0)}{CL_{\alpha_f}} \tag{6.43}$$

$$\alpha_{oj} = -\frac{CL_{j\mu} \quad (\alpha = 0)}{CL_{\alpha j}} \tag{6.44}$$

Stalling angles:

For the wing in a free stream

$$\alpha_{max_1} = \frac{1.6\pi}{CL_{\alpha_1}} \quad \frac{AR}{\sqrt{AR^2 + 4}} \quad \alpha_{max_{2D}} \tag{6.45}$$

For the unblown part of the wing

$$\alpha_{max_f} = \alpha_{max_1} \tag{6.46}$$

For each part in a jet

$$\alpha_{max_{jo}} = .8 \left(1 + \frac{2}{\sqrt{AR^2 + 4}}\right) \alpha_{max_{2D}} \tag{6.47}$$

$$\alpha_{max_{j\mu}} = (1 - \mu^2)\ \alpha_{max_{jo}} + \mu^2\ \alpha_{max_1} \tag{6.48}$$

Lift and drag of the blown and unblown parts of the wing:

For the unblown part of the wing

$$CL_f = CL_{\alpha_1} \sin(\alpha_f - \alpha_{of}) \ , \quad \alpha_f - \alpha_{of} \leq \alpha_{max_f}$$

$$CL_{\alpha_1} \tan \alpha_{max_f} \cos(\alpha_f - \alpha_{of}) \ , \quad \alpha_f - \alpha_{of} > \alpha_{max_{j\mu}} \tag{6.49}$$

For each part in a jet

$$CL_{j\mu} = CL_{\alpha_j} \sin(\alpha_{wj\mu} - \alpha_{oj\mu}), \quad \alpha_{wj\mu} - \alpha_{oj\mu} \leq \alpha_{max_{j\mu}}$$

$$CL_{\alpha_j} \tan \alpha_{max_{j\mu}} \cos(\alpha_{wj\mu} - \alpha_{oj\mu}),$$

$$\alpha_{wj\mu} - \alpha_{oj\mu} > \alpha_{max_{j\mu}} \tag{6.50}$$

Calculate CD_f and $CD_{j\mu}$ from (6.36) and (6.37) using the above values of CL_f and $CL_{j\mu}$

Lift and drag of the complete wing:

Replace (6.30) and (6.31) by

$$\bar{V}^2\bar{S}CL_w = \left(S - \sum_{jets} S_{wj}\right) V^2 CL_f + \sum_{jets} S_{wj} V_j^2 (CL_{j\mu} \cos\epsilon - CD_{j\mu} \sin\epsilon) \tag{6.51}$$

$$\bar{V}^2\bar{S}CD_w = \left(S - \sum_{jets} S_{wj}\right) V^2 CD_f + \sum_{jets} S_{wj} V_j^2 (CL_{j\mu} \sin\epsilon + CD_{j\mu} \cos\epsilon) \tag{6.52}$$

F. Total forces

Symbols:

CL_W	lift coefficient due to wing
CL_T	lift coefficient due to propeller thrust
CL_N	lift coefficient due to propeller normal force
CD_W	drag coefficient due to wing
CD_T	drag coefficient due to propeller thrust
CD_N	drag coefficient due to propeller normal force

Contribution of propeller thrust to total lift and drag:

Each actuator is inclined through the sum of the angle of attack plus its incidence i_j, therefore

$$\overline{V}^2\overline{S}CL_T = \sum_{\text{jets}} T \sin(\alpha + i_j) \tag{6.53}$$

and regarding the thrust as a negative drag

$$\overline{V}^2\overline{S}CD_T = -\sum_{\text{jets}} T \cos(\alpha + i_j) \tag{6.54}$$

Contribution of propeller normal force to total lift and drag:

$$\overline{V}^2\overline{S}CL_N = \sum_{\text{jets}} S_p V_j^2 CN \cos(\alpha + i_j) \tag{6.55}$$

$$\overline{V}^2\overline{S}CD_N = \sum_{\text{jets}} S_p V_j^2 CN \sin(\alpha + i_j) \tag{6.56}$$

where CN is given by (6.5) and (6.6).

Total lift and drag:

$$CL = CL_W + CL_T + CL_N \tag{6.57}$$

$$CD = CD_W + CD_T + CD_N \tag{6.58}$$

where CD is negative if the propeller thrust exceeds the drag of the other components.

7. Comparison of the theory with tests

The formulas of section 6 have been incorporated in a computer program for quick estimation of the characteristics of V/STOL configurations. This section presents comparisons between the predictions obtained with this program and experimental data. The data was obtained from the following NASA reports:

(1) TN 3307, An Investigation of a Wing-Propeller Employing Large-Chord Plain Flaps and Large Diameter Propellers for Low-Speed Flight and Vertical Take-Off, by Richard E. Kuhn and John W. Draper, 1954.
(2) TN D17, Wind Tunnel Investigation of Effect of Ratio of Wing Chord to Propeller Diameter with Addition of Slats on the Aerodynamic Characteristics of Tilt-Wing VTOL Configurations in the Transition Speed Range, by Robert T. Taylor, 1959.
(3) TN D1586, Aerodynamic Data on a Large Semispan Tilting Wing with 0.6 Diameter Chord, Single Slotted Flap, and Single Propeller Rotating Up at Tip, by Marvin P. Fink, Robert G. Mitchell, and Lucy G. White, 1964.
(4) TN D3375, Aerodynamic Data on a Large Semispan Tilting Wing with 0.5 Diameter Chord, Double Slotted Flap, and Both Left and Right-Hand Rotation of a Single Propeller, by Marvin P. Fink, Robert G. Mitchell, and Lucy G. White, 1966.
(5) TN D4448, Large-Scale Wind-Tunnel Tests of a Deflected Slip-stream STOL Model with Wings of Various Aspect Ratios, by V. Robert Page, Stanley O. Dickinson, and Wallace H. Deckert, 1968.

These were selected because they cover a representative range of configurations. Tests with and without flap deflection will be considered separately.

A. Unflapped Wings

Comparisons are presented in fig. 3 - 9. Each figure shows

(a) a sketch of the configuration with pertinent data
(b) the variation of CL_α with CT
(c) the variation of CL with α for selected thrust coefficients
(d) polar curves of CL against CD for selected thrust coefficients

All the aerodynamic coefficients are referred to the slipstream velocity

$$CT = \frac{T}{\frac{1}{2}\rho V_j^2 S_p}$$

$$CL = \frac{L}{\frac{1}{2}\rho V_j^2 S}$$

$$CD = \frac{D}{\frac{1}{2}\rho V_j^2 S}$$

so that the static case is represented by CT = 1.0, and the lift coefficient decreases as the thrust coefficient increases and the velocity ratio decreases. The drag includes the thrust so that, at small angles of attack, CD is negative.

The assumed angles of zero lift and maximum lift for the two dimensional airfoil section are recorded in each figure. Generally, the lift slope of the free wing was calculated by the method of De Young and Harper (ref. 1). This method was incorporated in the program. In the cases of TN D17 and TN D4448, however, this method was found to give very poor agreement. Values were then assumed for the lift slope of the free wing which yielded agreement with the power-off measurements. The low lift slope recorded in TN D17 might be due to the low Reynolds number at which those tests were conducted. In the case of TN D4448, separation at the wing fuselage junction may have caused a loss of lift.

It can be seen that the theory and the measurements are generally in good agreement. The largest divergences are in the region of the stall, as might be expected, considering the approximate treatment of the stall. When the thrust coefficient is large enough, the stall is suppressed because the jet is aligned with the wing, while the contribution of the unblown part of the wing is negligible. At lower thrust coefficients, there may be separate stall breaks for the blown and unblown parts of the wing. Since no allowance for profile drag was included in the calculations, the theoretical drag curves should be to the left of the experimental points. At high thrust coefficients, the apparent profile drag coefficient is reduced because the drag coefficient of sections outside the slipstream is referred to the higher velocity in the slipstream. In the case of the medium span wing in TN D4448, the theoretical drag curve is to the right of the experimental points. This is because

the reported thrust coefficient based on wing area of 3.8 is not consistent with the measured drag coefficient of -4.0. Generally the induced drag is the dominant component of the drag.

B. Flapped Wings

Comparisons for some representative flap deflections are shown in fig. 10 - 16. Each figure shows

(a) a sketch of the configuration including the flap geometry
(b) the variation of CL with α for selected thrust coefficients
(c) polar curves of CL against CD for selected thrust coefficients

In this case, the program requires data on the following properties of the two dimensional section:

(1) zero lift angle without flap deflection
(2) the flap effectiveness α/δ_{2D}
(3) the flap angle
(4) the chord extension due to the flaps
(5) the angle of maximum lift with the flaps deflected

The assumed values are recorded in the figures.

According to the standard wing theory, a change in the camberline should alter the zero lift angle but not the lift slope of a two dimensional airfoil. If the lift coefficient is referred to the original wing area, flap deflection would then cause an increase in the lift slope proportional to the chord extension. On a three dimensional wing, the increase should be slightly less than this because of the reduction in aspect ratio. In the case of TN D4448, the increase in lift slope measured power off was much greater than the increase in wing area. The values of CL_α power off and α/δ used in the calculations were selected to give reasonable agreement in the absence of power effects. In all the other cases CL_α power off was calculated by the program for the true planform with chord extension, but referred to the original wing area.

The agreement between the theory and the tests is fair. The largest source of error is again the prediction of the stalling angle under power. It appears that the application of power sometimes delays the stall. There is a tendency to underestimate the lift slope at medium thrust coefficients. Also, the profile drag can become important when flaps are deflected through large angles, with a consequent separation of the flow.

C. Static tests of flap turning effectiveness

It would be possible to improve the prediction of the performance of flapped wings if more was known about the effect of the jet on the flap effectiveness α/δ. Tests have generally been made of wings with propellers attached to them so that the angle of attack of the wing in the jet was fixed, and only the flap angle was varied. As a result, the flap effectiveness cannot be directly determined; but if theoretical values of CL_α are assumed for the wing in the jet, it is possible to impute values of α/δ.

When the aircraft is static, the performance can conveniently be measured by the angle θ through which the jet is turned. For conservation of momentum

$$\sin\theta = \frac{L}{T}$$

Now the turning angles of rectangular wings in rectangular jets is shown in fig. 3 of Part 1. For a given jet width, the turning effectiveness θ/α of the wing increases as its chord is increased towards a limiting value for a wing of infinite chord or zero aspect ratio. This limiting value is plotted in fig. 17. It is generally less than unity but increases towards unity as the jet width increases. For a square jet

$$\theta/\alpha_{\max} = .5$$

The limiting turning effectiveness of a wing spanning a circular jet can be determined by slender wing theory. In the static case, the result of Graham et al. (ref. 6) reduces to

$$CL_\alpha = \frac{\pi AR}{2}\left(1 - \frac{4}{\pi^2}\right)$$

Then if B and c are the jet diameter and wing chord

$$L_\alpha = \frac{1}{2}\rho V_j^2 BcCL_\alpha$$

$$= \rho V_j^2 \pi \frac{B^2}{4}\left(1 - \frac{4}{\pi^2}\right)$$

while

$$T = \rho V_j^2 \frac{\pi B^2}{4}$$

Since θ/α equals L_α/T, it may be deduced that for a circular jet

$$\theta/\alpha_{max} = 1 - \frac{4}{\pi^2} = .595$$

The inability of a wing to deflect a jet through its full angle of attack has a simple physical explanation. Sketch 2(a) shows a view of the cross plane. The pressure differential Δp is zero at the jet boundary, negative in the center of the jet above the wing, and positive below it. The pressure gradient induces an inward flow above the wing and an outward flow below it. To conform the surface velocity to the angle of attack of the wing, there must be a downward flow. When this is superposed on the spanwise flows, the streamlines in the cross plane have a shape like that depicted in sketch 2(b). They converge above the wing and diverge below it. The average downward velocity is less than the downward velocity $V_j \alpha$ at the wing surface, and the average deflection angle θ is less than α. It is thus an edge effect which prevents the wing turning the jet through the full wing angle. As the jet becomes wider, the influence of the boundary is progressively diminished until finally the theory predicts that an infinitely wide jet would follow round the wing surface, in agreement with the well known Coanda effect.

Kuhn has digested the results of a number of tests of flapped wings in jets (ref. 7). In fig. 18, he gives a curve of the turning effectiveness of flaps as a function of their chord. A detailed analysis of numerous experiments has been made and some typical results are shown in fig. 19 - 20. It can be seen that for some flap configurations, θ/δ has been measured as high as .75. If the theoretical maximum value of θ/α is substituted in the relation

$$\theta/\delta = \theta/\alpha \quad \alpha/\delta$$

then Kuhn's curve would imply values of the α/δ greater than unity. The precise value imputed to θ/α_{max} by the theory depends on the application of the boundary

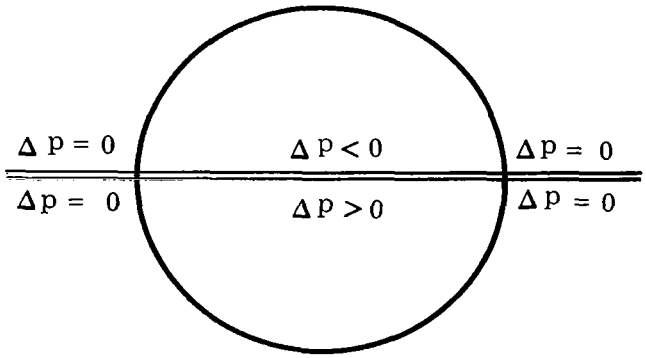

(a) Pressure gradients

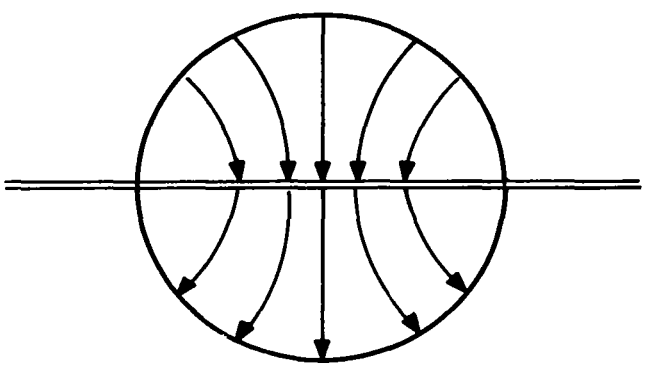

(b) Streamlines

Sketch 2. Flow in the Cross Plane of a Jet Over a Wing

condition without regard for jet deflection and distortion. Nevertheless the preceeding physical agreement indicates that the deflection angle of a narrow jet should be substantially less than the wing trailing edge angle. It may be concluded that the flap effectiveness α/δ can be close to unity. The formulas (4.3) and (4.4) in section 4 were designed to take account of this.

8. Conclusions

The determination of the lift and drag of a wing in the slipstream of several propellers requires massive calculations even when the problem is simplified by using the equations of an ideal fluid, ignoring slipstream deflection and distortion, and linearizing the boundary conditions. The use of a rectangular jet to approximate the slipstream permits standard imaging techniques to be used to treat the case of a static wing propeller combination. The effect of forward speed can be treated approximately by multiplying the interference potential by a scalar strength factor derived with the aid of studies of elliptic jets. By introducing the idea of the equivalent mass flow influenced by the wing, it is possible to find simple formulas which closely approximate the results of the detailed calculations. These formulas provide the basis of a method suitable for engineering calculations which shows good correlation with existing experimental data for wings without flaps.

The method can also be used to predict the lift and drag of propeller-wing-flap combinations if suitable values are assumed for the flap effectiveness α/δ in a jet. Experimental evidence suggests that the flap effectiveness is substantially increased in a jet and may be close to unity. Because of edge effects, it can be expected that a wing will not deflect a jet through the full angle of attack. Yet static tests of flaps in jets indicate that the turning ratios of flaps may even exceed the theoretical maximum value for wings of infinite chord. There is a need for tests in which the jet producing device is removed from the wing so that both angle of the wing in the jet and the flap angle can be varied to give precise measurements of CL_α , CL_δ and α/δ . It is possible that jet distortion is important, and it would lead to a better insight into the problem if observations were also made of the final shape of the jet cross section.

Two principal computer programs have been developed

(1) for the calculation of the lift of a symmetric wing in a rectangular jet according to the theory of Part 1.
(2) for the prediction of the characteristics of practical V/STOL configurations according to the engineering method described in Part 2.

These are available through the COSMIC Computer Library, Computer Software Management and Information Center, Barrow Hall, University of Athens, Georgia 30601.

REFERENCES:

1. DeYoung, John and Harper, Charles W.: Theoretical Symmetric Span Loading at Subsonic Speeds for Wings Having Arbitrary Planform. NACA TR 921, 1948.

2. DeYoung, John: Propeller at High Incidence. J. of Aircraft, Vol. 2, No. 3, May 1965, pp. 241-250.

3. Lowry, John G. and Polhamus, Edward C.: A Method for Predicting Lift Increments Due to Flap Deflection at Low Angles of Attack in Incompressible Flow. NACA TN 3911, 1957.

4. DeYoung, John: Spanwise Loading for Wings and Control Surfaces of Low Aspect Ratio. NACA TN 2011, 1950.

5. Hayes, William C., Jr., Kuhn, Richard E., and Sherman, Irving R.: Effects of Propeller Position and Overlap on the Slipstream Deflection Characteristics of a Wing-Propeller Configuration Equipped with a Sliding and Fowler Flap. NACA TN 4404, 1958.

6. Graham, E. W., Lagerstrom, P. A., Licher, R. M., and Beane, B. J.: A Preliminary Theoretical Investigation of the Effects of Propeller Slipstream on Wing Lift. Douglas Rep. SM 14991, 1953.

7. Kuhn, Richard E.: Semiempirical Procedure for Estimating Lift and Drag Characteristics of Propeller-Wing-Flap Configurations for Vertical and Short Take-Off and Landing Airplanes. NASA Memo. 1-16-59L, 1959.

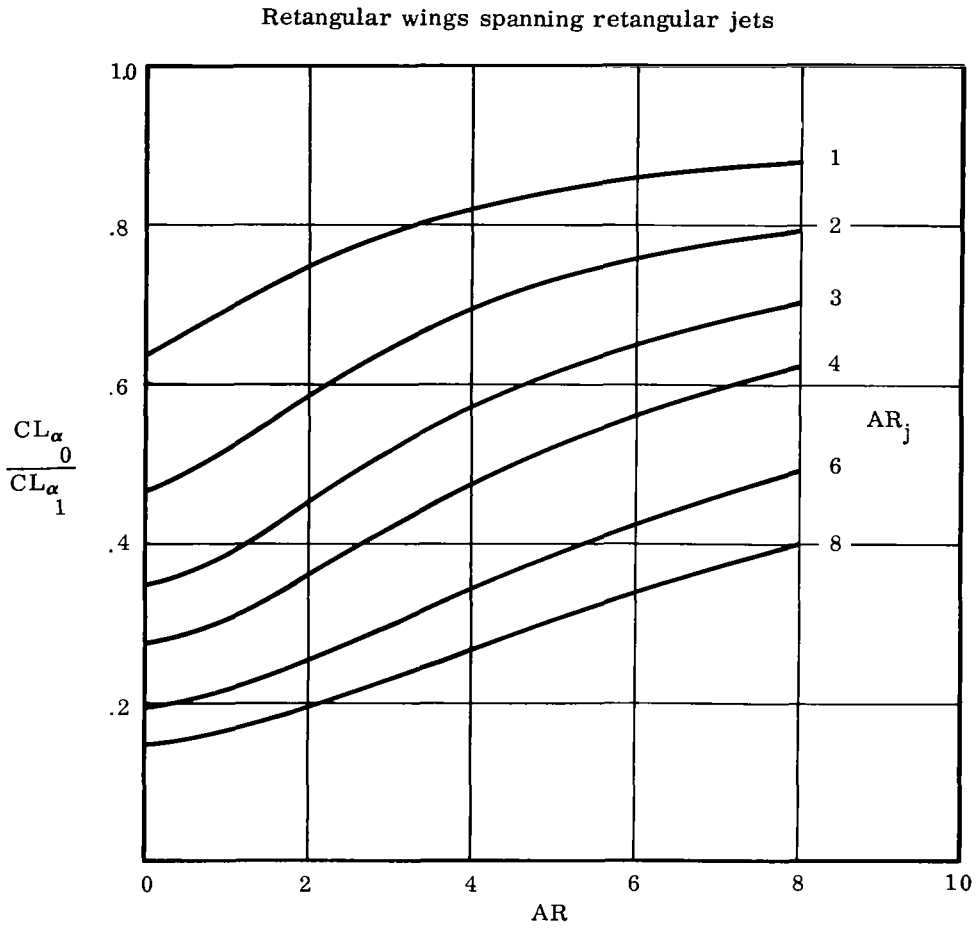

Figure 1. Ratio of Lift in a Static Jet to Lift in a Free Stream

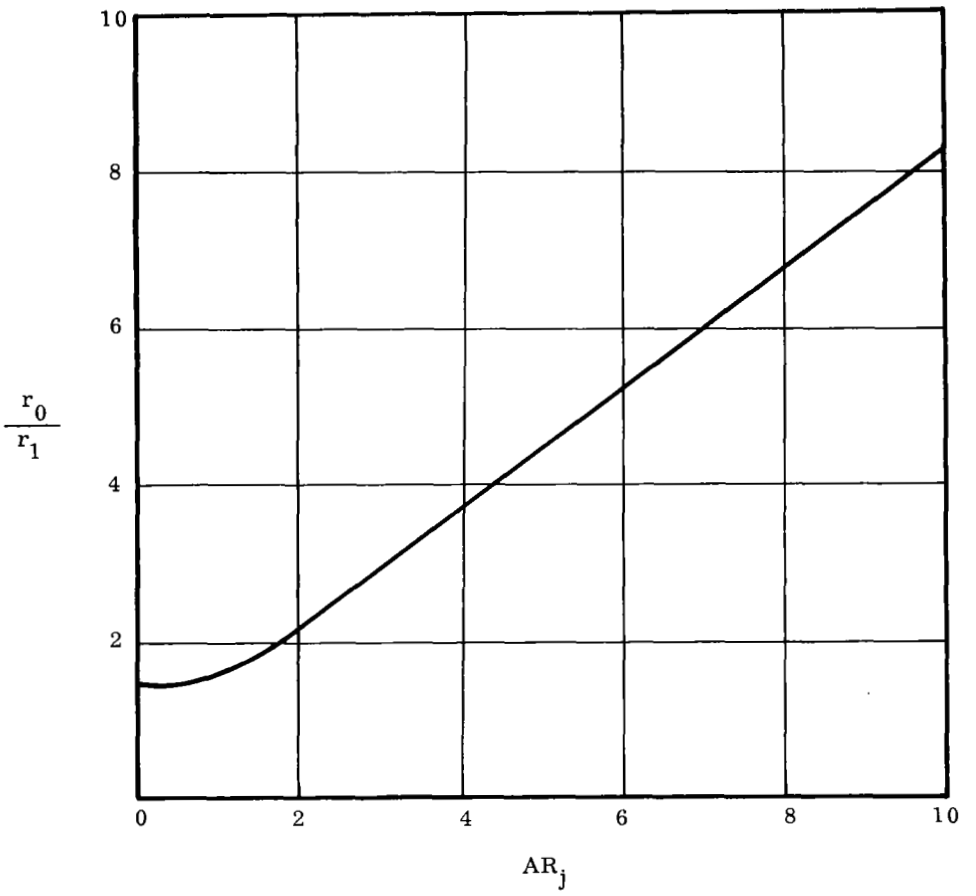

Figure 2. Ratio of Induced Drag in a Static Jet to Induced Drag in a Free Stream

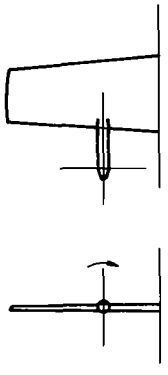

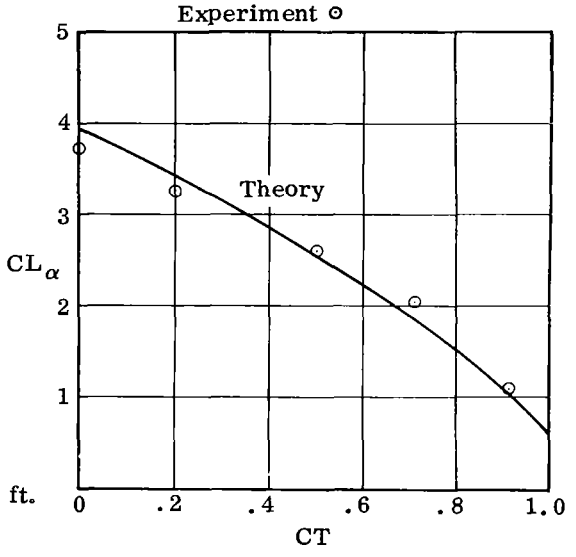

Span	6.83 ft.	Area	10.25 sq. ft.
AR	4.55	Taper	.714
Section	NACA 0015	$\alpha_{zero\ lift}$	0°
$\alpha_{max\ CL}$	14.0^o	Prop D	2.0 ft.

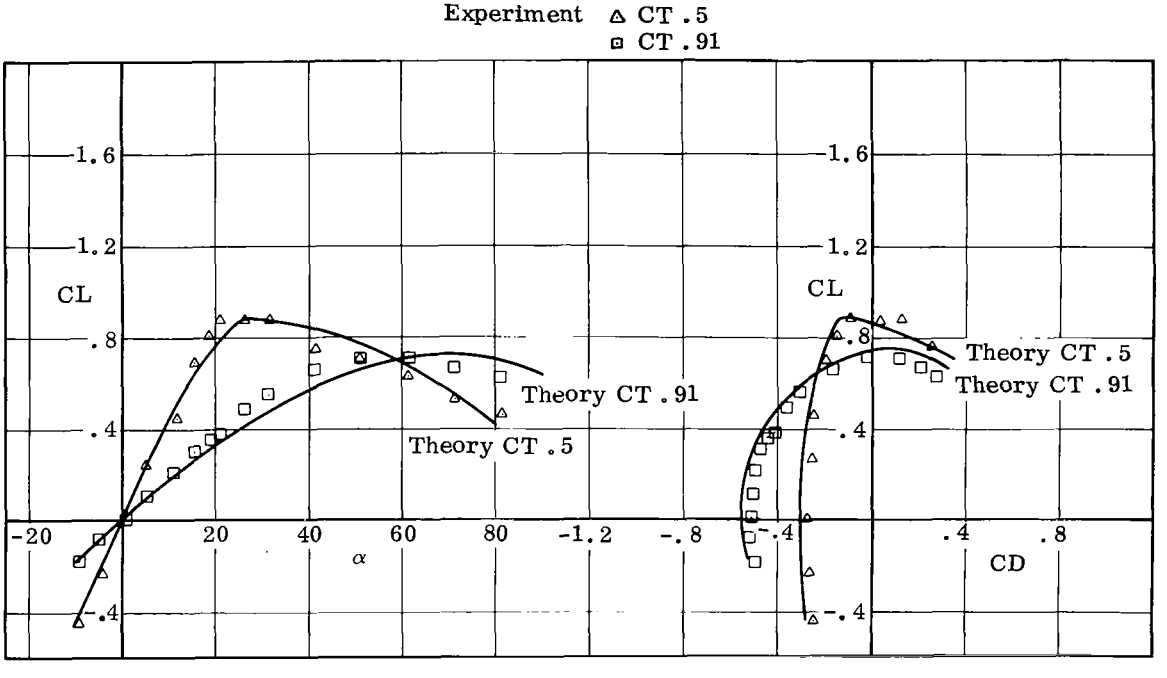

Figure 3. Correlation with TN 3307 (2 Propellers); Coefficients Referred to Slipstream Velocity

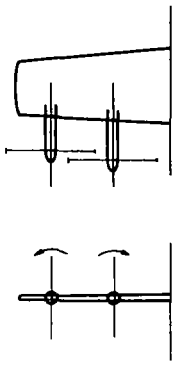

Span	6.83 ft.	Area	10.25 sq. ft.
AR	4.55	Taper	.714
Section	NACA 0015	α zero lift	0°
α max CL	14.0°	Prop D	2.0 ft.

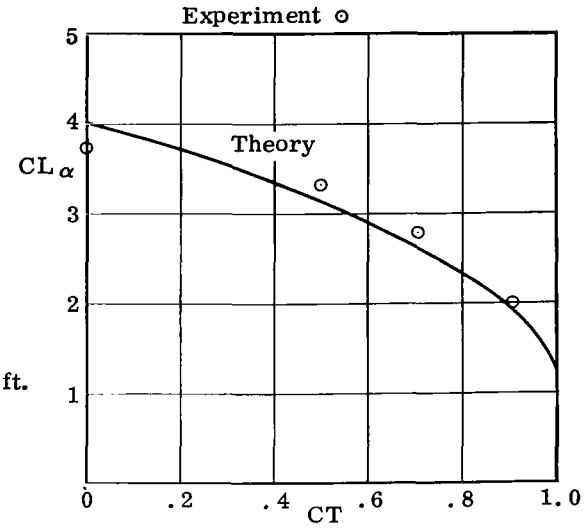

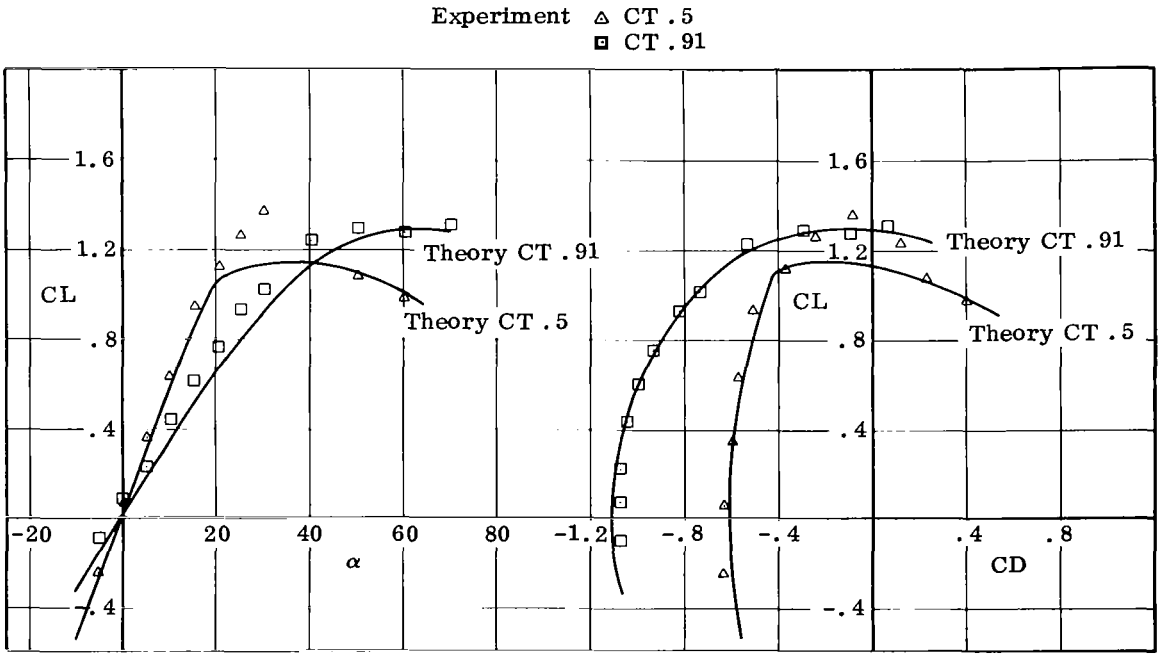

Figure 4. Correlation with TN 3307 (4 Propellers); Coefficients Referred to Slipstream Velocity

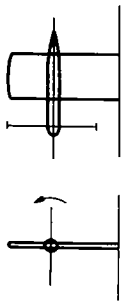

Span	5.0 ft.	Area	5.0 sq. ft.
AR	5.0	Taper	1.0
Section	NACA 0015	α zero lift	0°
α max CL	14.0^{o}	Prop D	2.0 ft.

CL_{α} power off to be 3.25 per radian

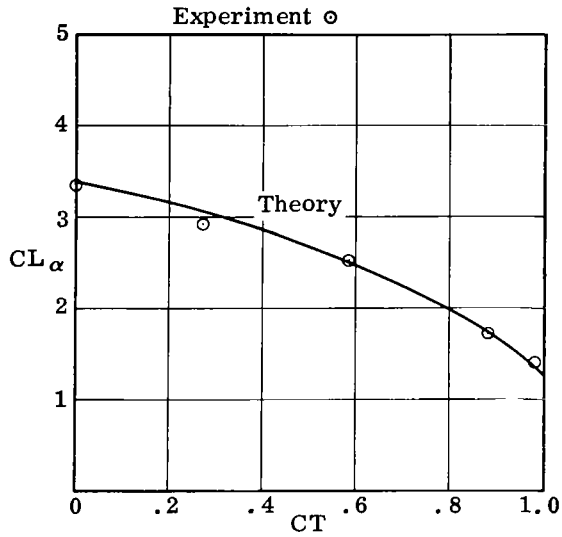

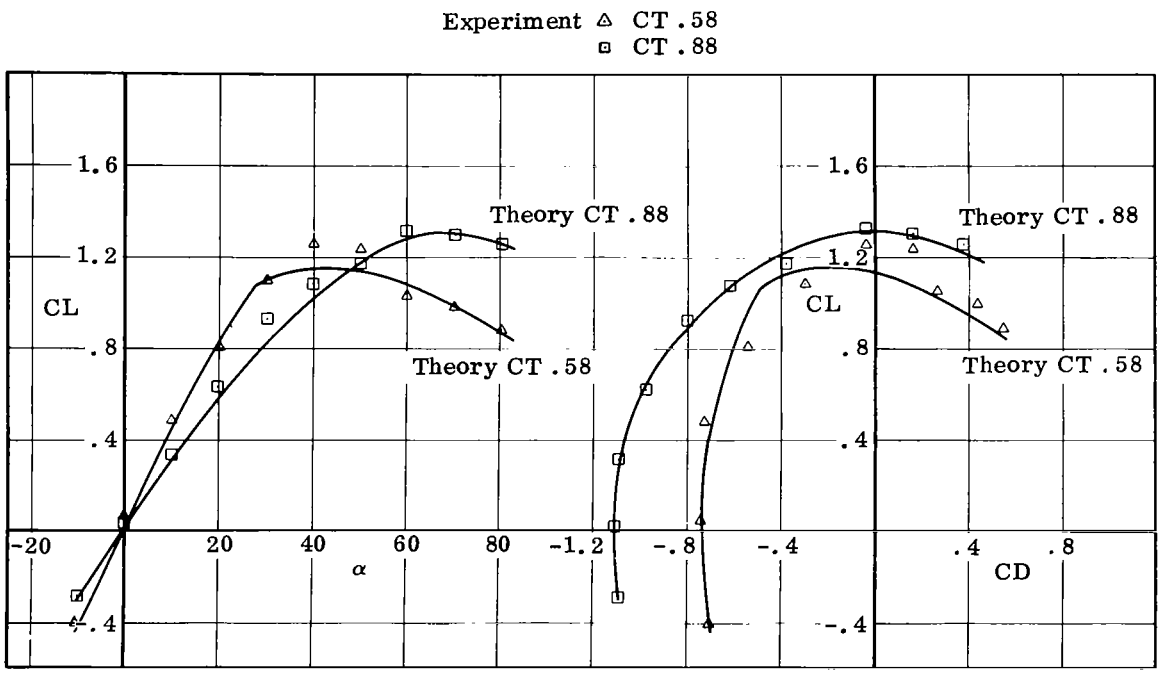

Figure 5. Correlation with TN D17 (Chord-Diameter Ratio .5); Coefficients Referred to Slipstream Velocity

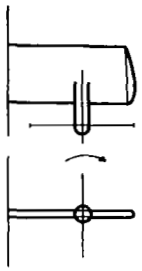

Span	13.8 ft.	Area	47.2 sq. ft.
AR	4.05	Taper	1.0
Section	NACA 4415	$\alpha_{zero\ lift}$	-4.5^{o}
$\alpha_{max\ CL}$	12.5^{o}	Prop D	5.67 ft.

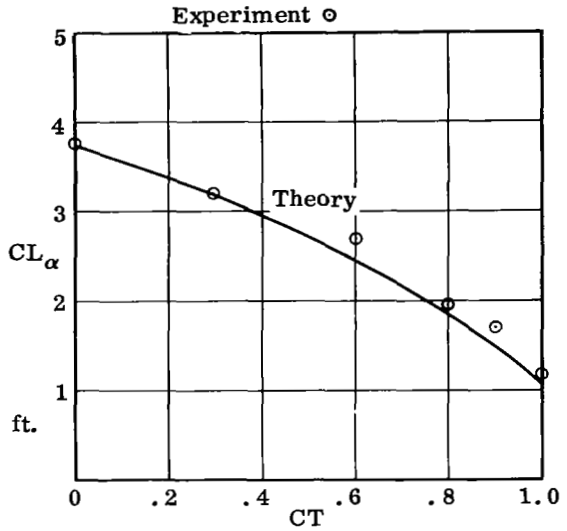

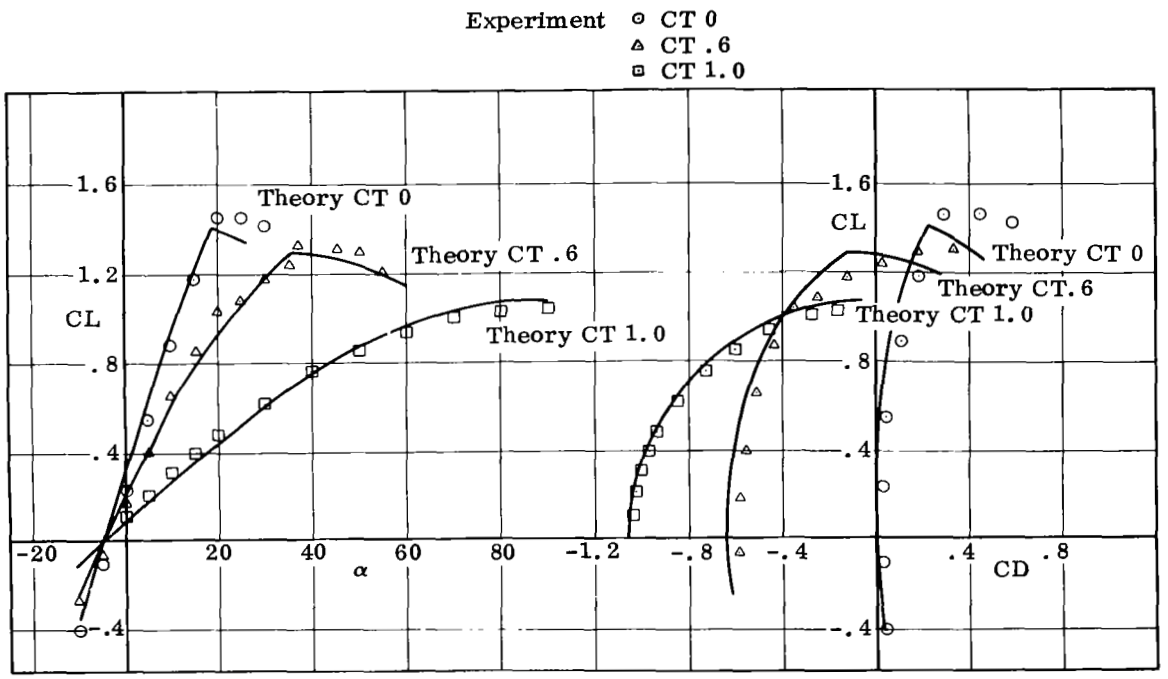

Figure 6. Correlation with TN D1586; Coefficients Referred to Slipstream Velocity

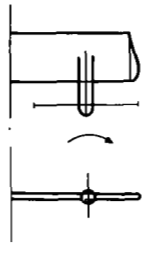

Span	13.8 ft.	Area	39.2 sq. ft.
AR	4.88	Taper	1.0
Section	NACA 4415	$\alpha_{zero\ lift}$	-4.5^{o}
$\alpha_{max\ CL}$	12.5^{o}	Prop D	5.67 ft.

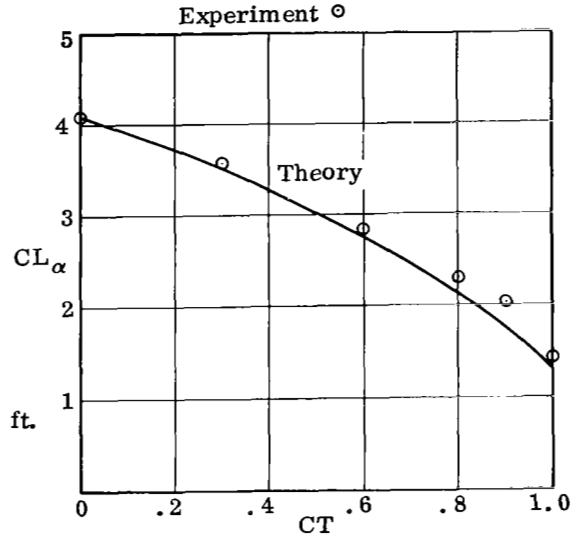

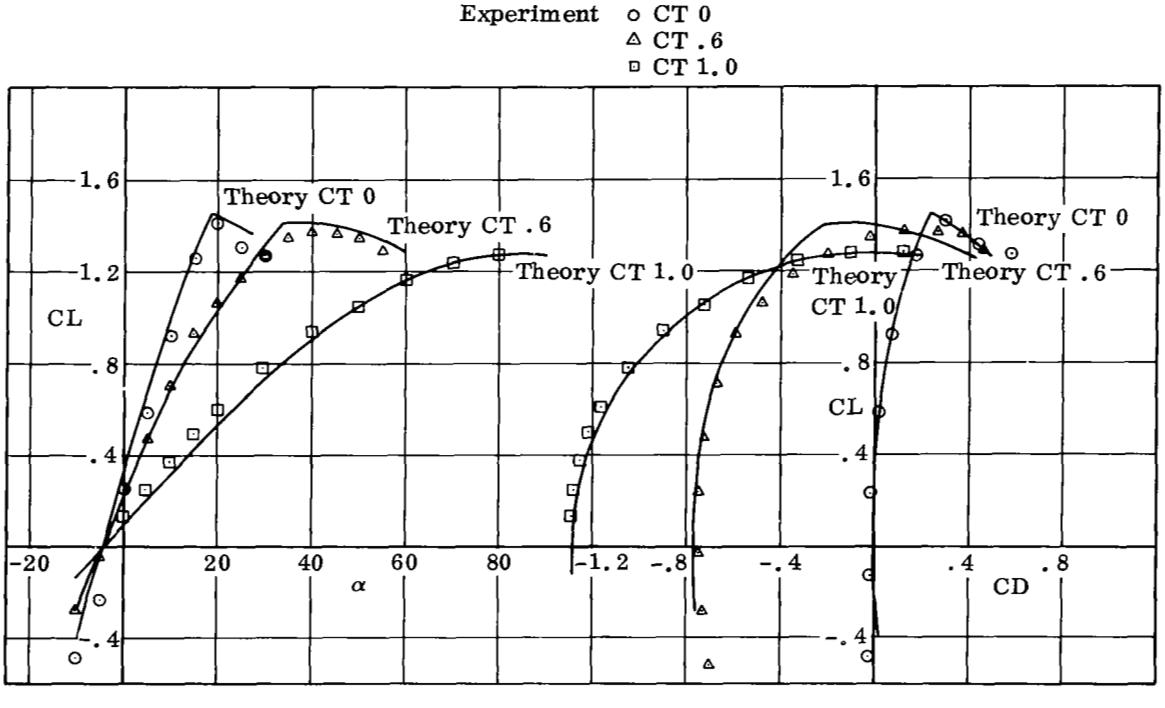

Figure 7. Correlation with TN D3375; Coefficients Referred to Slipstream Velocity

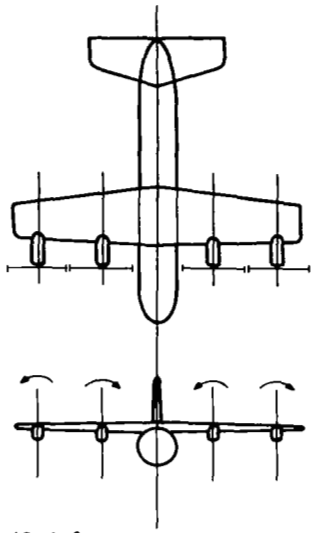

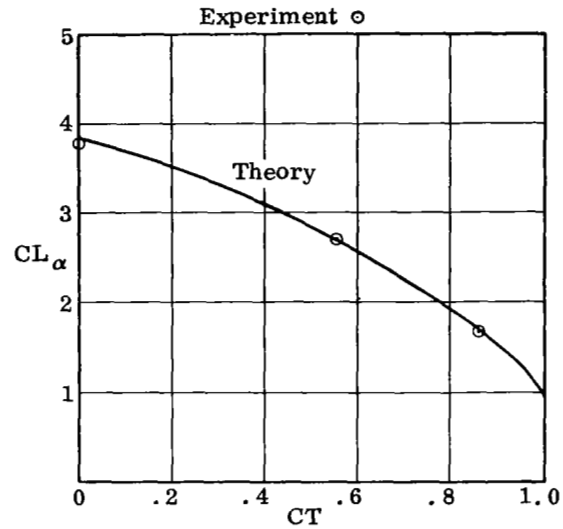

Span	43.3 ft.	Area	329 sq. ft.
AR	5.71	Taper	.554
Section	NACA 63_2 416	$\alpha_{zero\ lift}$	-2.5°
$\alpha_{max\ CL}$	15.5°	Prop D	9.3 ft.
Fuselage D	6.0 ft.		

CL_α power off taken to be 3.70 per radian

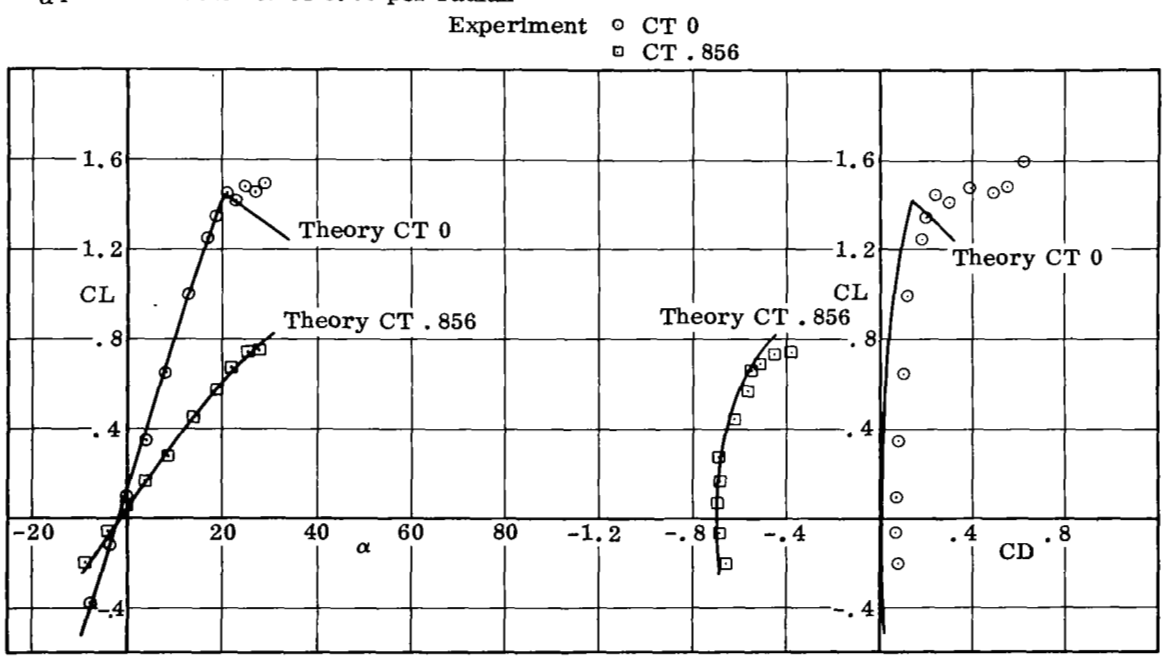

Figure 8. Correlation with TN D4448 (Short Wing); Coefficients Referred to Slipstream Velocity

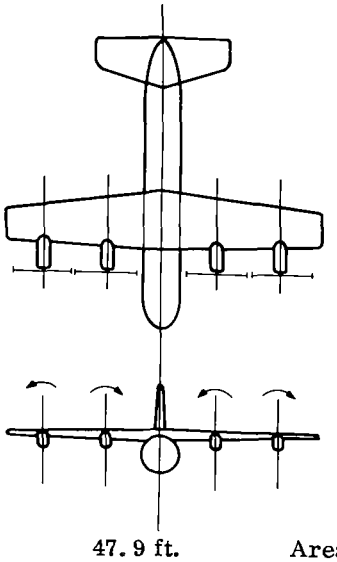

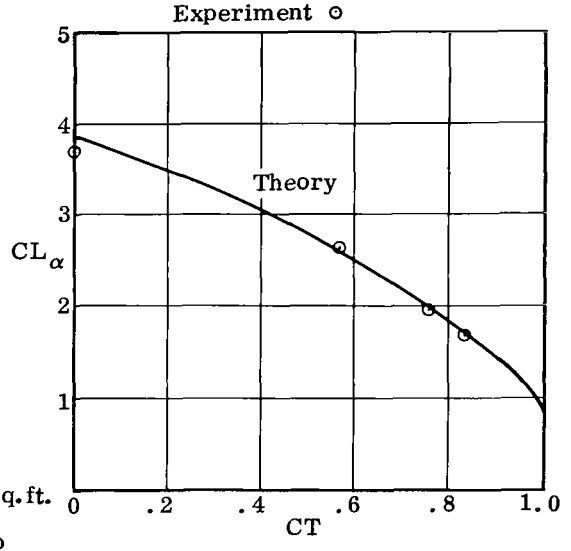

Span	47.9 ft.	Area	353 sq.ft.
AR	6.52	Taper	.507
Section	NACA 63_2-416	$\alpha_{zero\ lift}$	-2.5°
$\alpha_{max\ CL}$	15.5°	Prop D	9.3 ft.
Fuselage D	6.0 ft.		

CL_α power off taken to be 3.75 per radian

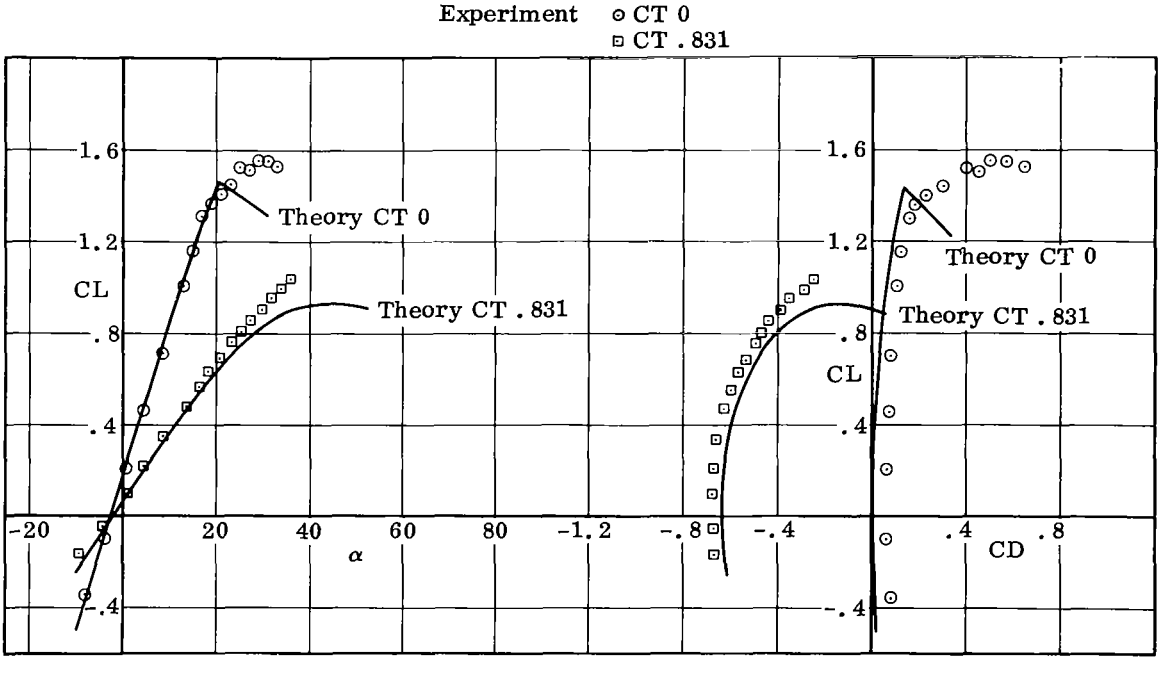

Figure 9. Correlation with TN D4448 (Medium Wing); Coefficients Referred to Slipstream Velocity

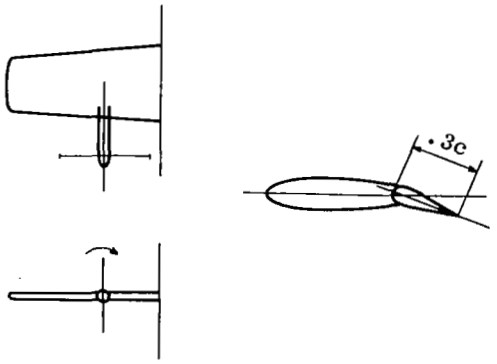

Span	6.83 ft.	Area	10.25 sq. ft.
AR	4.55	Taper	.714
Section	NACA 0015	$\alpha_{zero\ lift}$	0°
δ flap	20°	Chord extension	0
α/δ_{2D}	.4	$\alpha_{max\ CL}$	12.0^o
Prop D	2.0 ft.		

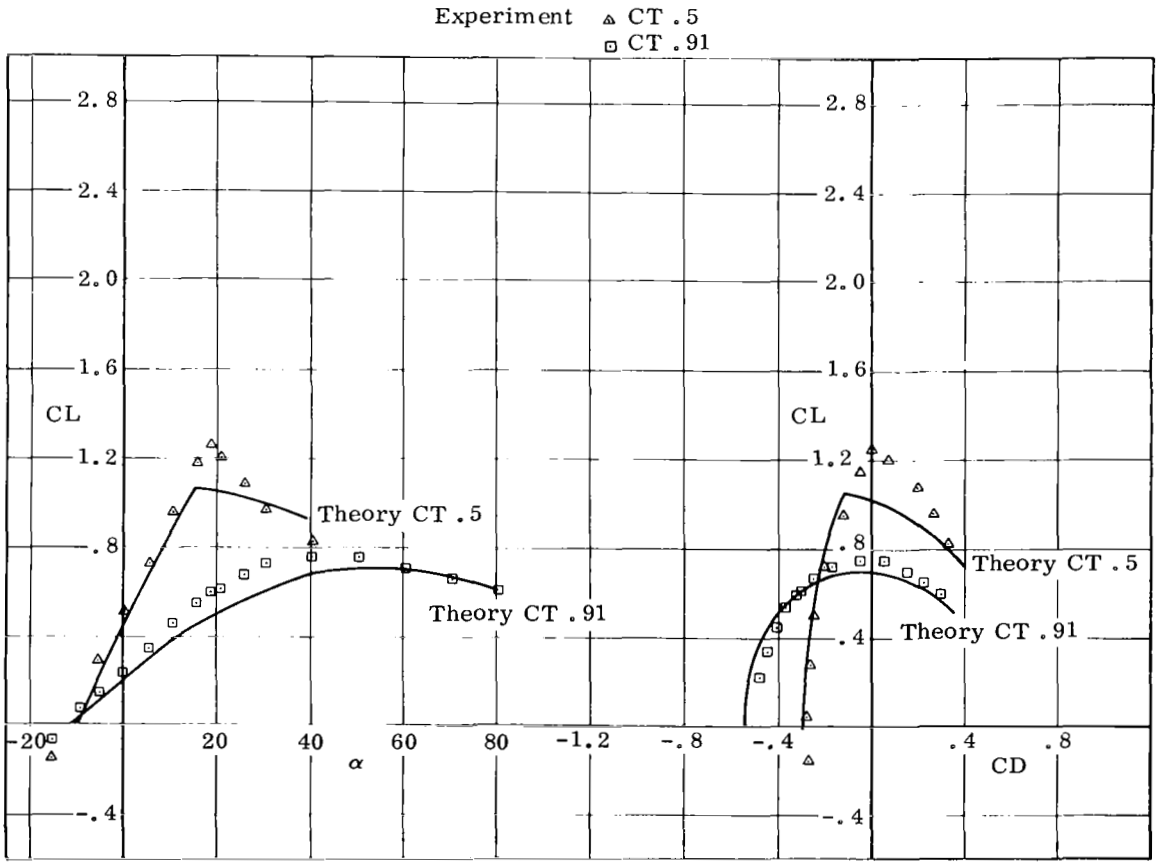

Figure 10. Correlation with TN 3307 (2 Propellers); Flap 20°; Coefficients Referred to Slipstream Velocity

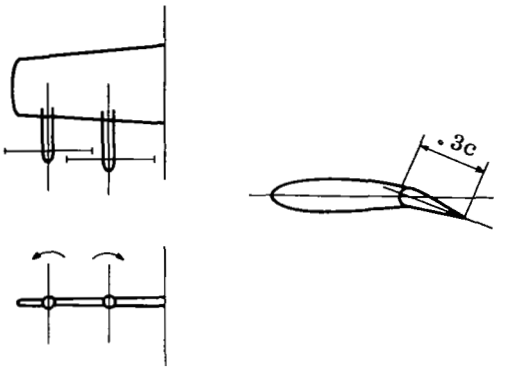

Span	6.83 ft.	Area	10.25 sq. ft.
AR	4.55	Taper	.714
Section	NACA 0015	$\alpha_{zero\ lift}$	0°
δ flap	20°	Chord extension	0
α/δ_{2D}	.40	$\alpha_{max\ CL}$	12.0^{o}
Prop D	2.0 ft.		

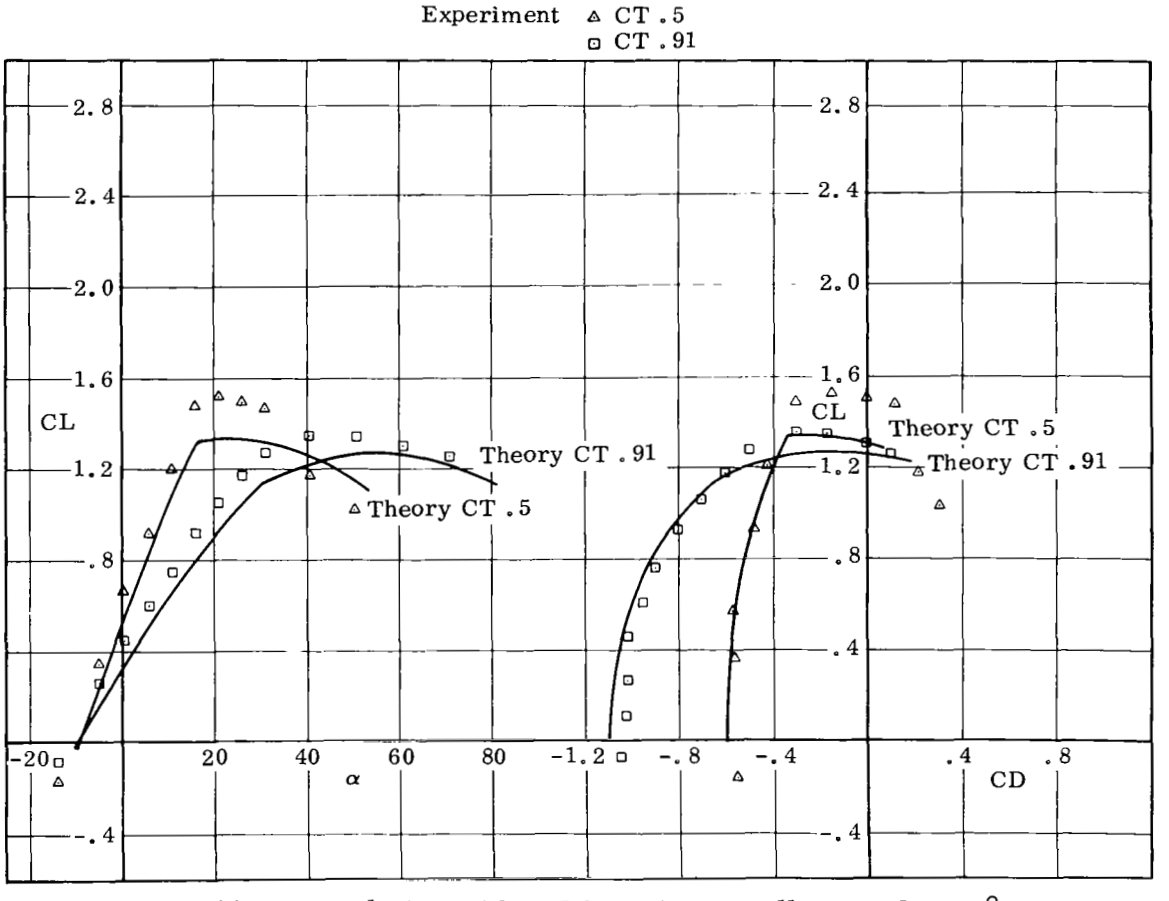

Figure 11. Correlation with TN 3307 (4 Propellers); Flap 20°; Coefficients Referred to Slipstream Velocity

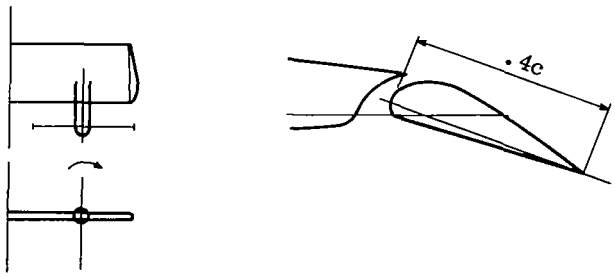

Span	13.8 ft.	Area	47.2 sq. ft.
AR	4.05	Taper	1.0
Section	NACA 4415	$\alpha_{\text{zero lift}}$	-4.5°
δ flap	20°	Chord extension	.025
α/δ_{2D}	.50	$\alpha_{\text{max CL}}$	12.5°
Prop D	5.67 ft.		

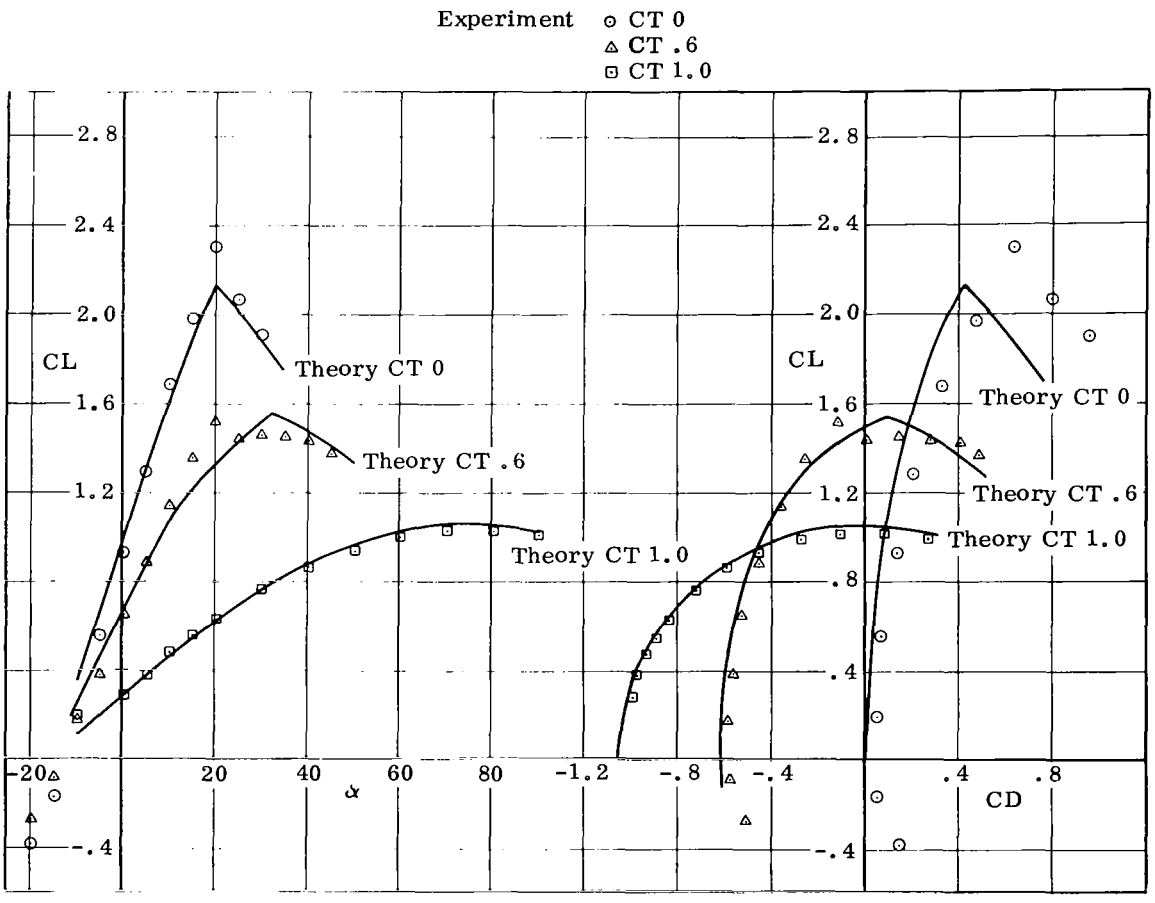

Figure 12. Correlation with TN D1586; Flap 20°; Coefficients Referred to Slipstream Velocity

Span	13.8 ft.	Area	47.2 sq. ft.
AR	4.05	Taper	1.0
Section	NACA 4415	α zero lift	-4.5°
δ flap	40°	Chord extension	.05
α/δ_{2D}	.40	α max CL	13.5°
Prop D	5.67 ft.		

Experiment ⊙ CT 0
△ CT .6
⊡ CT 1.0

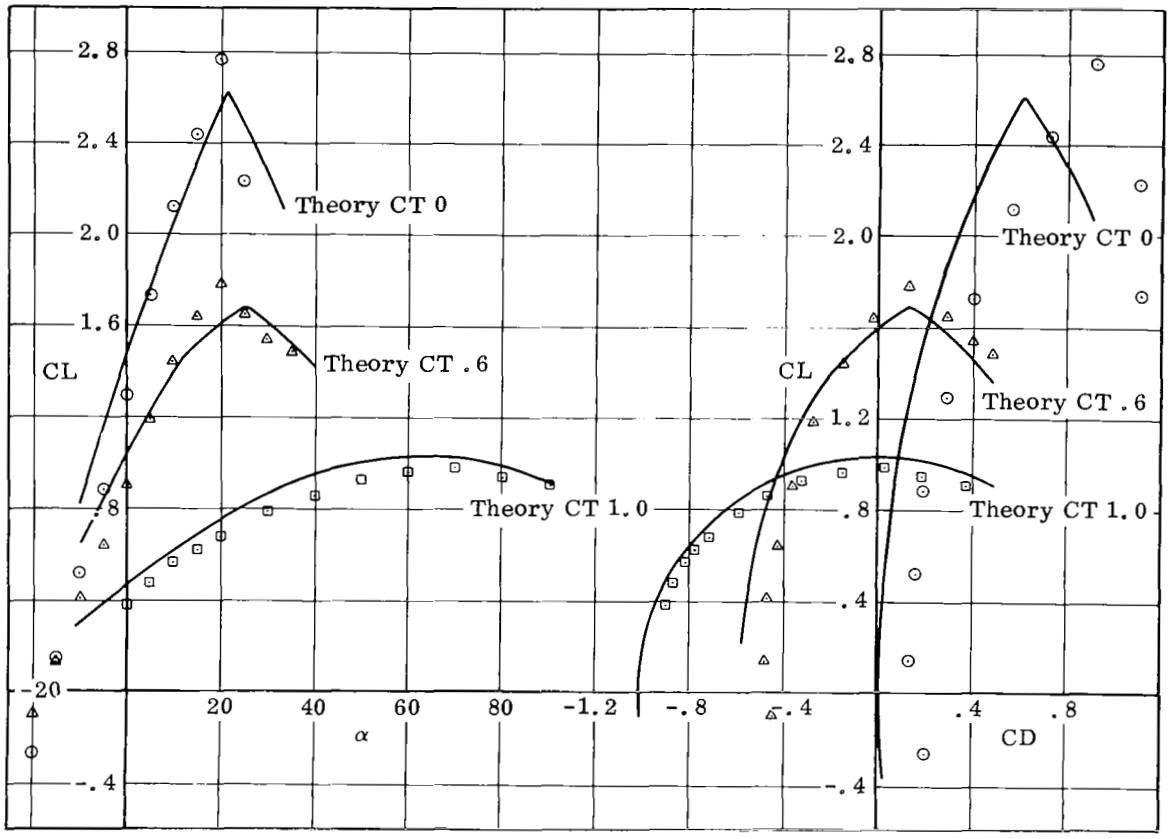

Figure 13. Correlation with TN D1586; Flap 40°; Coefficients Referred to Slipstream Velocity

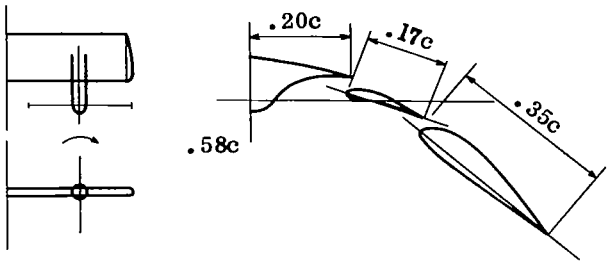

Span	13.8 ft.	Area	39.2 sq. ft.
AR	4.88	Taper	1.0
Section	NACA 4415	$\alpha_{\text{zero lift}}$	-4.5°
δ flap	40°	Chord extension	.30
α/δ_{2D}	.50	$\alpha_{\text{max CL}}$	7.5°
Prop D	5.67 ft.		

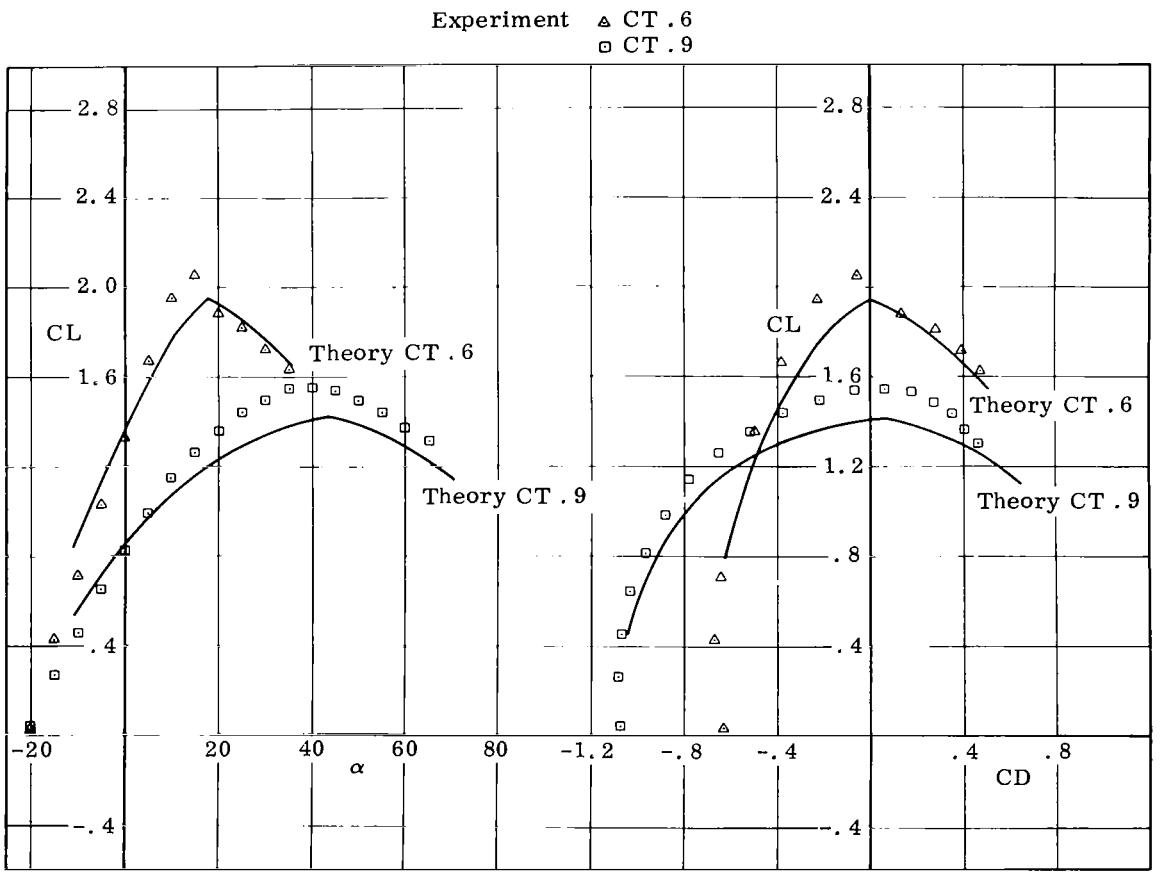

Figure 14. Correlation with TN D3375; Flap 40°; Coefficients Referred to Slipstream Velocity

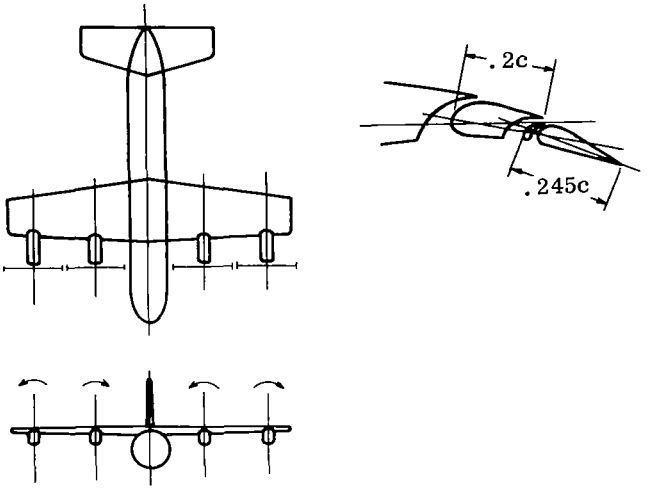

Span	43.3 ft.	Area	329 sq. ft.
AR	5.71	Taper	.554
Section	NACA 63_2 416	$\alpha_{zero\ lift}$	-2.5°
δ_{flap}	20°	Chord extension	.05
α/δ_{2D}	.25	$\alpha_{max\ CL}$	17.5°
Prop D	9.3 ft.	Fuselage D	6.0 ft.

CL_{α} power off with no flap deflection taken to be 4.35 per radian

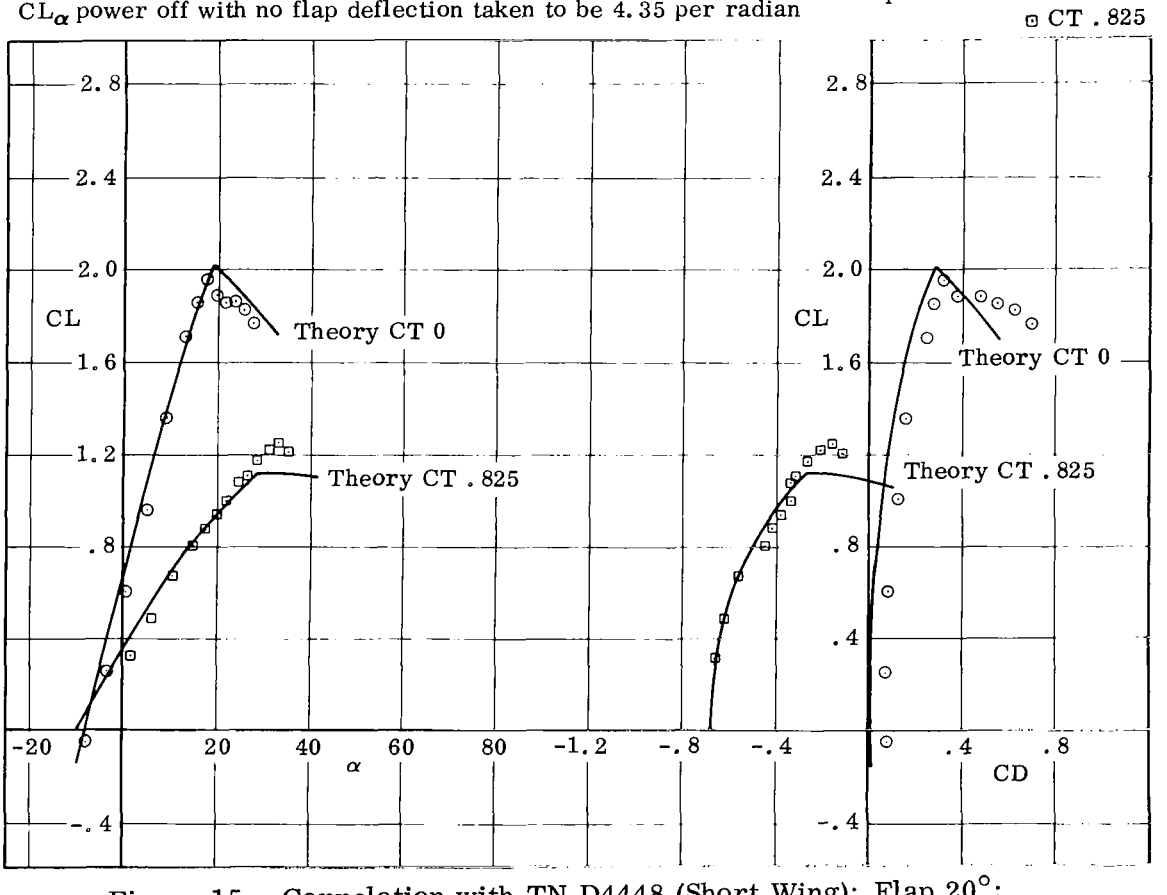

Figure 15. Correlation with TN D4448 (Short Wing); Flap 20°; Coefficients Referred to Slipstream Velocity

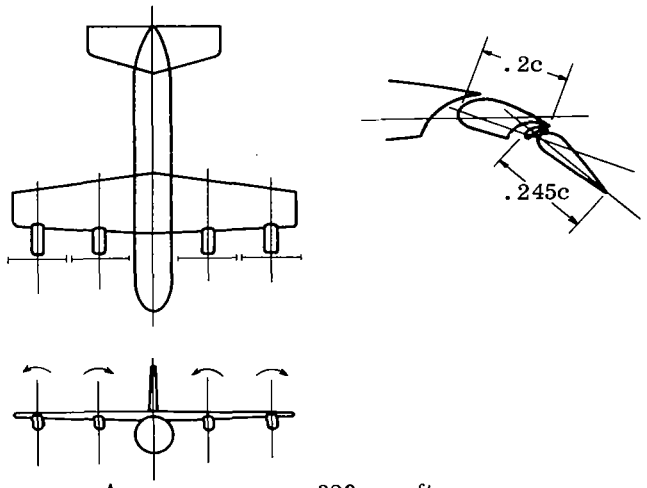

Span	43.3 ft.	Area	329 sq. ft.
AR	5.71	Taper	.554
Section	NACA 63_2 416	$\alpha_{zero\ lift}$	-2.5°
δ_{flap}	40°	Chord extension	.10
α/δ_{2D}	.25	$\alpha_{max\ CL}$	18.5°
Prop D	9.3 ft.	Fuselage D	6.0 ft.

Experiment ○ CT 0 □ CT .829

CL_{α} power off with no flap deflection taken to be 4.35 per radian

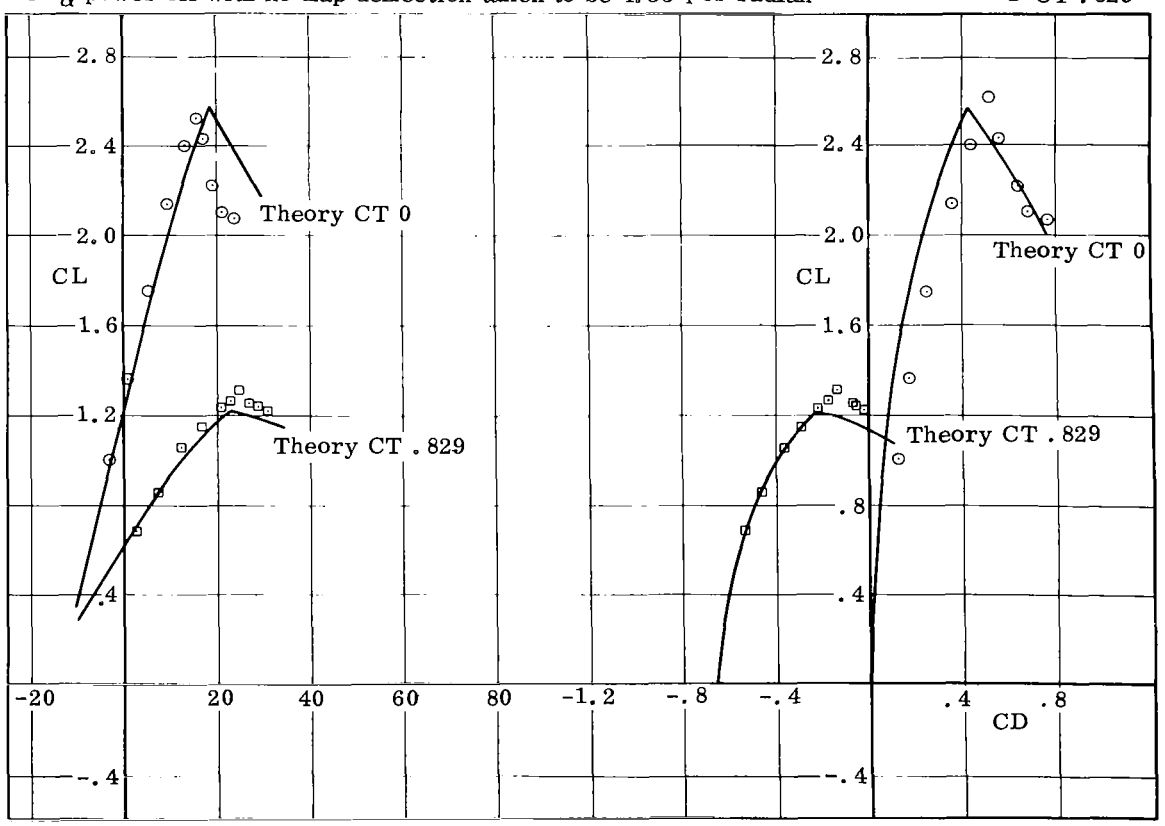

Figure 16. Correlation with TN D4448 (Short Wing); Flap 40°; Coefficients Referred to Slipstream Velocity

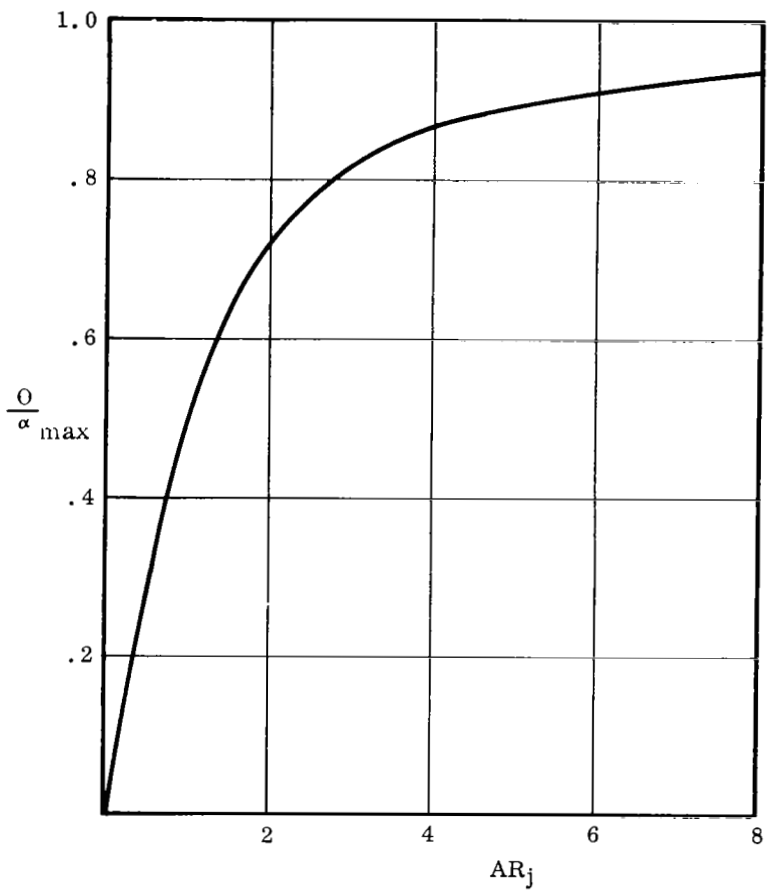

Figure 17. Effect of Jet Width on Limiting Turning Ratio

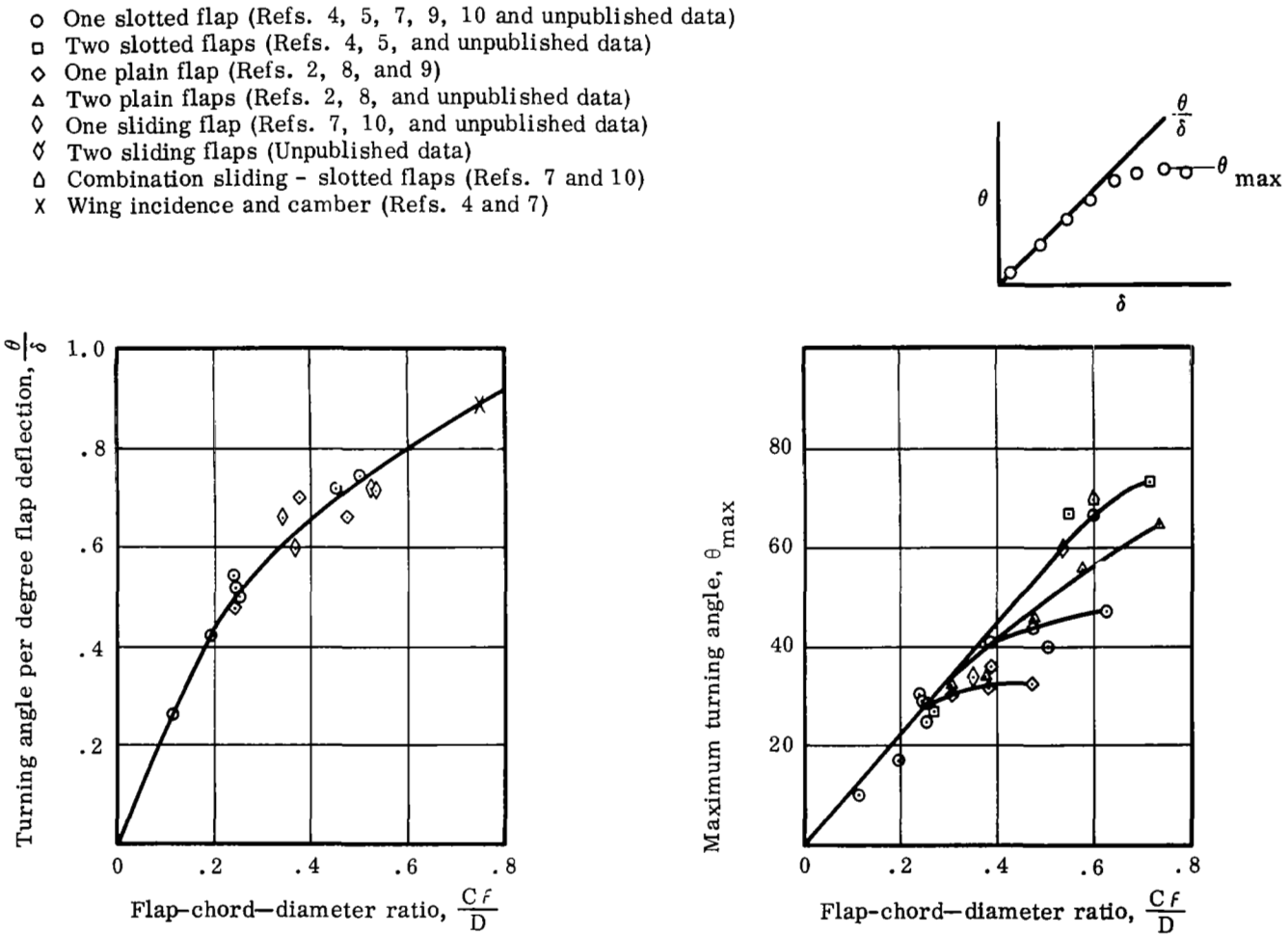

Figure 18. Variation of Turning Angle with the Ratio of Total Flap Chord to Propeller Diameter for Various Flap Configurations in Hovering Out of Ground-Effect Region (Reproduced from NASA Memorandum 1-16-59L. Reference Numbers Are for the List of References in This Report.)

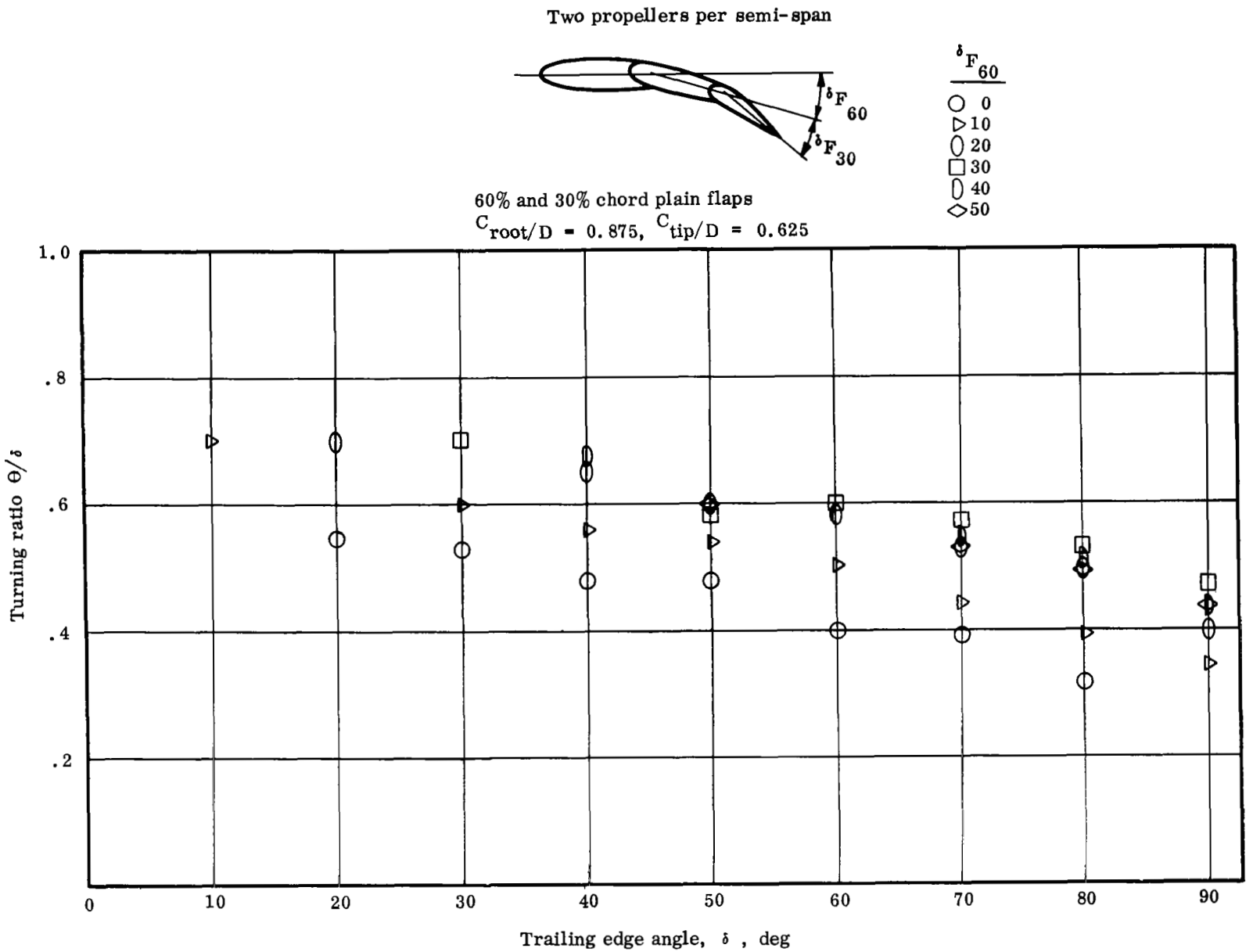

Figure 19. Flap Data from TN 3307

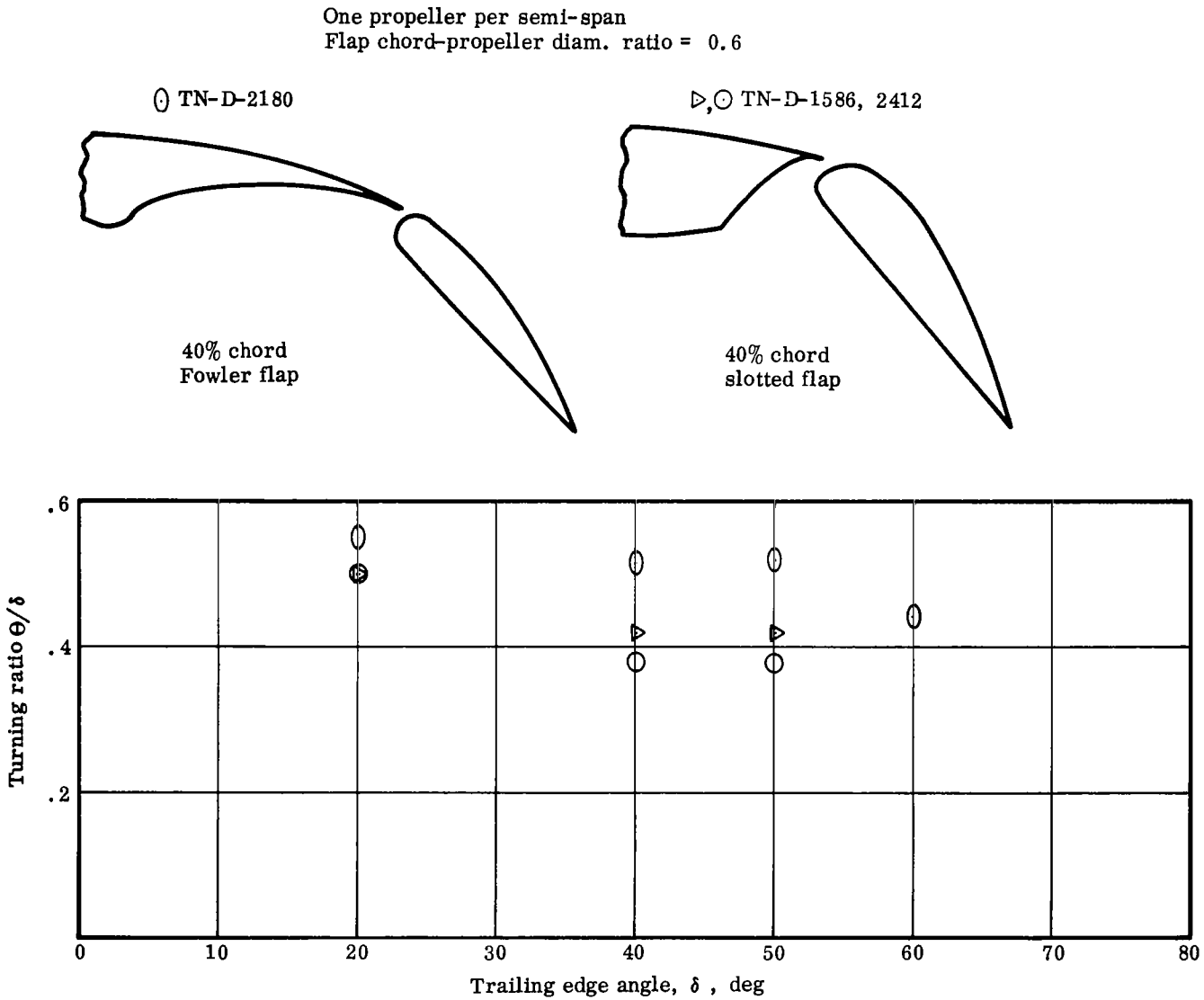

Figure 20. Typical Flap Data

Appendix A Slipstream contraction

In order to calculate the loads on the wing, it is necessary first to determine the dimensions and velocity of each jet. Because the slipstream contracts to preserve the mass flow as the velocity is increased through the actuator, the dimensions of the jet at the wing quarter chord line will be smaller than those of the actuator.

The velocity field inside a jet can be approximated by representing the jet edge as a column of closed vortices stacked together. A circular jet is then formed by a cylinder of ring vortices. The induced velocity may be calculated by the Biot Savart law in exactly the same way as the magnetic field due to a wire carrying an electric current. According to this, the velocity due to a segment of length ds of a vortex of strength Γ is

$$dq = \frac{\Gamma ds}{4 \pi r^2 \sin\theta}$$

where r is the distance to the segment and θ is the angle to its direction. When this is integrated, the velocity at a point x on the center line of a jet of radius R_p due to a ring vortex at a point $\bar{x}$ is

$$u(x) = \frac{\Gamma R_p^{\,2}}{2\left[R_p^{\,2} + (\bar{x} - x)^2\right]^{3/2}}$$

Let N be the number of ring vortices per unit length. Then the total axial velocity due to a cylinder of semi-infinite length is

$$u(x) = \frac{N\Gamma}{2} \int_0^\infty \frac{R_p^{\,2}\, d\bar{x}}{\left[R_p^{\,2} + (\bar{x}-x)^2\right]^{3/2}} = \frac{N\Gamma}{2}\left(1 + \frac{x}{\sqrt{R_p^{\,2} + x^2}}\right)$$

Thus

$$\frac{u(x)}{u(o)} = 1 + \frac{x}{\sqrt{R_p^{\,2} + x^2}}$$

The velocity far downstream is twice the velocity at the actuator, in agreement with propeller momentum theory.

The induced longitudinal velocity at points on the plane $z = 0$ due to a closed rectangular vortex of height H_p and span B_p is

$$u(x,y) = \frac{\Gamma}{4\pi}\left\{\frac{2\left(\frac{H_p}{2}\right)}{(\bar{x}-x)^2+\left(\frac{H_p}{2}\right)^2}\left[\frac{\frac{B_p}{2}+y}{\sqrt{(\bar{x}-x)^2+\left(\frac{H_p}{2}\right)^2+\left(\frac{B_p}{2}+y\right)^2}} + \frac{\frac{B_p}{2}-y}{\sqrt{(\bar{x}-x)^2+\left(\frac{H_p}{2}\right)^2+\left(\frac{B_p}{2}-y\right)^2}}\right]\right.$$

$$+\frac{2\left(\frac{B_p}{2}+y\right)\left(\frac{H_p}{2}\right)}{\left[(\bar{x}-x)^2+\left(\frac{B_p}{2}+y\right)^2\right]\sqrt{(\bar{x}-x)^2+\left(\frac{H_p}{2}\right)^2+\left(\frac{B_p}{2}+y\right)^2}}$$

$$\left.+\frac{2\left(\frac{B_p}{2}-y\right)\left(\frac{H_p}{2}\right)}{\left[(\bar{x}-x)^2+\left(\frac{B_p}{2}-y\right)^2\right]\sqrt{(\bar{x}-x)^2+\left(\frac{H_p}{2}\right)^2+\left(\frac{B_p}{2}-y\right)^2}}\right\}$$

,et

$$\xi = \frac{x}{B_p/2} \quad ; \quad \eta = \frac{y}{B_p/2} \quad ; \quad AR_p = \frac{B_p}{H_p}$$

'hen integrating from $\bar{x} = 0$ to ∞

$$u(\xi, \eta) = \frac{N\Gamma}{2\pi} \left[\tan^{-1} AR_p(1+\eta) + \tan^{-1} AR_p(1-\eta) + \tan^{-1} \frac{1}{AR_p(1+\eta)} \right.$$

$$+ \tan^{-1} \frac{1}{AR_p(1-\eta)}$$

$$+ \tan^{-1} \frac{AR_p^{\,2}(1+\eta)\xi}{\sqrt{AR_p^{\,2}\xi^2 + 1 + AR_p^{\,2}(1+\eta)^2}}$$

$$+ \tan^{-1} \frac{AR_p^{\,2}(1-\eta)\xi}{\sqrt{AR_p^{\,2}\xi^2 + 1 + AR_p^{\,2}(1-\eta)^2}}$$

$$+ \tan^{-1} \frac{\xi}{(1+\eta)\sqrt{AR_p^{\,2}\xi^2 + 1 + AR_p^{\,2}(1+\eta)^2}}$$

$$\left. + \tan^{-1} \frac{\xi}{(1-\eta)\sqrt{AR_p^{\,2}\xi^2 + 1 + AR_p^{\,2}(1-\eta)^2}} \right]$$

The arc tangent terms can be combined to yield

$$u(\xi,\eta) = \frac{N\Gamma}{2}\left[1 + \frac{1}{\pi}\tan^{-1}\frac{\xi}{1+\eta}\sqrt{AR_p^{\,2}\xi^2+1+AR_p^{\,2}(1+\eta)^2} + \frac{1}{\pi}\tan^{-1}\frac{\xi}{1-\eta}\sqrt{AR_p^{\,2}\xi^2+1+AR_p^{\,2}(1-\eta)^2}\right] \tag{A2}$$

A similar treatment leads to the same formula for the velocity at points in the plane $y = 0$, with η replaced by $\frac{2z}{H_p}$ and AR_p by $\frac{1}{AR_p}$.

According to (A2) the induced velocity is constant throughout the cross section at $\xi = 0$ and ∞. In fact it is well known from the theory of electromagnetic solenoids that this is true for a cross section of arbitrary shape. The increase $\frac{u(\xi,\eta)}{u(0,\eta)}$ in the velocity at different heights when $\xi = \frac{1}{AR_p}$ or $x = \frac{1}{H_p}$ is tabulated below:

	$AR_p = 1$	2	∞
$\eta = 0$	1.667	1.565	1.50
.5	1.698	1.600	1.50
1	1.760	1.760	1.75

It can be seen that the velocity is still nearly independent of the position in the cross section. The velocity will therefore be taken everywhere as that at the center line,

$$\frac{u(x)}{u(0)} = 1 + \frac{2}{\pi}\tan^{-1}\left[\frac{2x}{H_pB_p}\quad H_p^{\,2} + B_p^{\,2} + 4x^2\right] \tag{A3}$$

The representation as a column of vortices does not allow for the contraction of the jet. This effect can be approximated by using (A1) and (A3) with the local jet dimensions, calculated so that the mass flow is constant. Let V_o be the external velocity and V_j the jet velocity far downstream. Then, the velocity at a distance x downstream is

$$V(x) = V_o + u(x)$$

and

$$V_j = V_o + u(\infty) = V_o + 2\,u(0)$$

Thus, if μ is the velocity ratio $\frac{V_o}{V_j}$

$$\frac{V(x)}{V_j} = \mu + \frac{1-\mu}{2}\,\frac{u(x)}{u(0)}$$

and

$$\frac{V(0)}{V_j} = \frac{1+\mu}{2}$$

Let S_p be the actuator area and S(x) the jet area. Then, for continuity of the mass flow

$$\frac{S(x)}{S_p} = \frac{V(0)}{V(x)} = \frac{1+\mu}{2}\,\frac{V_j}{V(x)}$$

or

$$\frac{S(x)}{S_p} = \frac{1}{1 + \left(\frac{1-\mu}{1+\mu}\right)\left(\frac{u(x)}{u(0)} - 1\right)} \tag{A4}$$

If the jet is circular and its radius is R(x) at a distance x downstream, then substituting (A1) in (A4)

$$\frac{R(x)^2}{R_p^{\,2}} = \frac{1}{1 + \left(\frac{1-\mu}{1+\mu}\right) \frac{x}{R_p^2 + x^2}} \tag{A5}$$

Similarly, for a rectangular jet substituting (A3) in (A4)

$$\frac{H(x)B(x)}{H_p B_p} = \frac{1}{1 + \left(\frac{1-\mu}{1+\mu}\right) \frac{2}{\pi} \tan^{-1} \left(\frac{2x}{H_p B_p} \sqrt{H_p^{\,2} + B_p^{\,2} + 4x^2} \right)} \tag{A6}$$

It is desired to replace both $H_p B_p$ by $H(x)B(x)$ and $H_p^{\,2} + B_p^{\,2}$ by $H^2(x) + B^2(x)$ in (A3). Now

$$H^2(x) + B^2(x) = \left[B(x) - H(x) \right]^2 + 2H(x)B(x)$$

When $B_p > H_p$, (A2) indicates that the velocity and corresponding pressure drop are larger at the side boundaries of the jet than they are at the top and bottom boundaries. Thus the absolute magnitude of the decrease in B(x) is greater than that of H(x). The proportionate decrease in H(x), however, can be expected to be greater than that of B(x), because in the limiting case, as the width of the jet is increased until it becomes an infinite strip, the area change must be accomplished by a vertical contraction, with H(x) approaching $\frac{1+\mu}{2} H_p$. A relation that approximates these two conditions is

$$B_p - B(x) = \left[H_p - H(x) \right] \quad AR_p \tag{A7}$$

(A6) may be solved using (A7) to give

$$B(x) = \frac{B_p}{2} \left[1 - \frac{1}{\sqrt{AR_p}} + \sqrt{\left(1 - \frac{1}{\sqrt{AR_p}}\right)^2 + \frac{4H(x)B(x)}{B_p^2}\sqrt{AR_p}} \right]$$

$$H(x) = \frac{B_p}{2\sqrt{AR_p}} \left[-\left(1 - \frac{1}{\sqrt{AR_p}}\right) + \sqrt{\left(1 - \frac{1}{\sqrt{AR_p}}\right)^2 + \frac{4H(x)B(x)}{B_p^2}\sqrt{AR_p}} \right] \tag{A8}$$

Then B(x) and H(x) may be found by substituting for H(x) B(x) on the right from (A6).

When R_p is replaced by R(x) in (A1) or H_p and B_p are replaced by H(x) and B(x) in (A3), it is found that at a distance downstream equal to the propeller diameter or actuator height, the velocity even in the static case has already reached a fraction .897 of its final value when the jet is circular, and fractions .873, .831 and .813 when the jet is rectangular with aspect ratios of 1, 2 and ∞. The effect of viscosity has been ignored in this treatment. Experimental measurements in air indicate that due to viscosity, the maximum velocity in fact occurs at about one propeller diameter downstream. It is generally reasonable therefore to assume that the slipstream has already reached its final state in the region of the wing. Then, for a circular jet

$$R = \frac{1 + \mu}{2} R_p \tag{A9}$$

and for a rectangular jet

$$B = \frac{1}{2\sqrt{AR_p}} \left(\sqrt{1 + AR_p + 2\mu \sqrt{AR_p}} + \sqrt{AR_p} - 1 \right) B_p$$

$$H = \frac{\sqrt{AR_p}\,(1 + \mu)\,H_p}{\sqrt{1 + AR_p + 2\mu \sqrt{AR_p}} + \sqrt{AR_p} - 1} \tag{A10}$$

$$\frac{B}{H} = \frac{1}{2(1+\mu)} \left(\sqrt{1 + AR_p + 2\mu \sqrt{AR_p}} + \sqrt{AR_p} - 1 \right)^2$$

Actually, since the velocity is not exactly uniform at points downstream, pressure variations would cause a jet that started rectangular to become rounded.

Appendix B Downwash in the slipstream

If the propellers are inclined to the free stream, they will deflect it so that the angle of attack of the wing in the slipstream will be altered.

The downwash can be determined from the inflow angle α_j as

$$\epsilon = E \alpha_j \tag{B1}$$

According to Ribner's analysis (ref. B1), the final downwash factor far downstream can be expressed in terms of the velocity ratio μ and the normal force coefficient at zero thrust as

$$E_\infty = \frac{1-\mu^2}{1+\mu^2} + \frac{\mu(2+\mu+\mu^2)}{4(1+\mu^2)^2} CN_\alpha \quad (T = 0) \tag{B2}$$

The normal coefficient can be estimated by De Young's method (ref. B2) as

$$CN_\alpha (T=0) = \frac{4.25\sigma}{1+2\sigma} \sin(\beta+8) \tag{B3}$$

where σ is the effective solidity and β is the blade angle in degrees at a radius fraction of 3/4.

Near the propeller, it will be assumed that the downwash varies along the longitudinal axis in the same way as the downwash at the center of a horseshoe vortex. If the propeller radius is R, the downwash factor at a distance x is then

$$E = \frac{E_\infty}{2} \left[1 + \frac{\sqrt{1 + \left(\frac{x}{R} + e\right)^2}}{\frac{x}{R} + e} \right] \tag{B4}$$

where e can be determined from the condition that the flow should be normal to the disk immediately behind it, or E = 1 when x = 0. This leads to

$$e = \frac{E_\infty}{2\sqrt{1-E_\infty}} \tag{B5}$$

Note that $E_\infty \rightarrow 1$ as $\mu \rightarrow 0$. In this case, $e \rightarrow \infty$ and $E \rightarrow 1$ for all x, in agreement with the absence of slipstream deflection when the aircraft is static.

When the jet is rectangular, the downwash will be assumed to vary like that of a horseshoe vortex of the same width B as the actuator, leading to the factor

$$1 + \frac{\sqrt{1 + \left(\frac{2x}{B} + e\right)^2}}{\frac{2x}{B} + e}$$

Now an infinitely wide jet can have no final downwash in the presence of an external stream, since the downwash in the entire crossplane at infinity must be uniform to preserve continuity of the flow. If the actuator is regarded as acting like a wing when it generates a normal force, the final downwash when $\mu > 0$ can be expected to be inversely proportional to its width. If E_∞ is calculated for the propellers represented by the actuator according to (B1), it is possible to allow for this effect by introducing a factor

$$\frac{\frac{2x}{B} + e}{\frac{2x}{H} + e}$$

where H is the actuator height. Combining the two factors, the downwash factor can be estimated as

$$E = \frac{E_\infty}{2} \; \frac{\frac{2x}{B} + e + \sqrt{1 + \left(\frac{2x}{B} + e\right)^2}}{\frac{2x}{H} + e} \tag{B6}$$

Then $E \rightarrow E_\infty \frac{H}{B}$ as $x \rightarrow \infty$ when $\mu > 0$, but E = 1 when $\mu = 0$.

References:

B1 Ribner, H. S.: Notes on the Propeller Slipstream in Relation to Stability. NACA ARR L4112a (WRL-25)

B2 DeYoung, John: Propeller at High Incidence, J. of Aircraft, Vol. 2, No. 3, May 1965, pp. 241-250.